The Impact of Self-Cycling Fermentation on the Production of Shikimic Acid in Populations of Engineered *Saccharomyces cerevisiae*

by

Roman Vincent Agustin

A thesis submitted in partial fulfillment of the requirements for the degree of

Master of Science

in

Chemical Engineering

Department of Chemical and Materials Engineering

University of Alberta

Abstract

Shikimic acid is an intermediary metabolite in the biosynthesis of aromatic amino acids in plants and microorganisms. It is also a precursor for the production of specialty chemical ingredients used in pharmaceutical, cosmetic, and healthcare products. However, the current commercial method of obtaining shikimic acid is a tedious and expensive process. The present study focuses on using *Saccharomyces cerevisiae* engineered to overproduce shikimic acid under a self-cycling fermentation (SCF) process to increase the yield, productivity, and specific productivity of this compound. SCF is an automated, unsteady state, semi-continuous mode of operation which has been shown to increase the specific productivity of biomolecules and induce synchrony in microbial populations.

The engineered *S. cerevisiae* was grown in batch cultures to quantify the increase in production of shikimic acid as compared to the unmodified strain. Shikimic acid titers between 0.08 to 0.13 $g \cdot L^{-1}$ were obtained during glucose metabolism. Subsequently, the engineered yeast strain was characterized in a 1-L batch fermenter for maximum shikimic acid production in preparation for SCF operation. It was determined that the most suitable time point at which cycling should be initiated is shortly after the depletion of glucose. In addition, the coupled readings of carbon dioxide evolution rate (CER) and its first derivative (dCER) proved to be an appropriate feedback control parameter to trigger cycling and to achieve stable SCF operation. SCF was then implemented and a shikimic acid titer of 0.39 $g \cdot L^{-1}$ was obtained after 23 cycles. This is a three-fold increase as compared to titers obtained in shake flask cultures during glucose metabolism and a four-fold increase as compared to the titer obtained after the first cycle. Moreover, the yield and after 21 cycles was 0.022 mol/mol-glucose. Furthermore, the integrated specific productivity after 23 cycles was 2.4×10^{-15} mol/(cell·h). This is a four-fold increase as compared to values obtained in batch studies. It is important to note that the use of the SCF system greatly improved the yield and specific productivity of shikimic acid in the engineered yeast strain. This shows great promise for an environmentally friendly alternative for the sustainable manufacture of this chemical.

Acknowledgements

First of all, I'd like to thank Dr. Sauvageau. You encouraged my interest in this interdisciplinary field of biology and engineering, especially when opportunities seemingly did not exist. You demonstrated how important (and fun) it is to foster a collaborative and creative work environment. Your reassurances were always timely. Your criticisms were always constructive. Thank you for continually encouraging me to loosen my grip on rigid plans, to explore the exciting fluidity of research, and to take ownership and pride in my work. You've been a mentor and a friend. It has been a complete privilege.

To all the past and present students, techs, and post-docs of the Sauvageau Lab: Thank you! To every "I have a quick question" I bombarded you with, to all the after-work drinks we consumed, you all have been a huge influence in my academic and personal growth. This does not even scratch the surface as to how privileged and thankful I am to have worked alongside each and every one of you. I've never met such a well-rounded group of overachievers!

Many thanks to the students and techs in the McCaffrey and Bressler Lab for making me feel welcome whenever I used their equipment. To Les who helped in the electrical side of setting up the fermenter system. To Becky for allowing me a safe space to unload my head and my heart. To the students in the office area for starting cake Monday.

To my friends and faf who have been there for me in this crazy journey: Thank you for reassuring me of my competence, for listening to my ideas and ramblings over many rounds of beer, for reminding me to laugh at every unfortunate 4 am sample-collection, and for walking through the muddy trenches with me. Seriously, you helped preserve my sanity – thank you!

And finally, to my family: I am so grateful for you. In all my excitement and complaints, you kept me grounded (and well-fed). Kuya, thanks for bragging about me – it's a bit embarrassing but I do appreciate it! Riva and Riza, the amount of times you both have made me laugh throughout this whole thing was more helpful than you can ever imagine. To mum and dad, thanks for always pushing me to achieve excellence. Onto the next dream!

Table of Contents

List of Tables

List of Figures

List of Abbreviations

ATP	Adenosine triphosphate
CA	Chorismic acid
CER	Carbon dioxide evolution rate
CO_2	Carbon dioxide
DAHP	3-Deoxy-D-arabinoheptulosonate 7- phosphate
dCER	First derivative of CER
DHS	3-Dehydroshikimic acid
DHQ	3-Dehydroquinic acid
DO	Dissolved oxygen
EPSP	5-enolpyruvylshikimate-3-phosphate
E4P	Erythrose-4-phosphate
[E]	Ethanol concentration
F	Synchrony index
GDLS	Genetic Design by Local Search
[G]	Glucose concentration

glf	Glucose facilitators
glk	Glucokinase
G6P	Glucose-6-phosphate
HPLC	High performance liquid chromatography
IR	Infrared
NAD^+	Nioctinamide adenine dinucleotide
$NADP^+$	Nicotinamide adenine dinucleotide phosphate
OD	Optical density
PDH	Pyruvate dehydrogenase
PEP	Phosphoenol pyruvate
ppSA	PEP synthase
PTS	PEP-dependent phosphotransferase
SCF	Self-cycling fermentation
[SA]	Shikimic acid concentration
SA	Shikimic acid
S3P	Shikimic acid-3-phosphate
tkta	Transketolase
TCA	Tricarboxylic acid
UV	Ultraviolet

1. Introduction

Shikimic acid is an intermediary metabolite in the biosynthesis of aromatic α-amino acids in plants and microorganisms (Enrich et *al.,* 2008). It is a precursor for the production of ingredients used in pharmaceutical, cosmetic, and healthcare products (Fossati, et *al.,* 2014). Industrially, it is used as a chiral starting material for the production of neuraminidase inhibitors for the treatment of influenza (Kim, et *al.,* 1997). The current commercial method of obtaining shikimic acid is by extraction from the Chinese star anise plant (*Illicium verum)* (Payne and Edmonds, 2005). This is a tedious and expensive process which involves harsh processing conditions resulting in yields of only roughly 3% (Ohira et *al.,* 2009). Thus, it is necessary to develop sustainable, high-yielding, and cost-effective alternatives to meet market needs.

Microbial production of shikimic acid via fermentation requires the engineering of the shikimic acid pathway to overproduce this metabolite from renewable carbon sources like glucose (Draths, et *al.,* 1999). This overproduction is achieved by the overexpression of enzymes that direct the carbon flux towards shikimic acid while blocking biochemical processes that consume it. Many studies in the metabolic engineering of *E. coli* and other bacteria to overproduce shikimic acid have been undertaken (Knop, et *al.,* 2001; Chandran et *al.,* 2003; Krämer, et *al.,* 2003; Ahn, et *al.,* 2008). However, yeast, which is emerging as a potent host for the production of high value plant-specific metabolites for industrial applications (Fossati, et *al.,* 2014), represents an advantageous vector for the production of shikimic acid. Currently, *Saccharomyces cerevisiae* is widely used as a cell factory for the production of bioethanol, therapeutic proteins, pharmaceuticals and nutritional products (Nevoigt, 2008). It is a model eukaryote often employed for the development of new fermentative processes due to its robustness towards a wide range of environmental conditions, its ease in genetic manipulation, and the extensive available information concerning its physiology and biochemistry (Nielsen and Jewett, 2008). Therefore, engineering the naturally-occurring shikimic acid pathway in yeast provides a viable method for high-yield production of shikimic acid.

The degree of substrate conversion and yields are dependent on the type of reactor and operating strategy chosen during fermentation. Despite high productivities for growth-associated products observed in continuous fermentations such as the chemostat, batch processes remain the method of choice for the synthesis of various products using engineered yeast strains (Shuler and

Kargi, 2002). This is because batch systems facilitate production of secondary metabolites. They also minimize back mutation of engineered strains commonly observed in chemostats (Shuler and Kargi, 2002). On the other hand, batch fermentations have long down times required for sterile medium preparation at the beginning of a process and clean up at the end of the fermentation period. This leads to decreased productivity. An alternative fermentation method called self-cycling fermentation (SCF) is an automated, unsteady state, semi-continuous mode of operation which has been shown to increase specific productivity of biomolecules (Sheppard and Cooper, 1990; McCaffrey and Cooper, 1995; Storms, e*t al.*, 2012). It can be used for increased biomass production and, by conjunction, primary metabolite production (Brown and Cooper, 1991) or configured to maximize formation of non-growth associated products (van Walsum and Cooper, 1993; McCaffrey and Cooper, 1995, Wentworth and Cooper, 1996). Furthermore, SCF operation leads to synchronized microbial cultures (Brown and Cooper, 1992; McCaffrey and Cooper, 1995; Wentworth and Cooper, 1996; Sauvageau, et *al.,* 2010; Storms, e*t al.*, 2012). The benefit of synchronized cultures includes the mitigation of product inhibition due to negative feedback loops, which consequently increases overall productivity and yield.

The present study proposes to take advantage of the coupled strategy of metabolically engineering *Saccharomyces cerevisiae* and implementing SCF operation to increase shikimic acid productivity and yield.

2. Literature Review

2.1 *Saccharomyces cerevisiae*

2.2.1 General characteristics

Saccharomyces cerevisiae is a unicellular eukaryote belonging to the kingdom Fungi, division Ascomycota (Walker, 2009). It is more commonly known as baker's or brewer's yeast. As one of the simplest eukaryotes, its genome size is only three times that of *Escherichia coli*; the chromosomes within the yeast nucleus range in size from 0.2 to 6 Mb (Van Zandycke, 2009). *S. cerevisiae* is stable in both haploid (16 chromosomes) and diploid (32 chromosomes) stages (Madigan, *et al.,* 2009). As such, it is widely recognized as an ideal eukaryotic model organism for genetic and biochemical studies.

Capable of growing under a large range of environmental conditions, *S. cerevisiae* is a facultative aerobe (Madigan, *et al.,* 2009). Like most organisms, its maximal growth rate occurs at optimal conditions. *S. cerevisiae* is best adapted at an optimal temperature of 32.3°C (Salvado, e*t al.,* 2011). The optimal pH range for growth is from pH 4 to pH 6 (Neelakantam and Power, 2005). It predominantly reproduces asexually by budding in both haploid and diploid stages (Oda and Ouchi, 2000; Madigan, *et al.,* 2009). However, some undergo sexual reproduction through mating, where two haploid yeast cells fuse to form a diploid. Subsequently ascospores are formed by meiosis (Madigan, *et al.,* 2009).

S. cerevisiae flourishes in environments with sugars. The growth curve of a proliferating yeast population follows that of a typical microbial growth cycle which includes the lag phase, exponential phase, deceleration phase, stationary phase, and death phase (Shuler and Kargi, 2002; Madigan, *et al.,* 2009). For many yeast strains cultured anaerobically, growth proceeds via fermentation and produces ethanol. Conversely, respiratory metabolism occurs when these strains are grown aerobically. When grown aerobically on glucose as the main carbon source however, *S. cerevisiae* can produce ethanol while its growth proceeds via fermentation (De Deken, 1965). This occurs at environmental glucose concentrations above 0.8 mM and is known as the *Crabtree effect* (Verduyn, *et al.,* 1984). The aerobic production of ethanol by *S. cerevisiae* is due to its limited respiratory capacity. At high glucose levels, the uptake of multiple hexose transporters increases the glycolytic rate within the cell. Consequently, pyruvate levels increase. This, in turn,

overwhelms the capacity of the pyruvate dehydrogenase complex (PDH) to shuttle pyruvate into the tricarboxylic (TCA) cycle. Thus, a carbon flux towards pyruvate decarboxylase for ethanol production occurs (Käppeli, 1986; Otterstedt, e*t al.*, 2004). Therefore, the aerobic growth of *S. cerevisiae* on glucose follows a diauxic growth pattern; a fast growth via aerobic fermentation of glucose is followed by a slow growth which involves the oxidation of the produced ethanol (De Deken, 1965). Simplified versions of the central intermediary metabolism of S. *cerevisiae* during growth in a batch culture on glucose and on ethanol are shown in Figure 2.1 and 2.2, respectively.

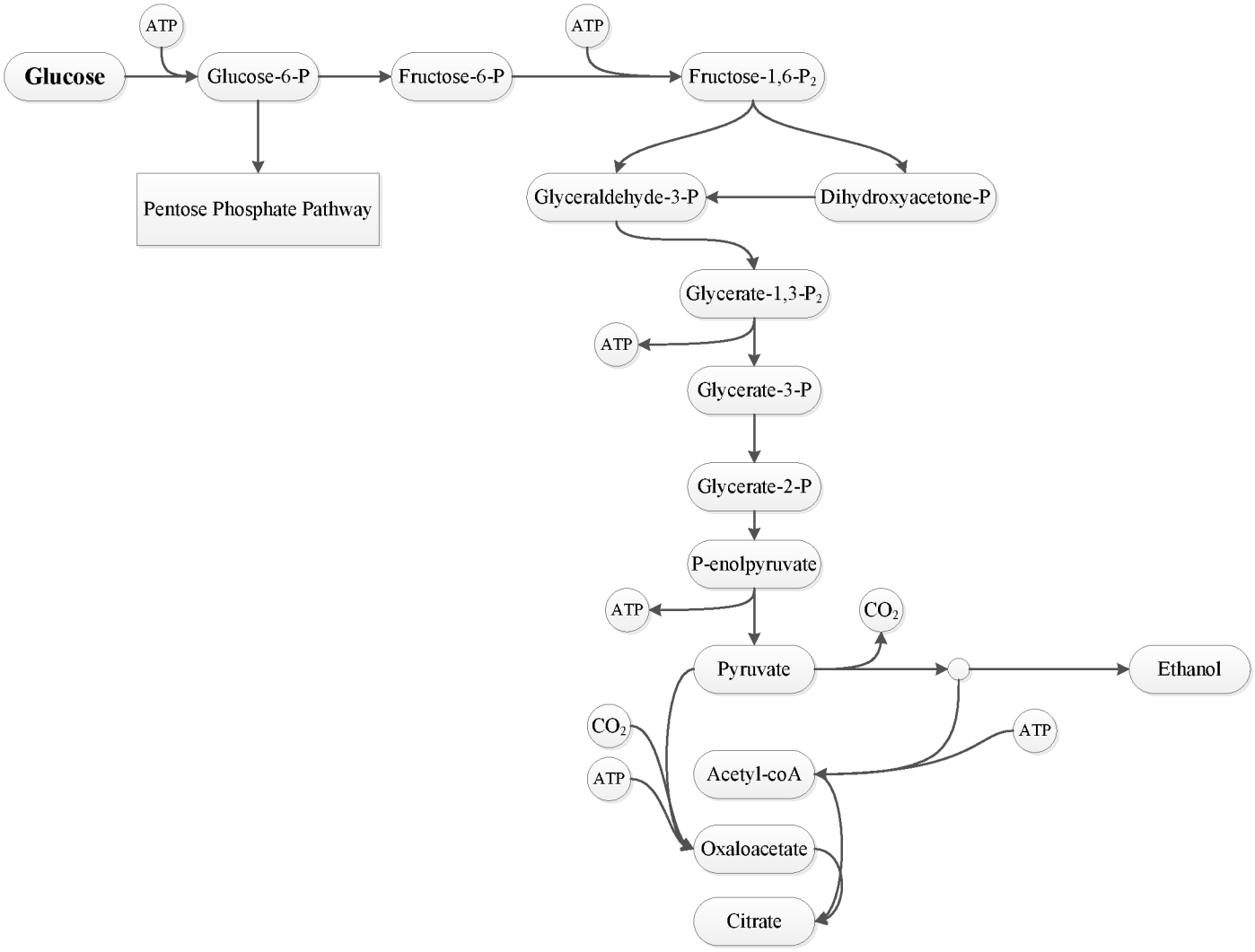

Figure 2.1. Glycolytic metabolism of *Saccharomyces cerevisiae* during growth on high concentrations of glucose.

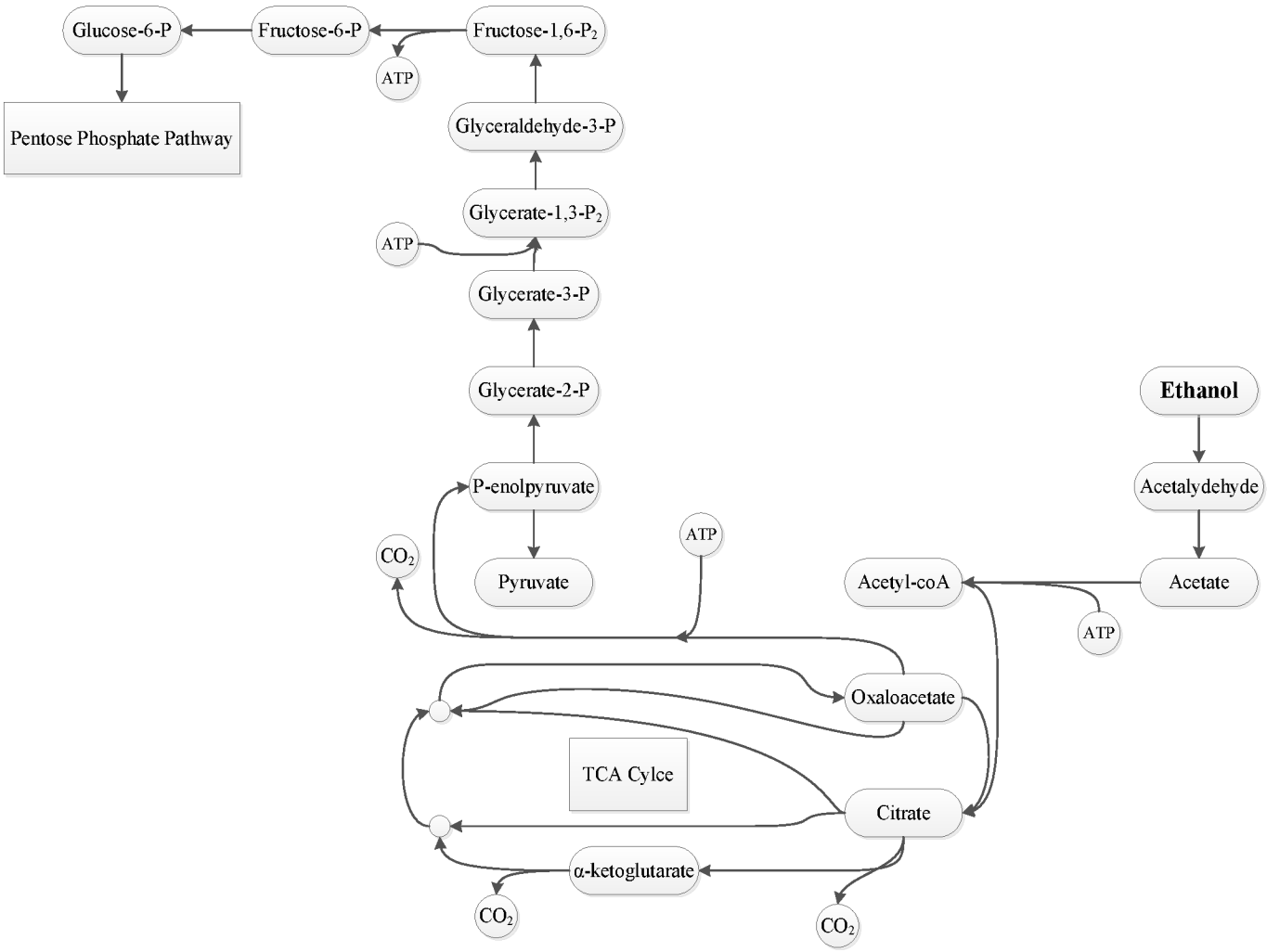

Figure 2.2 Metabolism of *Saccharomyces cerevisiae* during growth on ethanol.

2.2.2 Yeast as microbial factories

As a model eukaryote, the development and optimization of yeast as a cell factory for industrial applications is an active area of multidisciplinary research. One area of optimization arises from the chosen type of yeast strain platform. Based on growth in various carbon sources, biomass yield on sugar, and transformation and sporulation efficiencies, it has been shown that strains from the CEN.PK family are a suitable platform for cell-factory research (van Dijken, e*t al.,* 2000; Ostergaard, e*t al.,* 2000; Nielsen and Jewett, 2008). The CEN.PK strain was used to investigate metabolic fluxes (Stansfield and Stark, 2007). It is derived from the yeast strain ENY.WA-1A which grew well in chemostat cultures. To knock out the slightly flocculent nature of the ENY.WA strain, it was mated with strain MC996A. The haploid strain of CEN.PK has a fast growth rate with a doubling time of roughly 80 minutes. Moreover, different variations of

auxotrophies are found in CEN.PK strains (ura3-52, his3-Δ1, leu2-3,112 and trp1-289) (Stansfield and Stark, 2007). Auxotrophy is the inability of a microbe to produce an essential organic compound necessary for growth from inorganic nutrients. For industrial applications, it is used as a selection marker for transformed lines.

Yeast has many fermentative industrial applications. Traditionally, it is involved in the food industry to make bread, beer, wine, and vitamin supplements. However, it is also used in the biofuel industry to produce ethanol. In addition, yeast has been utilized in the production of chemicals by engineering synthetic pathways (Crumplen, *et al.,* 1989; Nevoigt, 2008; Curran, *et al.,* 2013, Gold, *et al.,* 2015). For the latter, the formation of products of interests from precursor metabolites through a platform yeast cell factory involves the manipulation of well-understood biochemical pathways. This can be done in three ways: the combination of existing pathways from different organisms into a host, the engineering of existing pathways, and *de novo* pathway design which combines the first two methods (Prather and Martin, 2008). In essence, yeast cell factory design is accomplished by bypassing natural feedback inhibition loops, rerouting metabolic flux, and constructing heterologous biosynthetic pathways. Thus, products such as alcohols, sugars, organic acids, aromatics, polyketides, insulin and other proteins can be synthesized from yeast hosts (Liu, *et al.,* 2013; Nielsen, 2013). Many of these chemicals are metabolically linked from glycolytic products such as pyruvate and acetyl-coA.

2.2 Shikimic Acid

2.2.1 General characteristics

Shikimic acid (3,4,5-trihydroxy-1-cyclohexene-1-carboxylic acid) (Figure 2.3) is an intermediate metabolite in the shikimic acid pathway involved in the synthesis of aromatic amino acids in plants and microorganisms (Ganem, 1978; Wilson, *et al.,* 1998; Herrmann and Weaver, 1999). Shikimic acid is a white crystalline organic acid with a melting point of 190°C (Snyder, 1973; Ghosh, *et al.,* 2012). It has a pK_a of 4.1 (yeast metabolome database, 2015). Its maximum absorbance in the UV range is recorded at λ=235 nm (Snyder, 1973). For many high performance liquid chromatography (HPLC) protocols however, it is observed at either 215 or 275 nm (Mousdale and Coggins, 1985). Only the α-isomer of shikimic acid (shown in Figure 2.3) has biological activity, even though many isomers have been characterized (Jiang *et al.,* 1997; Kranich *et al.,* 2007). Further physicochemical properties have been described by Bohm (1965).

With its six-carbon ring structure which contains three chiral carbons and a carboxylic acid functional group, shikimic acid is regarded as an important enantiomerically pure metabolite for the synthesis of biologically useful products (Krämer, *et al.,* 2003). Currently, it is used in the manufacture of a viral neuraminidase inhibitor called Oseltamivir which is used as an avian flu drug (Kramer, *et al.,* 2003; Ghosh, *et al.,* 2012); its synthesis from shikimic acid has been discussed previously (Kim, *et al.,* 1997, 1998; Rohloff, *et al.,* 1998).

2.2.2 Shikimic acid pathway

The shikimic acid pathway is found in various plants and microorganisms. It has been demonstrated that the pathway operates in the same manner in cells of plants, parasites, bacteria, yeast, and moulds. Differences that arise are in the structure of the enzymes related to the pathway and their mode of regulation (Gientka and Duszkiewicz-Reinhard, 2009). In yeast, the shikimic acid pathway undergoes seven catalytic steps where carbohydrate metabolism feeds into the synthesis of aromatic α-amino acids (Figure 2.3). It begins with the condensation of erythose-4-phosphate (E4P) from the pentose phosphate pathway (Figure B10 in Appendix B) and phosphoenol pyruvate (PEP) from glycolysis (Floss, *et al.,* 1972; Herrmann and Weaver, 1999). The shikimic acid pathway ends in the production of chorismate, a precursor for the synthesis of L-tyrosine, L-phenylalanine, L-tryptophan, and p-aminobenzoic acid (Floss, *et al.,* 1972; Herrmann and Weaver, 1999). Upon condensation of PEP with E4P, 3-deoxy-D-arabino-heptulosonate-7-phosphate (DAHP) is produced; the enzyme that catalyzes this step is DAHP synthase (Floss, *et al.,* 1972). Next, DAHP loses its phosphoryl group and undergoes cyclization to 3-dehydroquinone (DHQ) via DHQ synthase and NAD^+ (Bender, 1998). A double bond is introduced to DHQ which forms 3-dehydroshikimic acid (DHS) by means of DHQ dehydratase. Subsequently, shikimic acid dehydrogenase catalyzes the reduction of DHS with NADP to form shikimic acid (SA). Shikimic acid is then phosphorylated to 3-phosphoshikimic acid (S3P) by means of shikimate kinase. Condensation between a second molecule of PEP and S3P follows to produce 5-enolpyruvylshikimate-3-phosphate (EPSP) via EPSP synthase. Finally, chorismate synthase reduces and cleaves a phosphoryl group from the produced intermediate to form chorismate (Bohm, 1965; Floss, *et al.,* 1972).

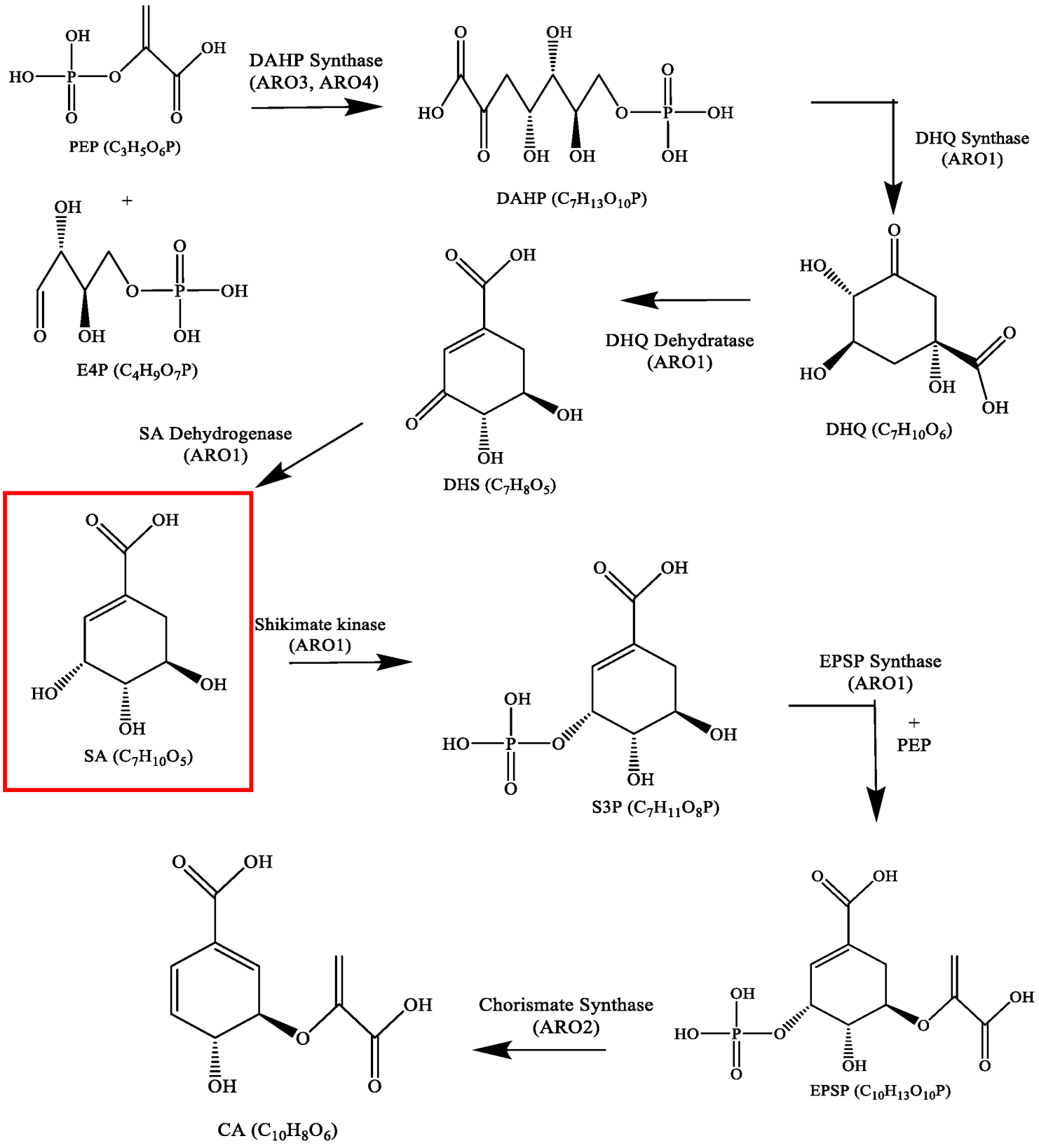

Figure 2.3 Shikimic acid pathway in *Saccharomyces cerevisiae.*

The shikimic acid pathway is tightly regulated to the needs of the cell since it leads to the formation of aromatic α-amino acids necessary for protein synthesis. When yeast cells are grown in complex medium rich in nutrients and amino acids, the genes responsible for the production of amino acids remain in pseudo-dormancy (Madigan, *et al.,* 2009; Gientka and Duszkiewicz-Reinhard, 2009). When placed under conditions of amino acid starvation, the synthesis of Gcn4p is induced; Gcn4p activates gene transcripts of multiple pathways for amino acid biosynthesis (Hinnebusch, 1988). It regulates protein formation by binding to the TGACTC fragments of the promoter present in several genes (Arndt and Fink, 1986). Specifically, it activates the synthesis of enzymes in the shikimic acid pathway by regulating the expression of their corresponding gene. In contrast, specific enzymes of the shikimic acid pathway are subject to inhibition in cultures where yeast cells have access to aromatic amino acids (Teshiba, *et al.,* 1986).

In *S. cerevisiae,* the first enzyme in the shikimic acid pathway, DAHP synthase, exist as an isoenzyme; it is encoded by two analogous genes called *ARO3* and *ARO4* located on chromosome IV and II, respectively. *ARO3* is subject to feedback inhibition by phenylalanine, whereas *ARO4* responds to tyrosine (Teshiba, *et al.,* 1986; Pravicini, *et al.,* 1989; Braus, 1991; Künzler, *et al.,* 1992). The five enzymes following DAHP synthase of the shikimic acid pathway are part of a complex multi-domain protein called the AROM protein; it is the product of the *ARO1* gene in yeast (Duncan, *et al.,* 1988). Its active centers (DHQ synthase, DHQ dehydratase, shikimic acid dehydrogenase, shikimate kinase, and EPSP synthase) are encoded by their respective sequences in the *ARO1* gene on chromosome IV (Duncan, *et al.,* 1988). In wild type strains of *S. cerevisiae,* the expression of the penta-functional AROM protein is regulated at a low level though its overexpression is feasible (Graham, *et al.,* 1993). It has been found that EPSP synthase is subject to *in vitro* inhibition by glyphosate, a growth inhibitor in bacteria, and displays antimycotic properties against various bacterial and yeast strains (Amrhein, *et al.,* 1983, Bode, *et al.,* 1986). When *S. cerevisae* was grown in medium containing glyphosate, shikimic acid was detected in the broth. Therefore, it was concluded that glyphosate blocks the shikimic acid pathway at a step after shikimic acid (Bode, *et al.,* 1986). In cultures with both glyphosate and aromatic amino acids in the medium, no shikimic acid is detected in the broth due to the inhibition of DAHP synthase by L-tyrosine and L-phenylalanine (Bode, *et al.,* 1984). Finally, chorismate synthase is encoded by the *ARO2* gene on chromosome VII (Braus, 1991).

2.2.3 Isolation from plant sources

Shikimic acid is found in plants but at low concentrations (Bohm, 1965; Dell and Frost, 1993; Herrmann and Weaver, 1999). It was first isolated from flowers of a highly toxic Japanese star anise (*Illicium anisatum*) in 1885 (Payne and Edmonds, 2005). Since then, it has been found in the leaves of sweetgum tree (*Liquidambar styraciflua*). It has been reported that shikimic acid can be extracted from the bark, wood, and seeds of American sweetgum trees, from which up to 3.7% (w/w) shikimic acid was obtained (Enrich, *et al.,* 2008; Martin, *et al.,* 2010). In addition, several varieties of spruce, pine, and fir have been known to produce shikimic acid; after undergoing hot water extraction (45-75°C), the needles of scots pine (*Pinus sylvestris*) yielded 1.6% (w/w) shikimic acid (Sui, 2008). Raghavendra, *et al.* (2009) outline other plant sources of shikimic acid. At present, the best source of shikimic acid are the plants of the genus *Illicium,* though most species are poisonous and thus not suitable for commercial production of this compound (Lederer, *et al.,* 2006). Currently, commercial production of shikimic acid is fueled by its extraction from the seeds of the Chinese star anise (*Illicium verum)* (Payne and Edmonds, 2005).

To obtain shikimic acid from plant tissue, a hot water extraction is generally the primary step in the extraction process. This is because shikimic acid is not soluble in non-polar solvents but highly-soluble in water (180 g·L^{-1} at 20°C) (Sui, 2008; Ohira, *et al.,* 2009). However, other water-soluble plant metabolites are found in the crude water extract and, thus, necessitate further downstream processing to produce pure shikimic acid. Approximately 1 kg of shikimic acid can be obtained from 30 kg of dry Chinese star anise seed pods (Ohira, *et al.,* 2009). Other extraction methods using complex formation (Sadaka and Garcia, 1999), acids (Harring, *et al.,* 1998; Mueller, 2003), and alcohols (Anderson, *et al.,* 2001) have been described.

2.2.4 Chemical synthesis

Shikimic acid was first chemically synthesized in the 1960s by the Diels-Alder reaction to form six membered rings (McCrindle *et al.,* 1960). However, the yield was low, at less than 15%. In 1982, the efficiency of the Diels-Alder reaction was improved to increase the shikimic acid yield to 29% (Koreeda and Ciufolini, 1982). Other methods of synthesizing shikimic acid chemically include the use of benzene as a starting material (Birch, *et al.,* 1988), palladium-mediated elimination reaction (Yoshida and Ogasawara, 2000), from sugars such as D-mannose (Dangschat and Fischer, 1950; Fleet, *et al.,* 1984), and from quinic acid and its derivatives (Kim,

et al., 1997; Rohloff, *et al.,* 1998). Despite the development of various ways to chemically synthesize shikimic acid, its production by these methods is too expensive for commercial use and requires the removal of enantiomers. Ultimately, the isolation of shikimic acid from the Chinese star anise remains the main source of this compound (Raghayendra, *et al.,* 2009; Ghosh, *et al.,* 2012).

2.2.5 Production in microbial strains

The engineering of the shikimic acid pathway has been centered most commonly on the bacterium *E. coli* (Knop, *et al.,* 2001; Yi, *et al.,* 2003; Johansson, *et al.,* 2005; Ahn, *et al.,* 2008; Escalante, *et al.,* 2010). Several differences in enzyme structure and regulation is observed in the shikimic acid pathway between *E. coli* and *S. cerevisiae*. In *E. coli*, three isoforms of the DAHP synthase exists which are encoded by the *AROF, AROG,* and, *AROH* genes; these are subject to feedback inhibition by L-tyrosine, L-phenylalanine, and L-tryptophan, respectively (Ghosh, *et al.,* 2012). The enzymes DHQ synthase, DHQ dehydratase, and shikimic acid dehydrogenase are encoded by the genes *AROB*, *AROD,* and *AROE*, respectively. Two versions of the enzyme shikimate kinase exist (I and II); they are encoded by the *AROL and AROK* genes, respectively. In *E. coli,* the enzymes DHQ synthase, DHQ dehydratase, and shikimic acid dehydrogenase are constitutively expressed whereas DAHP synthase and shikimate kinase are transcriptionally regulated. The rate limiting enzymes of the shikimic acid pathway in *E. coli* are DHQ synthase and shikimate kinase (Dell and Frost, 1993). Furthermore, shikimic acid dehydrogenase is subject to inhibition by shikimic acid (Dell and Frost, 1993). Figure B11 in Appendix B shows the shikimic acid pathway in *E. coli.*

The overproduction of shikimic acid in *E. coli* has been based on genetic manipulations to alter both the central carbon metabolism and the shikimic acid pathway itself. The modification of the central carbon metabolism is essential to increase the levels of PEP and E4P, both precursor substrates into the aromatic amino acid pathway. The engineering of the pentose phosphate pathway to increase the supply of E4P has been achieved through the overexpression of transketolase (*tktA*) (Knop, *et al.,* 2001). This resulted in an increase of shikimic acid yield from 0.12 to 0.18 mol/mol-glucose and concentration from 38 to 52 $g \cdot L^{-1}$ in fed-batch operation. Similarly, modification performed on the glycolytic pathway to increase the supply of PEP involved the overexpression of PEP synthase (ppSA) (Chandran, *et al.,* 2003). This resulted in a

shikimic acid yield of 0.23 mol/mol-glucose and a concentration of 66 $g \cdot L^{-1}$. Further manipulations which include the inactivation of the PEP-dependent phosphotransferase (PTS) operon and the overexpression of the non-PTS glucose transporter such as glucose facilitators (glf) and glucokinase (glk) in conjunction with the overexpression of the *tktA* gene resulted in shikimic acid concentrations up to 71 $g \cdot L^{-1}$ (Gibson, *et al.,* 2001; Chandran, *et al.,* 2003). In addition, by supplementing the minimal medium with yeast extract, cultures of engineered *E. coli* were able to produce shikimic acid to a concentration of 85 $g \cdot L^{-1}$ (Chandran, *et al.,* 2003).

Modifications of the shikimic acid pathway for fermentative production of shikimic acid falls into two similar approaches. The first uses engineered *E. coli* strains deficient in both the *AROK* and *AROL* gene (Draths, *et al.,* 1999). In this method, the shikimic acid pathway was blocked after the synthesis of shikimic acid by eliminating the metabolic step into S3P. The alternative genetic modification focuses on EPSP synthase deficient strains (Iomantas, *et al.,* 2002). In this method, the shikimic acid pathway is blocked after the production of S3P. In both approaches, introduction of a feedback resistant DAHP synthase gene called *AROF4br* increases the carbon flux towards the shikimic acid pathway from the central carbon metabolism. This gene can be combined with the *AROB* gene to overcome the rate limiting DHQ synthase. Moreover, the introduction of an additional *AROE* gene can compensate for the feedback inhibition caused by shikimic acid (Draths, *et al.,* 1999). However, overexpression of shikimic acid dehydrogenase (encoded by the *AROE* gene) resulted in the reduction of dehydroshikimic acid to quinic acid (Draths, *et al.,* 1999). In earlier studies of metabolically engineered *E. coli* strains, shikimic acid concentrations were low due to the simultaneous production of quinic acid (Knop, *et al.,* 2001). This is because a microbe-catalyzed equilibrium reaction occurs between shikimic acid and quinic acid. In 1999, Draths, *et al.* obtained a shikimic acid concentration of up to 27 $g \cdot L^{-1}$ with dehydroshikimic acid and quinic acid concentrations of 4.4 $g \cdot L^{-1}$ and 12.6 $g \cdot L^{-1}$, respectively. The accumulation of these by-products complicates downstream processing and purification of shikimic acid (Knop, *et al.,* 2001). Thus, the overexpression of the *AROE* gene was found to interfere with shikimic acid productivity due to the formation of quinic acid (Draths, *et al.,* 1999).

Knop, *et al.,* (2001) found that the equilibrium process that results in the consumption of shikimic acid to make dehydroshikimic acid and quinic acid is fueled by the uptake of shikimic acid into the cell. Thus, the reduction of shikimic acid uptake activity was explored as a means to

minimize quinic acid concentration (Draths, *et al.,* 1999). This was accomplished by either increasing glucose availability or introducing a glucose analogue in the medium. Increasing the availability of glucose reduced the quinic acid formation by 90% (Draths, *et al.,* 1999). However, no reduction in dehydroshikimic acid was observed while shikimic acid concentration decreased by 25%. When methyl-α-d-glucopyranoside, a glucose-mimic, was added to the medium, the concentration of shikimic acid increased from 28 to 35 $g \cdot L^{-1}$ in a culture of engineered *E. coli* (Knop, *et al.,* 2001). Furthermore, the yield increased from 0.14 to 0.19 mol/mol-glucose while the concentration of quinic acid decreased from 19 to 2.8 $g \cdot L^{-1}$.

2.2.6 Engineering the shikimic acid pathway in yeast

Despite the successful overproduction of shikimic acid in bacterial strains, development in yeast strains is attractive since genetic manipulations performed in the shikimic acid pathway can be coupled with heterologous biosynthetic pathways for the production of high value plant-specific secondary metabolites. As mentioned previously, *S. cerevisiae* is an ideal host organism for industrial production of specialty chemicals because it offers advantages which include tolerance to lower temperatures, easier separations, no phage contamination, and suitability in large-scale fermentation (Curran, *et al.,* 2013). In addition, *S. cerevisiae* naturally prefers lower pH environments as compared to *E. coli* which is a condition better suited for the formation of di-acids (Curran, *et al.,* 2013). *S. cerevisiae* has been used successfully as a host for heterologous models that use precursors from the shikimic acid and aromatic amino acid pathways to produce compounds such as naringenin, resveratrol, vanillin, p-hydroxybenzoic acid, p-hydroxycinnamic acid, and p-amino benzoic acid (Wang and Yu, 2012; Wang, *et al.,* 2011; Hansen, *et al.,* 2009; Jiang, *et al.,* 2005; Naesby, *et al.,* 2009; Vannelli, *et al.,* 2007; Krömer, *et al.,* 2012). Though rational metabolic engineering techniques applied to *E. coli* to alleviate feedback inhibition resulted in high concentrations of aromatic amino acids and its related precursor metabolites, these same principles do not achieve the same result in yeast (Curran, *et al.,* 2013). This suggests that the shikimic acid and aromatic amino acid biosynthetic pathways are highly regulated through local and global transcription machinery in yeast. A comprehensive omics analysis of amino acid formation in yeast has demonstrated the high degree of allosteric and transcriptional regulation in amino acid pathways that are controlled by factors such as Gcn4p (Moxley, *et al.,* 2009).

In yeast, two reactions in the aromatic amino acid pathway are subject to feedback inhibition. The first is the catalytic step into the shikimic acid pathway involving the two isoenzymes for DAHP synthase. Hartmann, *et al.,* (2003) showed that a single substitution in the ARO4 protein at position 229 from lysine to leucine deregulates the enzyme and causes it to become feedback insensitive to L-tyrosine. The second is a reaction downstream from chorismate; it involves chorismate mutase which is subject to allosteric regulation. It is encoded by the *ARO7* gene (*Ball*, *et al.,* 1986). Chorismate mutase is stimulated by L-tryptophan and inhibited by L-tyrosine. Substituting a serine residue at position 141 with glycine removes the effects of both aromatic amino acids (Shnappauf, *et al.,* 1998; Luttik, *et al.,* 2008). Of the two reactions, Luttik, *et al.* (2008) illustrated that DAHP synthase exerts a stronger degree of regulation on the formation of aromatic compounds in *S. cerevisiae.*

In addition to the localized changes incorporated in the shikimic acid and aromatic amino acid pathways, changes in the central carbon metabolism of *S. cerevisiae* to improve the availability of the precursors PEP and E4P were investigated by Gold, *et al.* (2015). A knockout strategy was proposed by a strain design algorithm called Genetic Design by Local Search (GDLS) to direct the flux towards L-tyrosine. This was coupled with the iMM904 model which maximizes biomass production during respiratory metabolism of glucose for wild-type and engineered yeast strains (Gold, *et al.,* 2015). The result was the deletion of the *Zwf1* gene. However, an NADPH deficiency was observed as a result of the deletion which caused an accumulation of DHS and subsequently, PEP. Relieving the NADPH deficiency through the addition of methionine was hypothesized to improve the thermodynamic favourability of DHS reduction to shikimic acid. Ultimately, methionine supplements in cultures of *Zwf1-* strains resulted in improved flux through the shikimic acid pathway (Gold, *et al.,* 2015).

2.3 Self-Cycling Fermentation (SCF)

2.3.1 General operation

In microbial fermentation processes, the cell is never at steady-state. Thus, an unsteady-state batch cultivation system unifies the dynamics of the process and the inherent dynamics of the cell-cycle. The self-cycling fermenter was developed for this purpose where information about the physiological state of a culture under specific environmental conditions can be extracted. SCF is an automated, unsteady-state, semi-continuous mode of operation where a series of cycles is

carried out in sequence (Brown, 2001). Each cycle consist of a filling step, a reaction phase, and an emptying or harvesting step. The length of the reaction phase is dictated by the gross metabolism of an organism which is signalled by a feedback control parameter. Once the control parameter signals the cessation of metabolism in the organism, exactly half of the fermenter contents are removed in the emptying step. Subsequently, this volume is replaced with fresh medium during the filling step (Brown, 2001). Interestingly, it was observed that the cycling process causes a synchronizing effect in the cell population.

2.3.2 Continuous phasing

Originally, continuous phasing, the predecessor of the SCF, was developed to study the overall metabolic capacity or the physiological state of an organism in a growing culture more accurately (Dawson, 1972; Brown, 2001). The problem with the reactor schemes for both chemostat and classical batch culture arises from the gross parameters that are measured; these parameters conflate the metabolism of a single microorganism with the average values obtained from the total cell population (Dawson, 1972; Brown 2001). Dawson proposed that to obtain a better picture of the physiological state of a microorganism, it is necessary to study cell populations whose growth cycles were completely aligned; the gross parameters of synchronized cell populations indicate the metabolic state of an individual cell more accurately. Cell populations with synchronized growth cycles have been obtained through selection and induction methods (Zeuthen, 1964; Burns, 1964; Lloyd, *et al.,* 1982; Sheppard and Dawson, 1999). In selection methods, cells at the same point in the growth cycle are selected from a population. This results in synchronous cultures. In induction methods, the cell population is subjected to a periodic forcing function where the period is equal to the natural doubling time of the organism. This results in synchronized cultures. Dawson (1972) developed a reactor system called continuous phasing which could generate populations of synchronized cells by addition of a limiting nutrient at a chosen interval. At the end of the chosen interval, the liquid volume in the fermenter was doubled by the addition of fresh nutrients. This results in a halving of the cell concentration. Subsequently, half of the reactor contents were removed which returned the system to its original liquid volume. Like SCF, the collection of fill, react, and emptying periods was termed a cycle. In subsequent experiments, the emptying step preceded the filling step.

In experiments with yeast, it was found that the cell cycle would adjust to the chosen period of the nutrient cycle (Dawson, 1972). Thus, it was concluded that the doubling time could be controlled by changing the period of the forcing function. However, continuous phasing of bacterial cells for the production of biosurfactant led to washout conditions when the forcing function was imposed too early (Sheppard and Cooper, 1990). In this case however, the dissolved oxygen profile was monitored during the fermentation period. Then, the system was set up where the addition of nutrients was not initiated until an increase in the dissolved oxygen curve was observed; the increase was used to indicate that growth had ceased. Using this strategy, the washout condition was avoided. Ultimately, the cycle time was dictated by the metabolism of the organism and not a chosen interval of the forcing function.

2.3.3 Incorporation of a feedback control strategy

Accordingly, SCF incorporates a feedback control to the continuous phasing technique to have the cells determine the period of a cycle. The feedback control scheme uses a monitored transient parameter to signal the cessation of growth of the inoculated organism. Usually, the complete removal of a limiting nutrient in the medium is the condition that causes the cessation of growth in a fermentation process. Therefore, the critical value of the monitored control parameter is related to the complete removal of the essential substrate. Once the critical value is obtained, the cycling process is initiated beginning with the emptying step. If the fermenter is filled with fresh nutrients at the moment nutrient exhaustion is observed, the cycle period equals the doubling time of the organism (Brown, 2001).

Therefore, one of the main challenges for SCF operation is the identification of an appropriate control parameter to signal the metabolism of the cell population. Dissolved oxygen has been used as the control parameter in many applications of SCF (Brown and Cooper, 1991; Sheppard and Cooper, 1991; van Walsum and Cooper, 1993; Sarkis and Cooper, 1994; McCaffrey and Cooper, 1995; Wentworth and Cooper, 1996, Hughes and Cooper, 1996). For this parameter to be successful however, the organism must use oxygen as the terminal electron acceptor. Thus, this control scheme is inappropriate for anaerobic fermentations. In addition, a change in dissolved oxygen must be observable which necessitates the system to proceed under a slight oxygen limitation. This condition may not be optimal for cell growth. Finally, the dissolved oxygen signal can lose its accuracy for long fermentation periods as the probe is prone to fouling. An alternate

control parameter that has been incorporated successfully in a denitrifying system with *Pseudomonas denitrificans* is the carbon dioxide evolution rate (CER) (Brown, *et al.,* 1999). Furthermore, the first derivative of the CER (dCER) has been used as the control parameter to obtain stable SCF operation in cultures of *E. coli* (Sauvageau, *et al.,* 2010, Storms, *et al.,* 2012). It has been shown that the use of the dCER allowed the SCF system to bypass the limitations that arise from using dissolved oxygen in the feedback control scheme.

2.3.4 Synchronization of cells

An interesting outcome of the cycling process during SCF operation is the synchronization of the cell population. Equation 2.1 outlines the synchrony index (Blumenthal and Zahler, 1962) used to analyze the degree of synchrony in the cell population induced by SCF operation.

$$F = \frac{N_t}{N_0} - 2^{\frac{t}{g}} \qquad \text{Equation 2.1}$$

where F is the synchrony index, N_t is the number of cells at the end of a time interval, N_0 is the number of cells at the beginning of a time interval, t is the time interval, and g is the doubling time of a culture growing under normal conditions. Under SCF operation, N_t/N_0 should have a value of 2 for any given cycle, t is the time necessary for the cells to double and g equals the cycle time. F has a maximum value of 1 if the entire population is completely synchronized, while an F-value of 0 indicates random cell division, hence no synchrony. Significant synchrony is assumed when the synchrony index is greater than 0.6 (Blumenthal and Zahler, 1962; Lloyd, *et al.,* 1982; Sauvageau, *et al.,* 2010). Studies incorporating SCF operation involving yeast and bacteria have shown that synchrony was obtained within the cell population (Brown and Cooper, 1991; Sarkis and Cooper, 1994; McCaffrey and Cooper, 1995; Wentworth and Cooper, 1996, Sauvageau *et al.*, 2010).

The synchronizing effect of the SCF facilitates the study of cell physiology at a larger scale. In classical batch systems, the cell mass and cell number both undergo exponential growth which implies that the average cell has a non-changing mass (Madigan, *et al.,* 2009). In synchronized cultures however, the growth of the cell population mimics that of an individual cell where cell number remains relatively constant while the cell mass increases continuously. Ultimately, the bulk parameters measured during synchronized growth becomes indicative of the physiology of an individual cell.

2.3.5 Applications of the SCF

Aside from the study of cell physiology, SCF has been utilized for many applications which include the production of primary and secondary metabolites, production of bacteriophages, and degradation of pollutants. The production of emulsin, a growth-associated bio-emulsifier, was performed successfully under SCF operation (Brown and Cooper, 1991). For the formation of non-growth associated metabolites, the cycles were extended to allow for production during stationary phase (McCaffrey and Cooper, 1995; Wentworth and Cooper, 1996). In other cases, a secondary tank was used after the SCF fermenter to maximize production of secondary products while maintaining normal SCF operation (van Walsum and Cooper, 1993; Sauvageau and Cooper, 2012; Storms, *et al.,* 2012). The compounds produced during these experiments included citric acid (Wentworth and Cooper, 1996), sophorolipids (McCaffrey and Cooper, 1995), surfactin (Sheppard and Cooper, 1990, 1991, van Walsum and Cooper, 1993), the antibiotic tetracycline (Zenaitis and Cooper, 1994), recombinant protein in *E. coli* (Storms, *et al.,* 2012), and bacteriophages (Sauvageau and Cooper, 2010).

Some SCF studies have investigated the biodegradation a pollutant of interest, which acted as the limiting nutrient consumed by the cell population. Since the limiting nutrient was completely depleted at every cycle during SCF operation, higher levels of biodegradation at faster rates were achieved in SCF compared to batch cultures (Sarkis and Cooper, 1994; Hughes and Cooper, 1996). Some of the pollutants investigated in these SCF experiments include toluene, p-xylene (Brown, *et al.,* 2000), oxidized nitrogen (Brown, *et al.,* 1999), phenol (Hughes and Cooper, 1996), and benzoate, 4-metoxybenzilidine-4-n-butylaniline, and p-anisaldehyde (Sarkis and Cooper, 1994).

A complete review of the technology, hardware and applications of the SCF system is found in Brown (2001).

3. Hypothesis and Objectives

3.1 Hypothesis

Using self-cycling fermentation (SCF) will increase the specific productivity and yield of shikimic acid in *Saccharomyces cerevisiae* engineered to optimize the shikimate pathway. This study is a proof of concept aimed to show that the coupled strategy of synthetic biology and induced synchrony via SCF is a viable alternative to current methods in obtaining high-value chemical ingredients.

3.2 Objectives

Four main objectives were developed according to the hypothesis of this study. The first objective was to evaluate and quantify the increase in production of shikimic acid by the engineered yeast strain compared to the parent strain. The second objective was to characterize the growth and metabolite production of engineered yeast in preparation for SCF operation. The third objective was to implement SCF and assess its impact on the biomass and shikimic acid yields in cultures of engineered yeast. Finally, the last objective was to analyze the degree of synchrony attained within the population of engineered yeast due to the implementation of SCF operation.

4. Materials and Methods

4.1 Yeast Culture and Medium

The yeast used in this study were strains of *Saccharomyces cerevisiae* kindly provided by Prof. Vincent Martin from the Department of Biology at Concordia University in Montréal, Québec. The parent yeast strain was CEN.PK 113-1A Matα. The engineered strain, genetically modified to overproduce shikimic acid, was CEN.PK113 Matα ΔURA Δ*aro3* Δ*aro4* with plasmid pYES *ura3*-[*ARO4fbr* + *AROB* + *AROD*] inserted; this strain was based on CEN.PK 113-13D. The engineered strain is a haploid of mating type α with deletions of the *ARO3* and *ARO4* gene, and the gene encoding for uracil. The pYES heterologous expression plasmid contains the gene encoding for uracil which acts as an auxotrophic selection marker (Invitrogen, 2009). The *ARO4fbr* gene encodes for the feedback insensitive version of the enzyme DAHP synthase (Draths, *et al.,* 1999). The *AROB* and *AROD* gene, derived from *E. coli,* encodes for the enzymes DHQ synthase and DHQ dehydratase, respectively (Dell and Frost, 1993). Figure 4.1 shows the genetic modifications performed on the shikimic acid pathway of the engineered strain.

The medium used was yeast nitrogen base (YNB) with $(NH_4)_2SO_4$ without amino acids (Sigma Aldrich, St. Louis, MO) at a concentration of 6.7 $g \cdot L^{-1}$ in deionized water (MilliQ, Millipore). The components of YNB without amino acids is described in Table A1 in Appendix A. Glucose (Fisher Scientific, Fair Lawn, NJ) was used as a carbon source at a concentration of 20 $g \cdot L^{-1}$ in inoculum cultures, shake flask experiments, 1-L fermenter experiments, and SCF experiments; a 200 $g \cdot L^{-1}$ stock solution of glucose was prepared and autoclaved separately from the YNB medium. Subsequently, the appropriate volume was added to the medium to achieve the desired final glucose concentration. When anhydrous ethyl alcohol (Commercial Alcohol, Brampton, ON) was tested as a carbon source, a concentration of 2% v/v in the medium was used.

For cryopreservation, yeast extract peptone dextrose (YPD) medium containing 10 $g \cdot L^{-1}$ of yeast extract (BD Bacto ™, Sparks, MD) and 20 $g \cdot L^{-1}$ of peptone (BD Bacto ™, Sparks, MD) in deionized water was used. Glucose was added to obtain a final concentration of 20 $g \cdot L^{-1}$. A 30% glycerol (Fisher Scientific, Fair Lawn, NJ) stock solution was prepared separately and added to achieve a final glycerol concentration of 15% in the medium. Initial cell banks were preserved at -80°C. Working cell banks were prepared from the initial cell bank and stored at -20°C.

Agar plates for the parent yeast strain were prepared by adding agar technical (BD Difco™, Sparks, MD) in YPD medium to a concentration of 15 g·L^{-1}. After addition of glucose, hard agar was poured immediately into petri dishes. Similarly, agar plates for the engineered yeast strain were prepared by adding 15 g·L^{-1} of agar technical and 1.92 g·L^{-1} of yeast synthetic drop-out media supplement (Sigma Aldrich, St. Louis, MO). The yeast synthetic drop-out media supplement used did not contain the amino acid Uracil; the composition of the synthetic drop-out media supplement is shown in Table A2 in Appendix A.

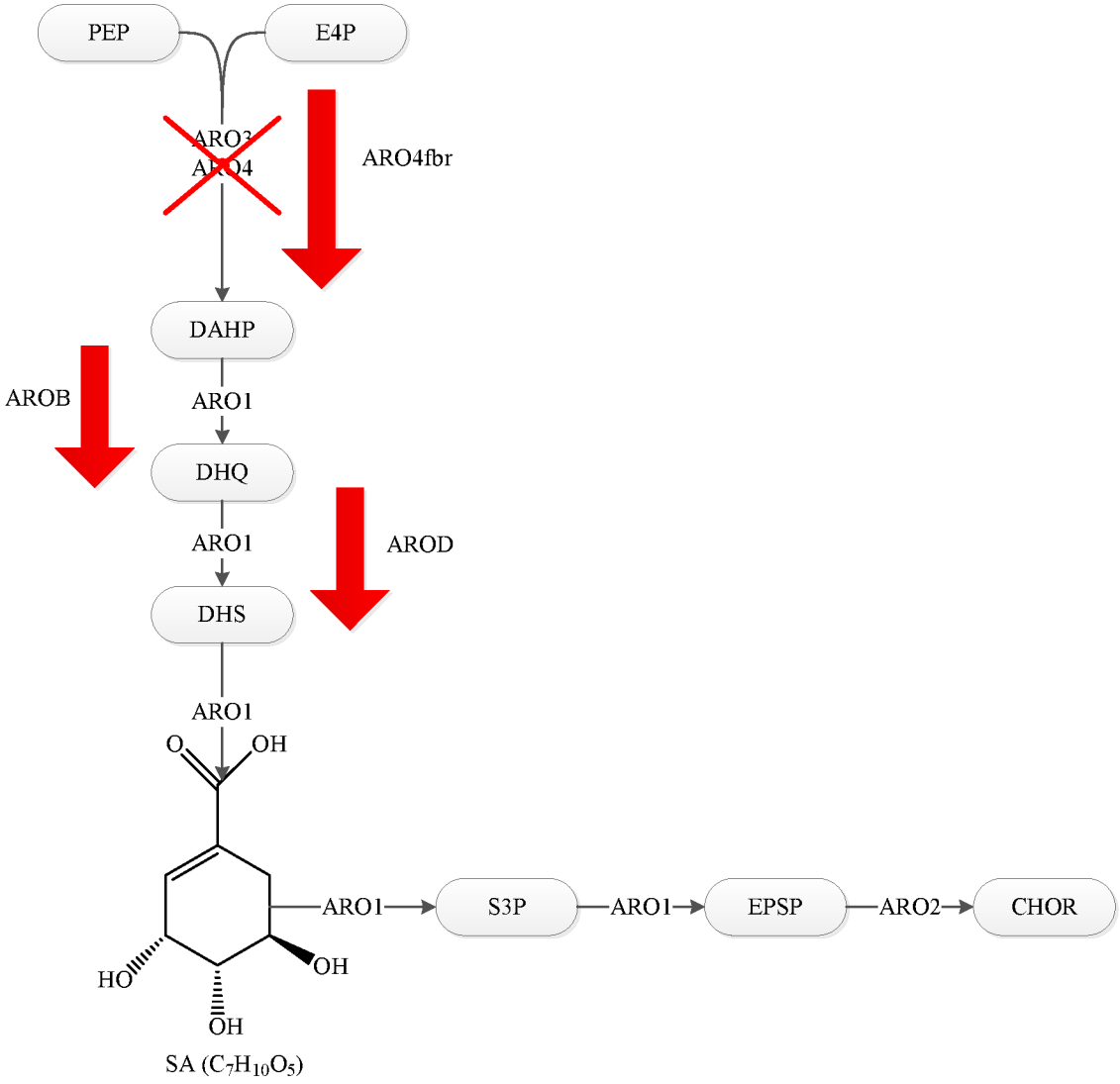

Figure 4.1 Genetic modifications performed on the shikimic acid pathway of *S. cerevisiae*.

4.2 OD_{600} and cell density measurements

Cell density was quantified 1) using a spectrophotometer (Ultrospec 50, Biochrom, Cambridge, UK) to measure the optical density of a 1-mL sample at a wavelength of 600nm and/or 2) by microscopy using a Petroff-Hausser counting chamber (Hausser Scientific, Horsham PA). For OD_{600} measurements, cell samples were diluted ten times in YNB medium with 2% glucose. For microscopy, cell samples were diluted five times in 0.2 mM disodium EDTA (Fisher Scientific, Fair Lawn, NJ). A 0.5M EDTA stock solution pH 8.0 was prepared. The pH was adjusted using sodium hydroxide (Fisher Scientific, Fair Lawn, NJ). Subsequently, the cells were viewed under a light microscope (Leica Mycrosystems, DMRXA2, Heerbrugg, Switzerland) equipped with a digital camera (QImaging, Retiga EX, Surrey, BC). Five measurements were taken for every sample. The cells were counted using the software ImageJ (open-sourced software from the NIH) and converted to cell density with units of cells·mL^{-1}.

The maximum replication rate and doubling time was determined during the linear portion of exponential growth on glucose. These were calculated using Equation 4.1 and 4.2, respectively (Shuler and Kargi, 2002).

$$\mu = \frac{\ln(N_2) - \ln(N_1)}{\Delta t} \qquad \text{Equation 4.1}$$

$$\tau'_d = \frac{\ln(2)}{\mu} \qquad \text{Equation 4.2}$$

where μ is the replication rate (h^{-1}), N_i is the cell number at time *i* (cell·mL^{-1}), t is the time in (h), and τ'_d is the doubling time with respect to cell number (h).

4.3 Measurement of shikimic acid concentration

1-mL samples from culture broths were transferred into a microcentrifuge tube and centrifuged (Eppendorf 5424R, rotor Eppendorf FA-45-24-11, Hamburg, Germany) for 2 minutes at 19,000×g and 22°C. The samples were then filtered using a 0.2 μm syringe filter (Fisher Scientific, Windsor, ON) and transferred into chromatography vials. The shikimic acid concentration was measured by high performance liquid chromatography (HPLC) (Agilent Technologies 1200 series). The column used was an Aminex HPX-87H organic acids analysis column (300 × 7.8mm I.D.; 9 μm particle diameter, Bio-Rad Labs, Watford, U.K.) with a guard

column, heated to a temperature of 60°C by a column heater (Bio-Rad Labs, Watford, U.K.). A mobile phase of 5 mM sulphuric acid (pH 2.2-2.3, Fisher Scientific, Fair Lawn, NJ) was eluted at a flow rate of 0.5 mL/min with a quaternary pump (G1311A). The column eluate was monitored at 215 nm using a UV detector (DAD, G1315D). The sample injection volume for measurement was 10 μL.

A standard calibration curve of pure shikimic acid (Sigma Aldrich, St. Louis, MO) was generated to convert the data obtained from HPLC into shikimic acid concentrations, as shown in Figure B1 in Appendix B.

4.4 Measurement of glucose and ethanol concentration

The same samples used for shikimic acid concentration measurements were quantified for its glucose and ethanol content. The glucose and ethanol concentration was measured by HPLC (Agilent Technologies 1200 series). The column used was a SupelcoGel PB carbohydrate column (300 mm length, 7.8 mm I.D., Sigma Aldrich, Bellefonte, PA) with a guard column at a temperature of 70°C. A mobile phase of sterile deionized water was eluted at a flow rate of 0.5 mL/min with a bin pump (G1312A). The column eluate was monitored with a refractive index detector - RID (G1362A). The sample injection volume for measurement was 10 μL.

A standard calibration curve was generated to convert the data obtained from HPLC into glucose and ethanol concentrations, as shown in Figure B2 and B3, respectively, in Appendix B.

4.5 Shake flasks

Cell cultures were grown in 125-mL shake flasks containing 25-mL of medium. Inoculation was performed as indicated in section 4.7 below. Cultures were then incubated at 30°C and 150 rpm in an incubator shaker (Infors HT, Ecotron, Bottmingen, Switzerland). Samples were taken periodically to measure growth or glucose, ethanol and shikimic acid concentrations.

4.6 Fermenter

Figure 4.2 shows a schematic diagram of the experimental fermenter setup. A custom-made, stainless steel fermenter (2 L, 10.5 cm I.D.) was used for both batch and SCF experiments. The agitation (250 rpm) was provided by a Rushton impeller (4 cm diameter) connected to a motor

(Fisher Scientific, Fair Lawns, NJ). The aeration rate was maintained at 845 std. $mL \cdot min^{-1}$ by a regulator combined to a gas rotameter (Cole Parmer, Chicago, IL). The rotameter calibration data is shown in Figure B4 in Appendix B. Air was delivered into the fermenter after passing through sterile deionized water and an in-line HEPA filter. The air exiting the fermenter passed through a glass condenser and an in-line HEPA filter. An IR-spectrometry CO_2 gas sensor (CO_2-BTA, Vernier) was positioned after the filter. The CO_2 measurements, representing the CER, were used as the cycling parameter for the SCF feedback control loop. The temperature was monitored by a K-type thermocouple (Model GKQSS-18G-10, Omega, Laval, QC) placed in a thermo-well. The fermenter temperature was maintained at $30^{\circ}C$ by a feedback control loop utilizing a 300 W heater (Model CIR-1032/120V, Omega, Laval, QC) in conjunction with the thermocouple.

In SCF experiments, two electro-optic level sensors (ELS-900 series, Gems Sensors, Plainville, CT) acted as the low and high level sensors and were placed at 0.5 L and 1 L of the working volume, respectively. These were used to control liquid volumes during the emptying and filling steps between cycles. A pump (Model 77201-60, Cole Parmer, Chicago, IL) was used to supply fresh sterile medium into the fermenter from a carboy containing 10 L of sterile medium and a stir bar (3" length, 0.5" diameter) placed on a 9" by 9" magnetic stirrer (Model 4815, Cole Parmer, Chicago, IL). A glass isolator was placed between the pump and the fermenter to avoid contamination of the fresh medium carboy. Two solenoid valves (Model SV125, Omega, Laval, QC) were used to facilitate the emptying and filling steps between cycles. The first was placed between the pump and the fermenter while the second was placed at the liquid outlet of the fermenter. A second glass isolator and a carboy were placed downstream from the second valve to collect the fermenter contents. A sampling port was used to take samples for cell counts, OD_{600}, and extracellular metabolite concentrations. The motor, the heater, the valves, the pump, and all sensors were connected to a computer via an OPTO 22 data acquisition board, which converted analog signals into digital ones. The unit was automated using a control scheme developed in LabView®. In addition, all obtained data was recorded through LabView®.

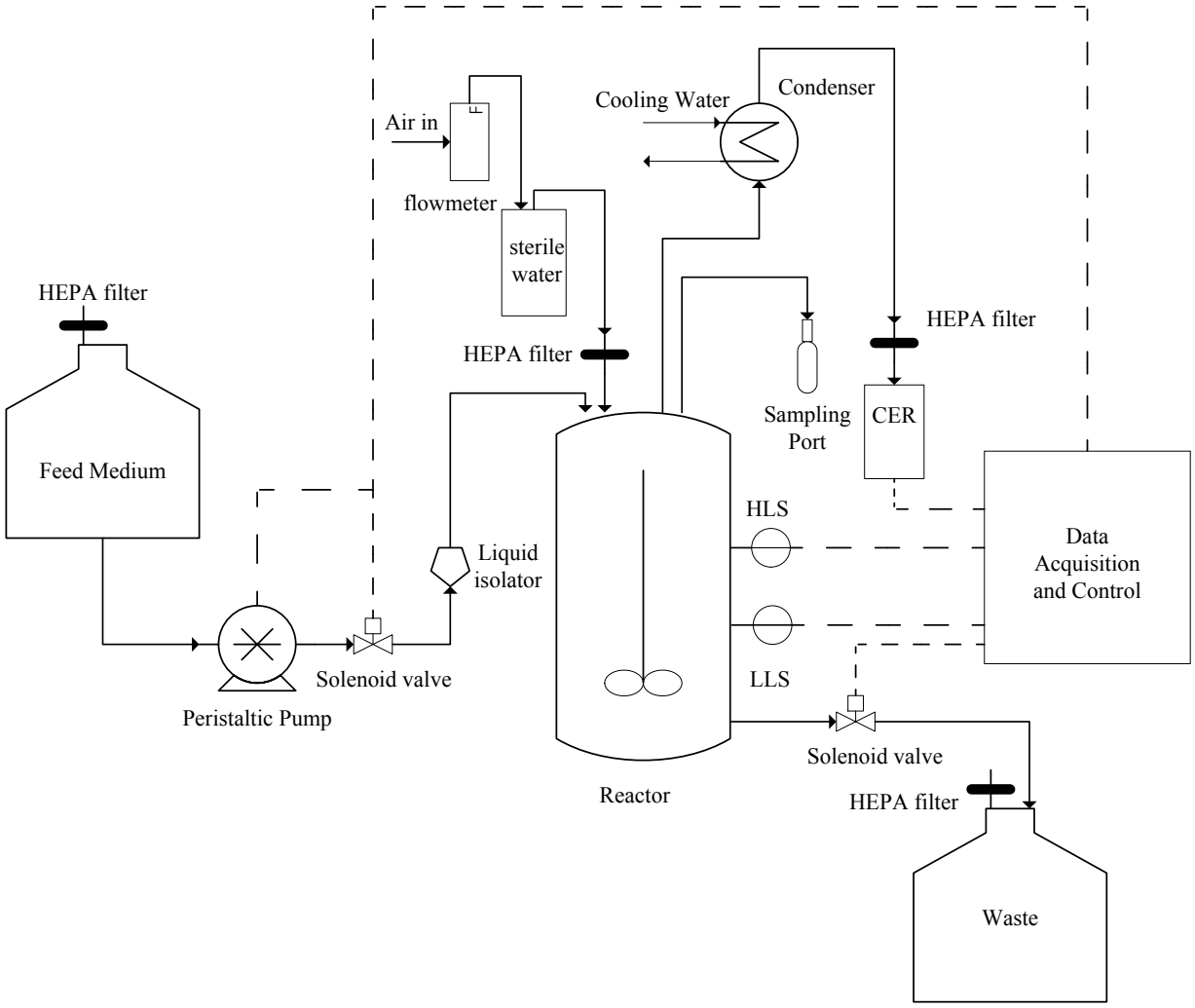

Figure 4.2 Schematic of the self-cycling fermentation setup. The motor connected to the Rushton impeller, and the temperature control loop are not shown. The high and low level sensors are used to control the pump and solenoid valves. The carbon dioxide sensor measures the CER and serves as feedback control parameter for cycling.

4.7 Inoculation loads

Shake flasks were inoculated either from working cell banks stored in -20°C or from agar plates stored in 4°C. For the former, 50 µL of cells were placed in a 125-mL shake flask containing 25-mL fresh medium. For the latter, three distinct colonies were taken and placed in a shake flask containing fresh medium. For both cases, the shake flasks were incubated for 48 hours before

transferring into another shake flask with fresh medium. After another 48 hours (corresponding to an OD_{600} of approximately 4.5-6), a 1% by volume inoculum was used to initiate batch or SCF experiments. Figure B5 and B6 in Appendix B show correlation curves between cell count and OD_{600} for growing cultures of the parent and engineered strain in shake flasks, respectively.

4.8 Carbon dioxide evolution rate (CER)

The observed CER was determined as the appropriate parameter to control the cycling condition for the SCF experiments. It was measured as the rate of CO_2 leaving the fermenter in the outlet stream. The observed CER was monitored by an IR-spectrometry CO_2 gas sensor which delivered data in units of ppm. Equation 4.3 provides the conversion from ppm to standard SI units of mol $CO_2 \cdot L^{-1} \cdot h^{-1}$; it assumes ideal gas behaviour.

$$CER = \frac{P}{RTV}\dot{Q}\left(CO_{2_{out}} - CO_{2_{air}}\right) \qquad \text{Equation 4.3}$$

where P is the atmospheric pressure (atm), R is the ideal gas constant ($atm \cdot L \cdot mol^{-1} \cdot K^{-1}$), T is the temperature of the air at the outlet (K), V is the working liquid volume of the fermenter (L), $\dot{Q}$ is the air volumetric flow rate ($L \cdot h^{-1}$), $CO_{2_{out}}$ is the value given the by CO_2 gas sensor (ppm), and $CO_{2_{air}}$ is the CO_2 concentration of the inlet air (ppm). The value of CER was recorded every 15 seconds.

The rate of change of CER (dCER) was calculated via a program in LabView® as developed and outlined by Sauvageau, *et al.* (2010). In this scheme, a linear regression is fit on the CER data collected in the previous 7 minutes, which represented the slope of the CER. This value was calculated and recorded every 15 seconds. The dCER had units of $mol \cdot L^{-1} \cdot h^{-2}$.

4.9 SCF operation

The first cycle of the SCF was initiated as a normal batch process with an inoculum size as outlined in section 5.7. When the cycling conditions – see Figure B7 in Appendix B for a schematic of the cycling conditions programmed in LabView® – were met, the emptying step was initiated. When emptying, the motor was turned off and the outlet valve was activated to facilitate the drainage to half of the fermenter liquid volume (0.5 L). Upon reaching half the original liquid volume, the low level sensor was activated which shut off the outlet valve. Then, the inlet valve

and pump were simultaneously activated which provided fresh medium into the fermenter until the original working volume of 1 L was attained, as signalled by the high level sensor. The activation of the high level sensor turned off the pump. After a 25 second time delay from the time the pump was shut off, the inlet valve was deactivated and the motor was turned on. This cycling operation was repeated for all cycles during SCF operation. The cycle time was defined as the period between the beginning of the filling step and the end of the emptying step.

In-cycle sampling was performed through the sample port to perform various measurements (OD600, cell counts, metabolite concentrations, pH). pH analysis was performed using a pH electrode (Fischer Scientific Accumet® 13-620-285) combined to a pH meter (Denver Instrument Ultrabasic benchtop 222691, Sartorius Corporation).

To analyze the growth and metabolite production of cells at the end of a cycle, the fermenter contents were collected into a sterile medium bottle during the emptying step. To follow the growth and production in extended cultures, 25 mL of the discharged fermenter contents were transferred into 125-mL shake flasks and incubated as outlined in section 5.5.

4.10 Plasmid retention

Triplicate non-selective YPD and selective YNB plates were prepared, as outlined in section 4.1. A culture of the engineered strain was inoculated in a shake flask, as outlined in section 4.7. After the culture was fully-grown, 100-µL samples were serially diluted in 900 µL of medium. This was repeated until a dilution factor of 10^8 was achieved. 10 µL from each dilution factor were then placed on YPD and YNB plates and let dry. Plates were stored at room temperature for 48 hours. Colony forming units were counted and compared between the selective and non-selective plate.

4.11 Impact of shikimic acid on engineered yeast strain

To analyze the effect of the presence of shikimic acid on a growing culture of the engineered strain, YNB liquid medium containing varying concentrations of shikimic acid (0.07 $g \cdot L^{-1}$, 0.30 $g \cdot L^{-1}$, and 0.90 $g \cdot L^{-1}$) was prepared in shake flasks prior to inoculation. Cultures were inoculated and grown for 96 hours at 30°C and 150 rpm. Metabolite concentration measurements were performed at the end of growth. A control shake flask without shikimic acid was prepared for comparison.

5. Results

5.1 Batch growth of yeast

In order to evaluate the effectiveness of genetically modified yeast to overproduce shikimic acid, the parent and engineered yeast strain were grown in batch cultures.

5.1.1 Biomass growth

The aerobic growth of parent and engineered yeast on glucose in YNB medium is shown in Figure 5.1. The figure shows that the parent strain reached an optical density of approximately 9, which corresponds to a cell concentration of 1.0×10^{8} cells·mL^{-1}; this is higher than the engineered strain, which reached an optical density of approximately 7.5, corresponding to a cell concentration of 9.0×10^{7} cells·mL^{-1}. The growth for both strains progressed steadily until approximately 24 h of fermentation, signalling the end of the exponential phase of growth. Then, the optical density continued to slowly increase thereafter. The time period of 6-15 hours was used to estimate the maximum replication rate (Equation 4.1) and doubling time (Equation 4.2) for both strains due to the linear nature of this time frame. The maximum replication rates for the parent and engineered strain were 0.360 h^{-1} and 0.337 h^{-1}, respectively. These correspond to doubling times of 1.93 h and 2.06 h, respectively.

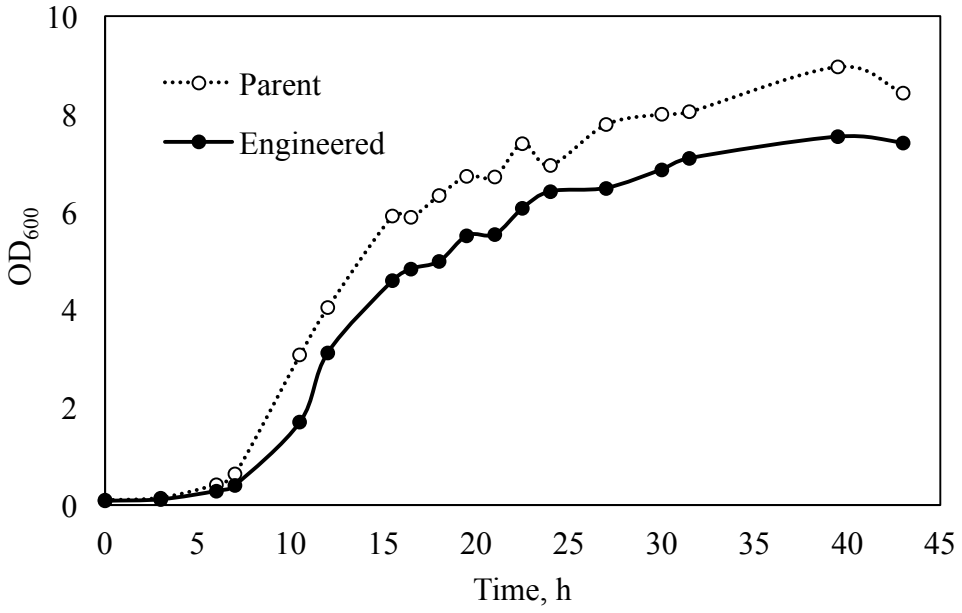

Figure 5.1 Growth of parent and engineered *S. cerevisiae* in YNB medium for 43 h.

5.1.2 Measurement of plasmid retention

Figure 5.2 illustrates the growth of the engineered strain on complex YPD and selective YNB agar plates. Should cells not retain the plasmid enabling the production of amino acids during growth, the number of cells growing on YNB plates would be expected to be significantly lower than those growing on YPD plates. As can be seen in Figure 5.2, the average number of colony forming units for the selective plate is slightly lower but within error of the non-selective plate. This suggests that there is no difference in proliferation of cell growth between each condition and confirms the plasmid retention in the engineered strain.

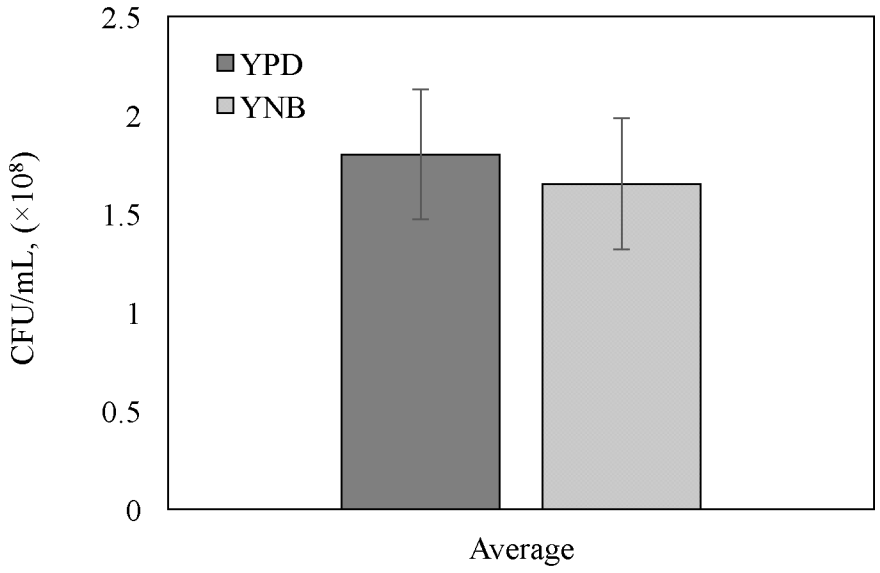

Figure 5.2 Growth of engineered *S. cerevisiae* on complex YPD and selective YNB agar plates after being cultured in YNB medium in shake flasks for 48 h.

5.1.3 Shikimic acid production

The aerobic growth of parent and engineered yeast strains in YNB medium for 73 h in shake flasks is presented in Figure 5.3. The optical density for the parent strain is slightly higher than that of the engineered strain. However, these values are within error of each other for the 16, 18, and 73 hour time points. In addition, a similar trend is observed here as in Figure 5.1: a sharp increase in optical density followed by a slower continued increase for both strains.

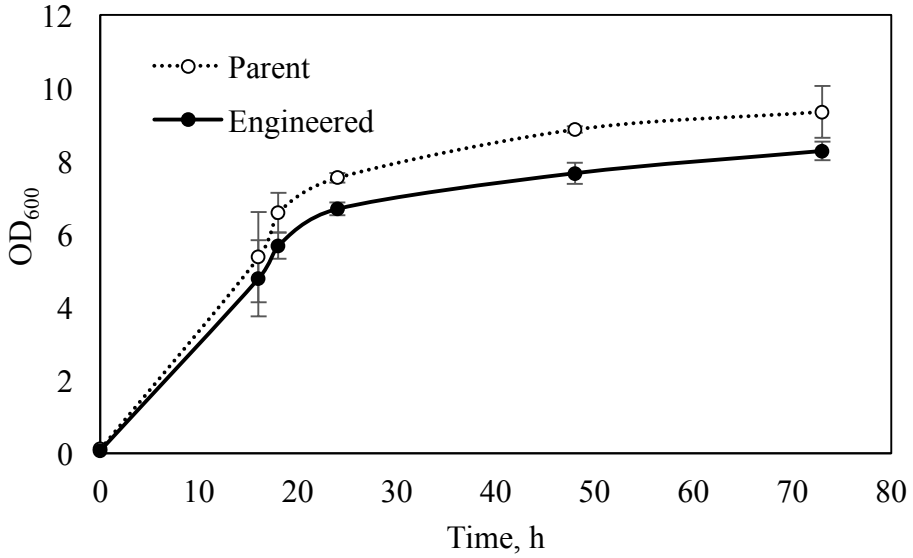

Figure 5.3 Growth of parent and engineered *S. cerevisiae* in YNB medium for 73 h.

Figure 5.4 shows the shikimic acid production of the parent and engineered yeast strain in YNB medium for 73 h. It shows that, for the parent strain, no shikimic acid is produced for the entire duration of fermentation. For the engineered strain, an average shikimic acid concertation of 0.13 $g \cdot L^{-1} \pm 0.018$ was obtained after 24 h, corresponding to the end of the exponential phase of growth. After 73 h, the shikimic acid concentration more than doubled to a value of 0.32 $g \cdot L^{-1} \pm 0.064$. To further the investigation, Figure 5.5 and Figure 5.6 illustrate the growth, shikimic acid production and glucose utilization of the engineered strain in YNB medium for 73 and 192 h, respectively. As can be seen in Figure 5.5, glucose, the primary carbon source, was almost completely utilized after 24 h of fermentation yet shikimic acid production continued throughout the stationary phase of growth. In addition, the increase in biomass slowed at 24 h but continued to slowly increase thereafter. Figure 5.6 shows that glucose was almost completely depleted after 24 h of growth; a shikimic acid concentration of 0.12 $g \cdot L^{-1}$ was obtained at this time. Again, biomass continued to increase slowly after 24 h. Furthermore, the shikimic acid concentration doubled to 0.20 $g \cdot L^{-1}$ at 47 h, and increased four-fold to 0.38 $g \cdot L^{-1}$ after 100 h. After this point, the shikimic acid concentration plateaued.

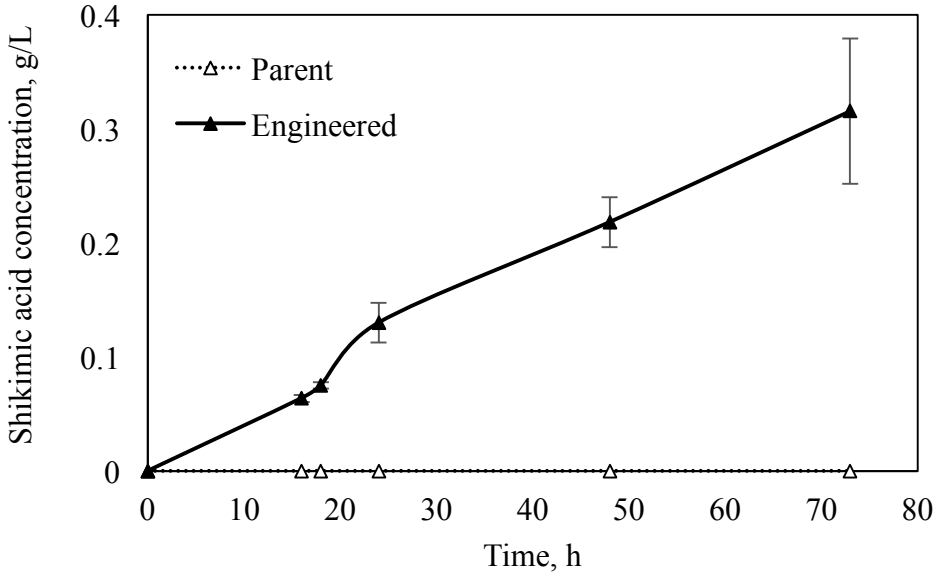

Figure 5.4 Shikimic acid production of parent and engineered *S. cerevisiae*.

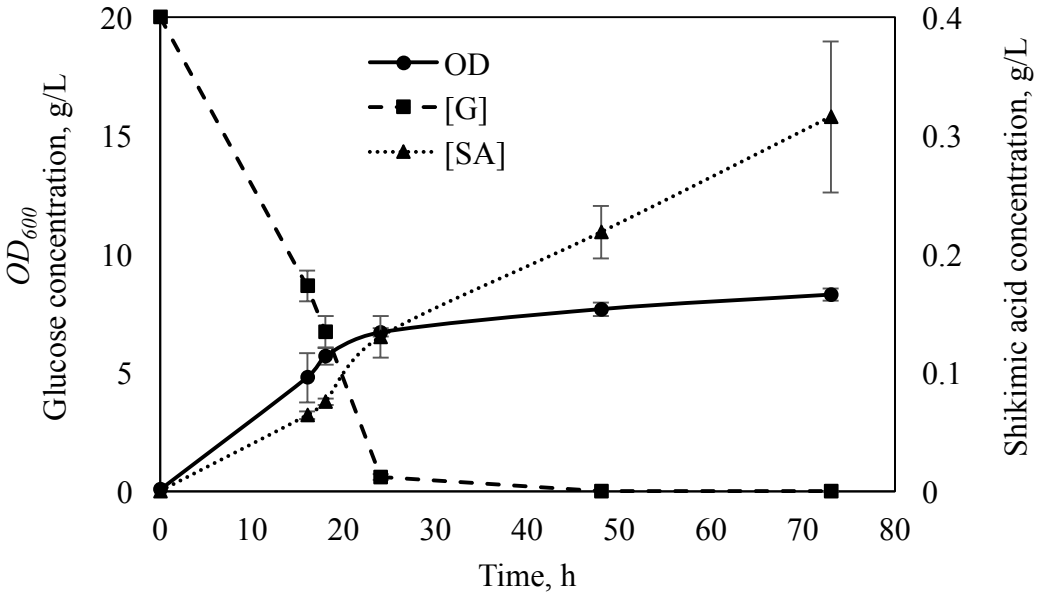

Figure 5.5 Growth (OD), shikimic acid production ([SA]), and glucose consumption ([G]) of the engineered *S. cerevisiae* cultured for 73 h.

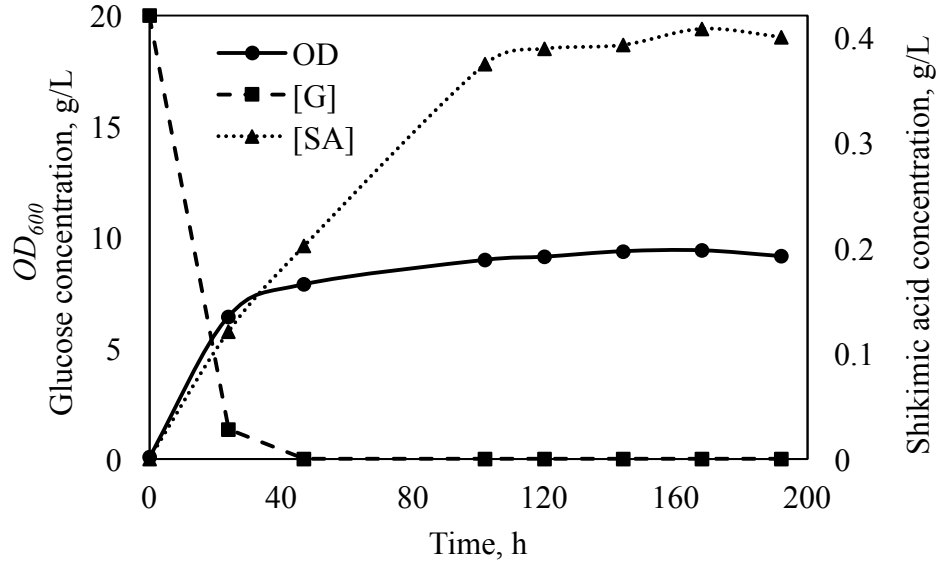

Figure 5.6 Growth (OD), shikimic acid production ([SA]) and glucose consumption ([G]) of the engineered *S. cerevisiae* cultured for 192 h.

5.1.4 Ethanol production

The growth, glucose consumption, and the production of shikimic acid and ethanol of the engineered strain in YNB medium is shown in Figure 5.7. Again, glucose was mostly depleted at approximately 25 h of growth. At this point, the shikimic acid concentration had reached 0.14 $g \cdot L^{-1}$ while the ethanol concentration peaked at approximately 0.74 v/v%. After 25 h, the ethanol concentration began to decrease until 96 h where it was completely depleted. In the period between 25 h and 96 h, the increase in optical density slowed down but continued to rise, indicative of diauxic growth between glucose and ethanol. Similarly, shikimic acid concentration continued to rise until 96 h of fermentation before stabilizing. A final shikimic acid concentration of approximately 0.58 $g \cdot L^{-1}$ was achieved.

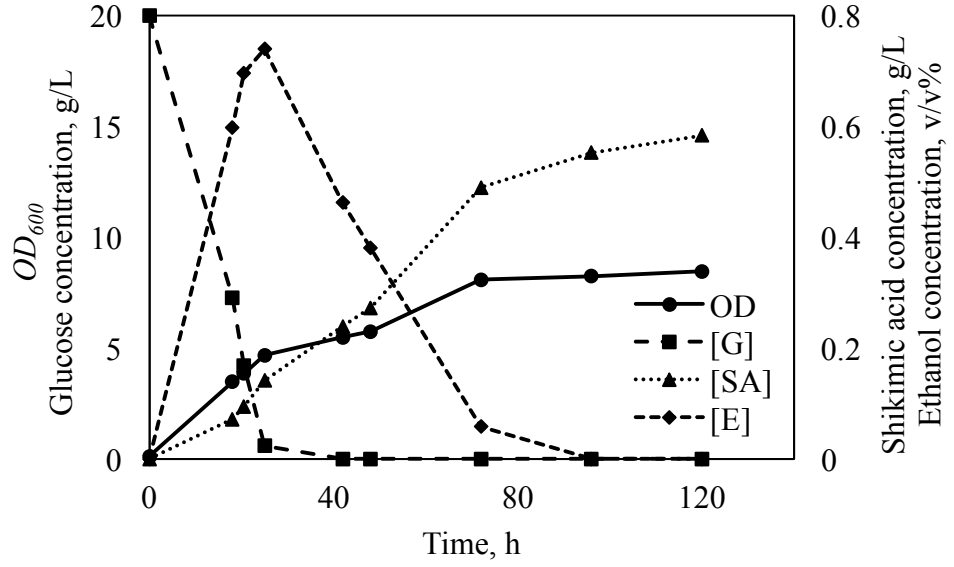

Figure 5.7 Growth (OD), glucose consumption ([G]), shikimic acid ([SA]) and ethanol ([E]) production of the engineered *S. cerevisiae* cultured for 120 h.

Figure 5.8 illustrates the glucose, ethanol and shikimic acid concentrations found in Figure 5.7 but converted to moles of carbon. From inoculation to the end of the first exponential phase (25 h of growth), approximately 0.67 moles of carbon from glucose was used to produce 0.25 moles of carbon of ethanol and 0.0057 moles of carbon of shikimic acid. During the slower, second exponential phase (between 25 and 96 h), approximately 0.016 moles of carbon of shikimic acid was produced from the produced ethanol to obtain a final concentration of approximately 0.022 moles of carbon of shikimic acid.

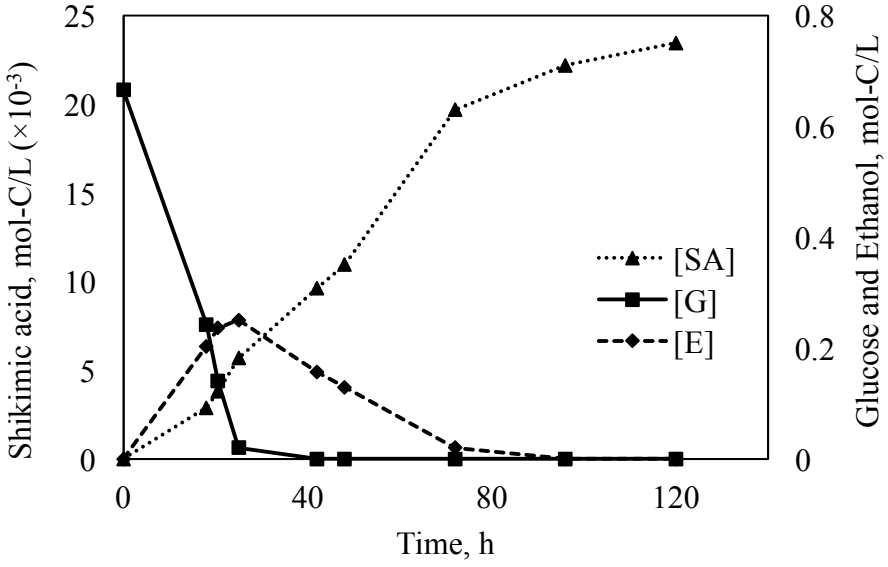

Figure 5.8 Glucose ([G]), ethanol ([E]) and shikimic acid ([SA]) concentrations in moles of carbon during the growth of the engineered *S. cerevisiae* cultured for 120 h.

5.1.5 Ethanol as a carbon source

The glucose, ethanol, and shikimic acid concentrations in moles of carbon during the growth of the engineered strain using glucose (A) or ethanol (B) as the primary carbon source is presented in Figure 5.9. Figure 5.9B illustrates that when ethanol is the primary carbon source, approximately 0.67 moles of carbon of ethanol was consumed after 72 h of culture to produce 0.016 moles of carbon of shikimic acid. This corresponds to a yield of 0.024 moles of carbon of shikimic acid per mol of carbon of ethanol. Shikimic acid production did not begin until after 25 h of growth despite the decrease in the concentration of moles of carbon in ethanol by approximately 0.30 moles of carbon. After 72 h, shikimic acid production stabilized at approximately 0.017 moles of carbon of shikimic acid. This value is 25% lower than the final shikimic acid concentration reached when glucose is the primary carbon source.

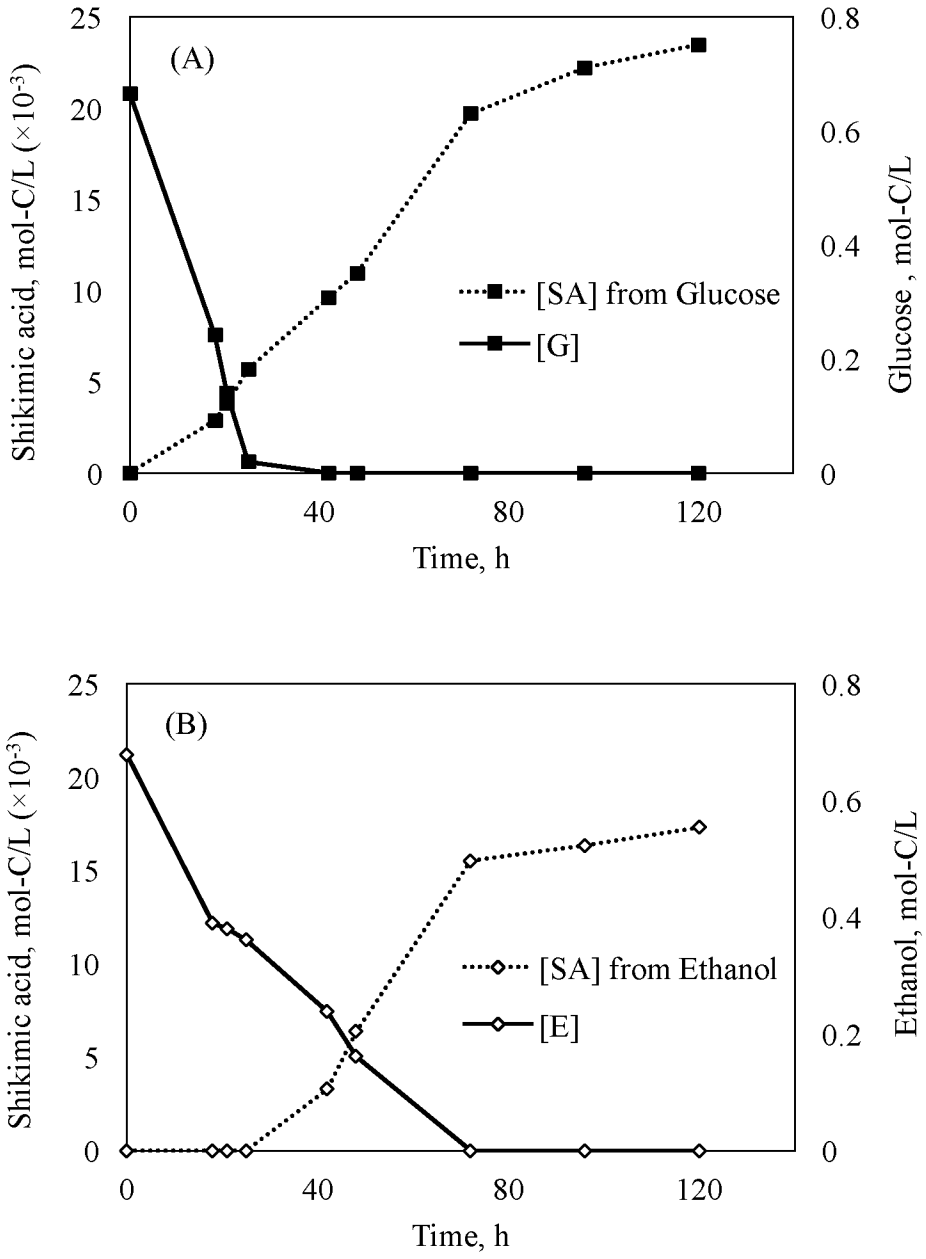

Figure 5.9 Glucose ([G]) and ethanol ([E]) consumption, and shikimic acid ([SA]) production in moles of carbon of the engineered *S. cerevisiae* cultured for 120 h using glucose (A) or ethanol (B) as the primary carbon source.

5.2 Characterization of engineered yeast

In order to prepare for SCF operation, the engineered yeast was characterized based on biomass growth, carbon-source consumption, carbon dioxide evolution rate (CER), and shikimic

acid production, selectivity, yield, and productivity in a 1-L batch fermenter. This is done to choose the most suitable time point to initiate cycling and the appropriate feedback control parameter for a stable SCF operation while maximizing shikimic acid productivity.

5.2.1 Biomass growth

The growth, glucose consumption, and ethanol and shikimic acid production of the engineered yeast strain in YNB medium were monitored for 160 h in a 1-L batch fermenter (Figure 5.10). The growth, carbon source utilization, and metabolite production profiles shown in Figure 5.10 are similar to those observed during growth of the engineered strain in shake flasks (see Figure 5.7). At the onset of stationary phase (21 h of growth), the optical density reached a value of 5.2 which corresponds to a cell concentration of 7.0×10^7 cells·mL^{-1}. At this time, the ethanol concentration was at its peak of 0.71 v/v%. In addition, the shikimic acid concentration reached 0.08 g·L^{-1}. These values were comparable to concentrations obtained in shake flask experiments at the same time point. However, after 160 h, the maximum optical density observed was lower, at approximately 6.4, which corresponds to a cell concentration of 8.0×10^7 cells·mL^{-1}. Furthermore, the peak shikimic acid concentration obtained was significantly reduced at 0.18 g·L^{-1}.

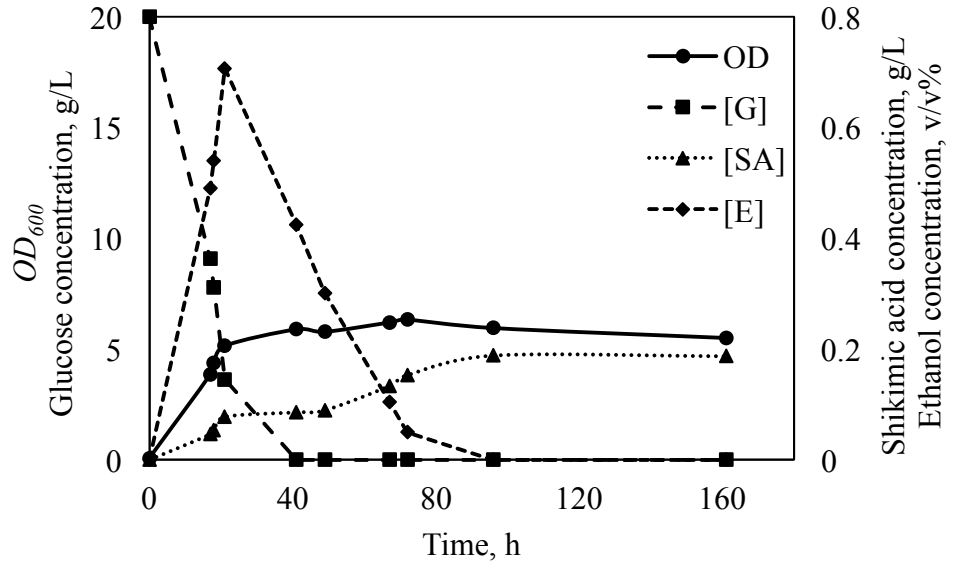

Figure 5.10 Growth (OD), glucose consumption ([G]), and ethanol ([E]) and shikimic acid ([SA]) production of the engineered *S. cerevisiae* in a 1-L batch fermenter.

5.2.2 Carbon-source consumption

Figure 5.11 presents the glucose, ethanol, and shikimic acid concentrations shown in Figure 5.10 but converted to moles of carbon. At 21 h of growth, approximately 0.54 moles of carbon of glucose was consumed to produce 0.23 moles of carbon of ethanol and 0.0031 moles of carbon of shikimic acid. After 96 h of growth, ethanol was fully consumed to produce 0.0076 moles of carbon of shikimic acid.

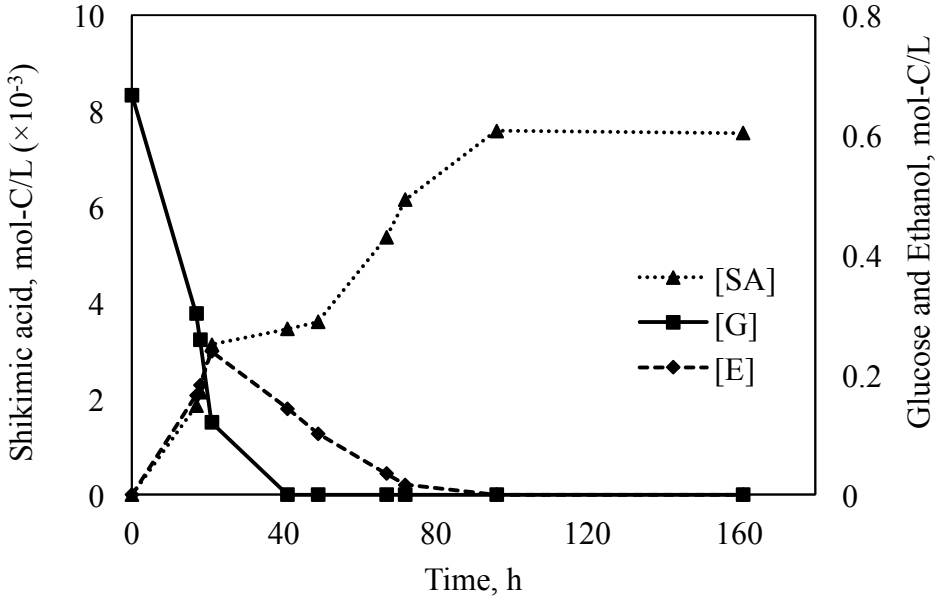

Figure 5.11 Glucose ([G]), ethanol ([E]) and shikimic acid ([SA]) concentrations in moles of carbon during the growth of the engineered *S. cerevisiae* in a 1-L batch fermenter.

5.2.3 Shikimic acid production: yield, selectivity, and productivity

The overall and instantaneous selectivity of shikimic acid over cell number and ethanol is shown in Figures 5.12 and 5.13, respectively. The overall selectivity over cell number is defined as the ratio between the total moles of shikimic acid produced per cell concentration as given by the correlation between OD_{600} and cell count found in Figure B6 of Appendix B. The overall selectivity over ethanol is given as the ratio of total moles of shikimic acid produced per mole of ethanol produced. The instantaneous selectivity over cell number is defined as the absolute value of the ratio of rate of formation of shikimic acid in moles per rate of change of cell concentration. Similarly, the instantaneous selectivity over ethanol is defined as the ratio of rate of formation of

shikimic acid in moles per rate of formation of ethanol in moles. The overall and instantaneous selectivity over ethanol curve stops at hour 21 because ethanol started to get consumed at this point, leading to negative values of instantaneous selectivity. Figure 5.12 shows that the overall selectivity over both cell number and ethanol increased slightly during the period of glucose consumption. During ethanol consumption, the overall selectivity over cell number did not increase until approximately 49 h of growth and it plateaued after 96 h of growth, corresponding to ethanol depletion. Similarly, Figure 5.13 shows that the instantaneous selectivity increased slightly during glucose consumption where a maximum was reached once glucose was almost completely depleted. During ethanol consumption, the instantaneous selectivity over cell number increased significantly where a maximum was reached at a time point between 67 and 72 h of growth.

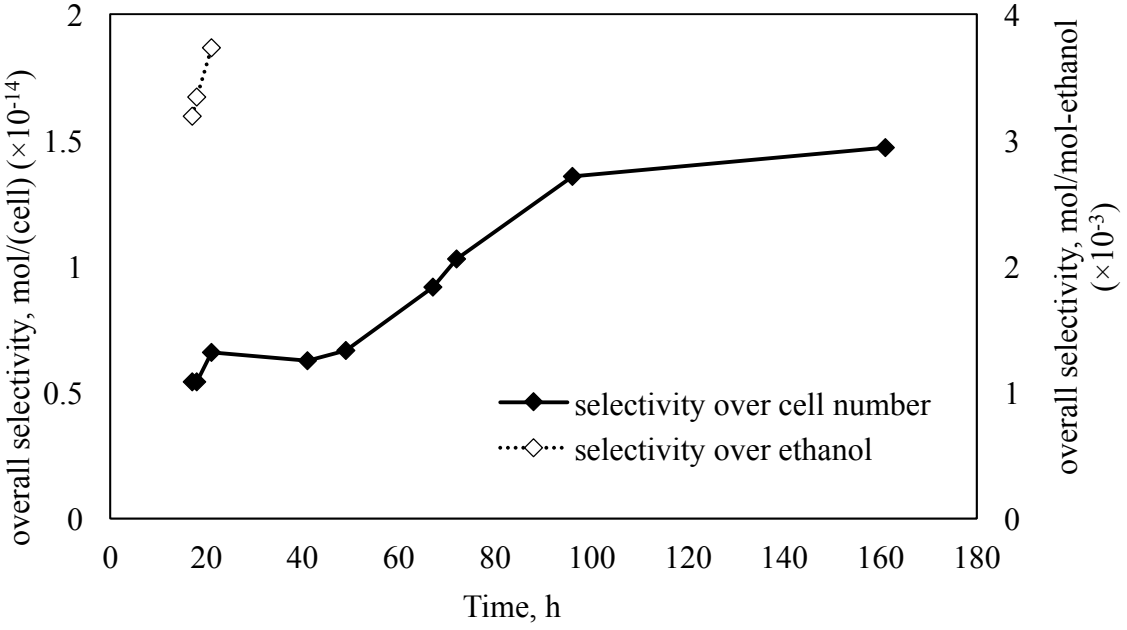

Figure 5.12 Overall selectivity of shikimic acid over cell number and ethanol during batch growth in a 1-L batch fermenter.

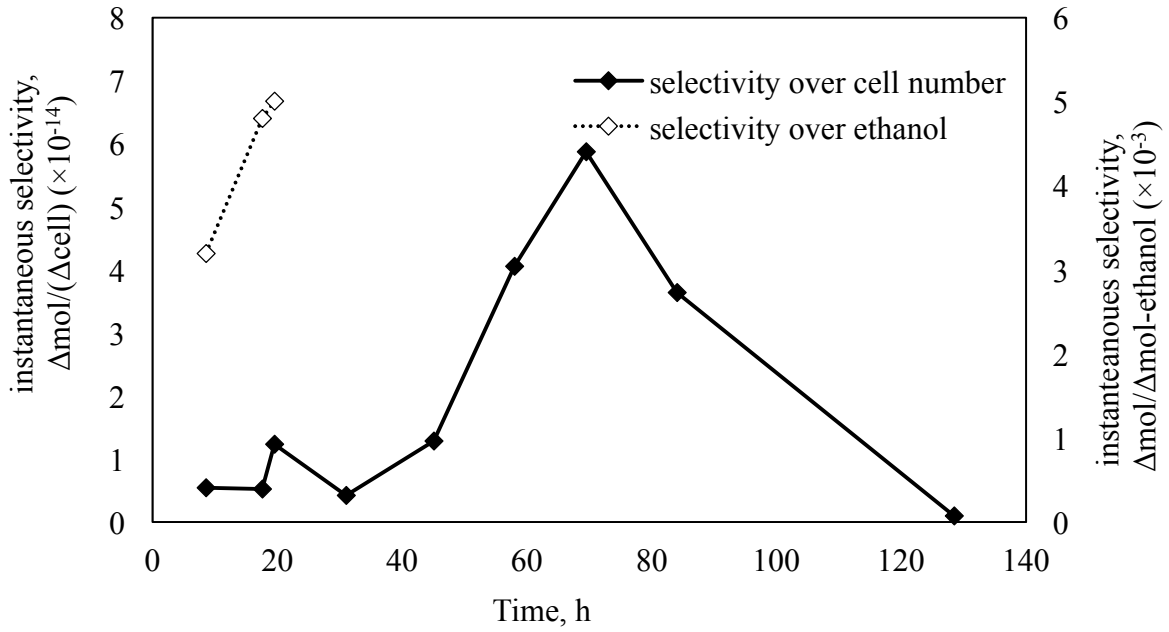

Figure 5.13 Instantaneous selectivity of shikimic acid over cell number and ethanol during batch growth in a 1-L batch fermenter.

Figure 5.14 presents the yield of shikimic acid on the total moles of carbon consumed during batch growth in a 1-L fermenter. The yield is defined as the ratio of moles of shikimic acid produced per total moles of carbon consumed. During glucose consumption, the moles of shikimic acid produced was divided by the moles of carbon of glucose consumed subtracted by the moles of carbon of ethanol produced. During ethanol and glucose consumption, the moles of shikimic acid produced was divided by both the decrease in moles of carbon of glucose and ethanol. Figure 5.14 shows that the yield reached a local maximum (1.72×10^{-3} mol shikimic acid/mol-C) once glucose was mostly consumed. Subsequently, the highest yield was obtained during ethanol consumption (1.21×10^{-2} mol shikimic acid/mol-C) when ethanol was fully consumed. The theoretical maximum yield of shikimic acid on one mole of glucose is 0.857 mol shikimic acid/mol-glucose (See Appendix C for sample calculation). This value was determined assuming that all of the carbon in glucose ends up in shikimic acid. In terms of moles of carbon of glucose, the theoretical maximum yield is 0.143 mol shikimic acid/mol-C. Finally, the theoretical maximum amount shikimic acid produced on 20 $g\cdot L^{-1}$ of glucose is 9.51×10^{-2} mol shikimic acid.

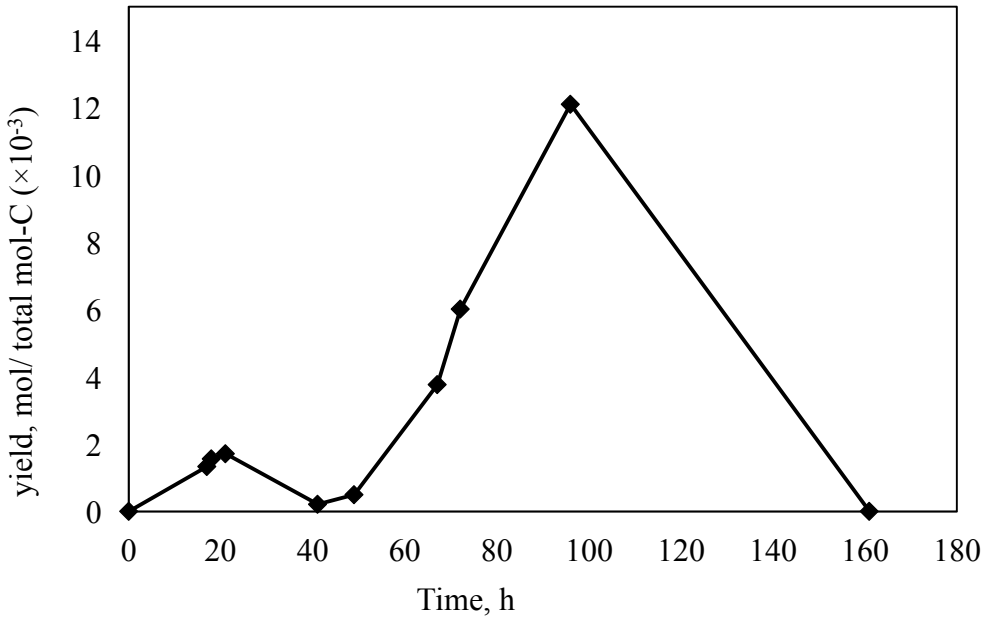

Figure 5.14 Yield of shikimic acid on the total moles of carbon consumed during batch growth in a 1-L batch fermenter.

The productivity and integrated specific productivity of shikimic acid is illustrated in Figure 5.15. The productivity was calculated by dividing the moles of shikimic acid produced per volume of batch by the amount of time it took to obtain the corresponding shikimic acid concentration. The specific productivity was calculated by dividing the moles of shikimic acid produced per volume of batch by the integral of cell number per volume of batch from time 0 to the sampling time. For both productivity and the integrated specific productivity, a maximum is reached at the end of glucose consumption where a value of 2×10^{-5} mol·(L·h)$^{-1}$ and 7×10^{-16} mol·(cell·h)$^{-1}$ were obtained, respectively.

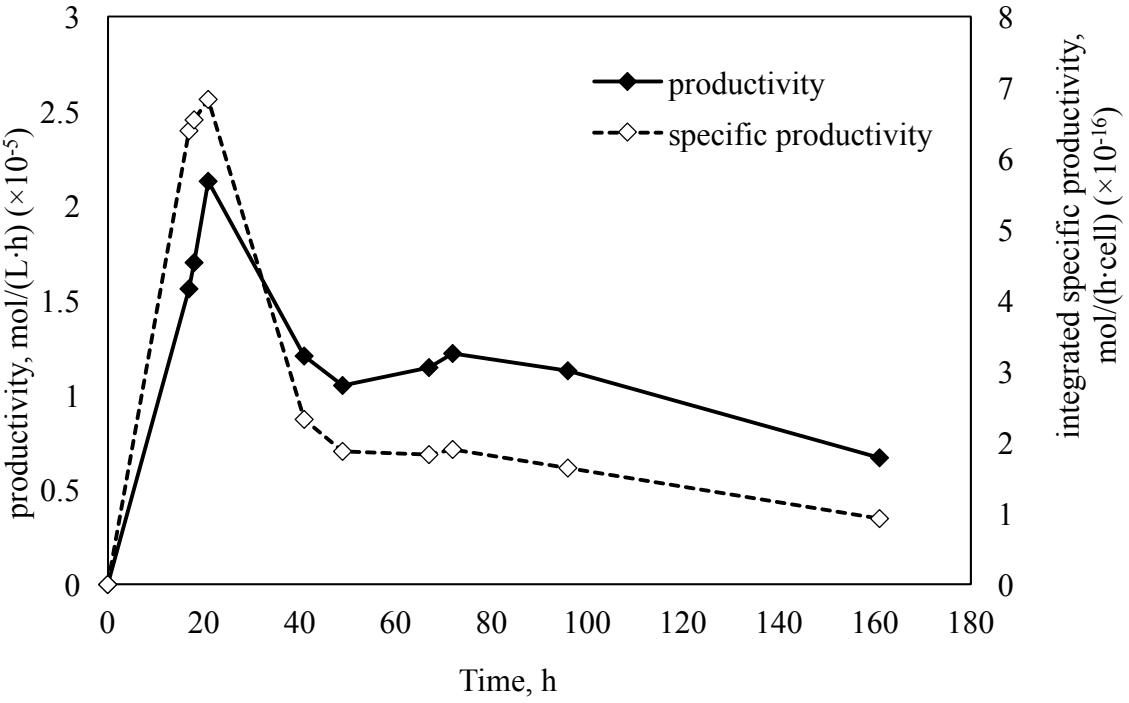

Figure 5.15 Productivity and integrated specific productivity of shikimic acid.

5.2.4 Carbon dioxide evolution rate

The observed carbon dioxide evolution rate during the growth of the engineered yeast strain in a 1-L batch fermenter is presented in Figure 5.16. The observed CER was calculated using Equation 4.3. Figure 5.16 shows that the CER increased as yeast population growth propagated during the first half of the glucose consumption process; this corresponds to the first 14 h of growth. After approximately 14 h of growth, a maximum in CER was observed at approximately 0.015 mol·h^{-1}. The CER remained at this approximate level until 22 h of growth where it rapidly dropped; this corresponds to the onset of glucose depletion and the end of the first exponential phase. After 25 h of growth, the CER level remained relatively stable at approximately 0.002 mol·h-^{1}. After 84 h of growth, the CER level dropped again and stayed at approximately 0.0002 mol·h^{-1} for the duration of the fermentation process; this corresponds to the depletion of ethanol and the onset of stationary phase.

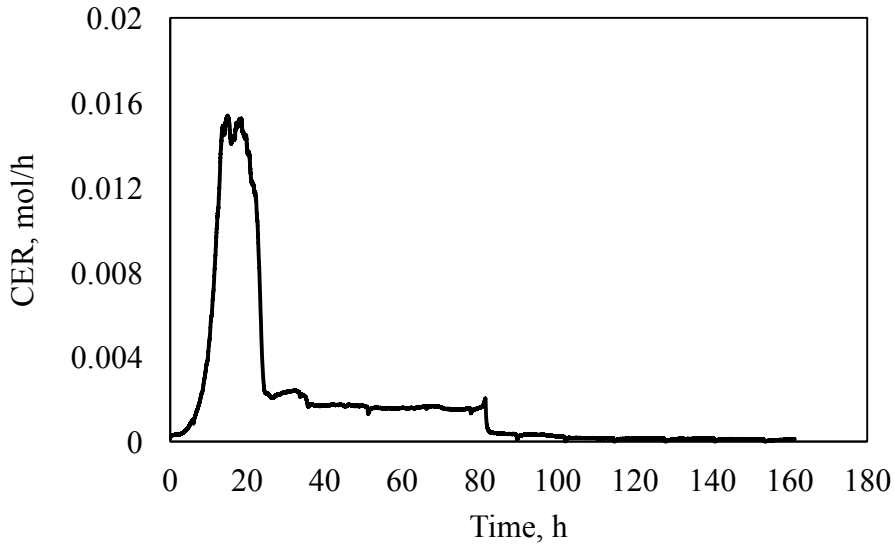

Figure 5.16 Observed CER during the batch growth of the engineered *S. cerevisiae* in a 1-L batch fermenter.

The observed CER in ppm (A) and the rate of change of CER (dCER) (B) during the batch growth of the engineered strain in a 1-L batch fermenter for the first 28 h of growth is shown in Figure 5.17. Figure 5.17A shows the increase in CER to approximately 7000 ppm after 14 h of growth. Similarly, the dCER increased during this time. Between 14-22 h of growth, the CER hovered between 6000-7000 ppm while the dCER dropped and hovered around the x-axis. After 22 h of growth, the CER and dCER dropped rapidly. Finally at approximately 25 h of growth, which corresponds to the end of the first exponential phase due to the depletion of glucose, the CER level dropped to approximately 1000 ppm. Furthermore, the dCER was zero at this point.

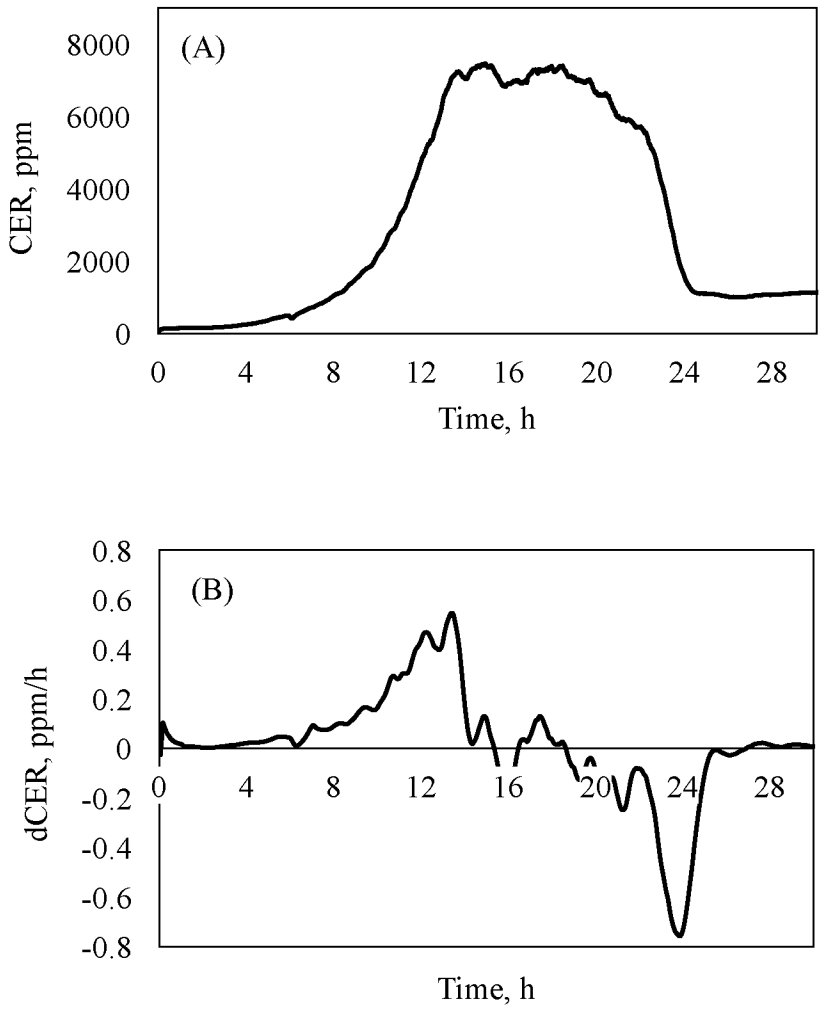

Figure 5.17 Observed CER in ppm (A) and the rate of change of CER (B) during the first 28 h of culture of the engineered *S. cerevisiae* in a 1-L batch fermenter.

5.3 Self-cycling fermentation operation

After characterization of the engineered yeast strain during batch growth in a 1-L batch fermenter, the condition chosen to trigger cycling during SCF operation was a combination of the CER and dCER.

5.3.1 Carbon dioxide evolution rate

The observed CER in moles per hour during SCF operation of the engineered yeast strain for 25 cycles is shown in Figure 5.18. Again, the observed CER was calculated using Equation 4.3. Figure 5.18 shows a consistent pattern of CER after 5 cycles. As in the batch process,

the maximum in CER obtained in the first cycle occurred between 14 and 15 h of growth, reaching a value of 0.016 mol·h^{-1}. A maximum CER of approximately 0.018 mol·h^{-1} was obtained for cycles 2, 3, and 5. Cycle 4 had a low CER due to an equipment upset unrelated to the growth of the yeast population. After 5 cycles, the average maximum CER was 0.013 mol·h^{-1} $\pm$ 0.0014.

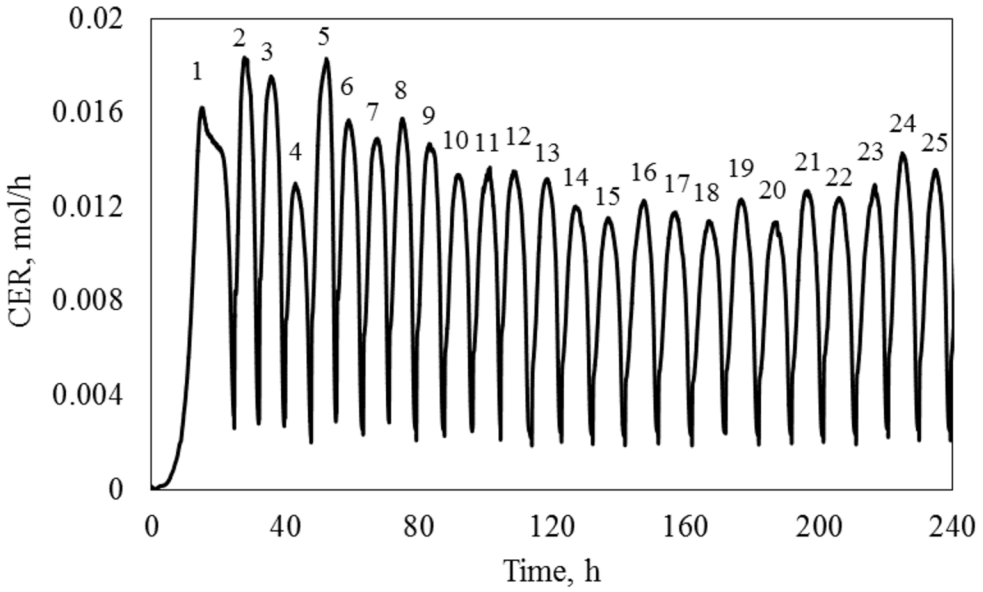

Figure 5.18 Observed CER during SCF operation of engineered *S. cerevisiae* for 25 cycles. Cycle numbers are shown above the mid-cycle data points.

Figure 5.19 presents the cycle times for the data in Figure 5.18. The cycle time is defined as the period between the addition of fresh medium and the end of the emptying step. After the first cycle, this period remained relatively constant at an average value of 8.87 h $\pm$ 0.77. Figure 5.19 shows that the cycle times from cycle 2 to 11 is at the lower end of the confidence interval at approximately 8.10 h. After 11 cycles, the cycle times increased to the higher end of the confidence interval at 9.64 h.

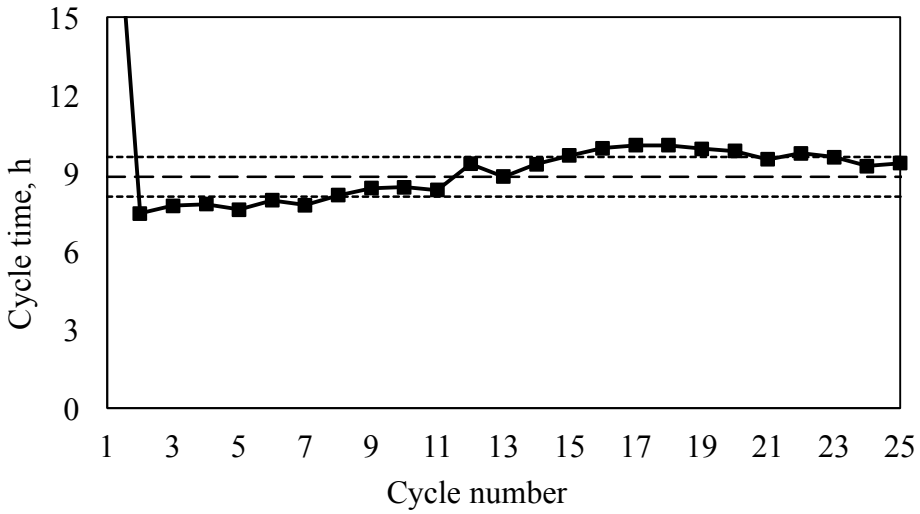

Figure 5.19 Cycle time of each cycle for 25 cycles of SCF operation.

Figure 5.20 presents the total moles of carbon dioxide evolved for each cycle for 25 cycles of operation. The total moles of carbon dioxide evolved for each cycle was calculated by determining the area under the CER curve shown in Figure 5.18. Figure 5.18 shows that the CER is higher for cycles before cycle 11, with the exception of cycle 1 and 4. Figure 5.19 shows that the corresponding cycle times for these cycles are shorter. Figure 5.20 illustrates that the inverse trend seen in Figure 5.18 and 5.19 produce a constant amount of carbon dioxide evolved for all cycles throughout the SCF experiment (average value of 0.090 moles $CO_2 \pm 0.0056$).

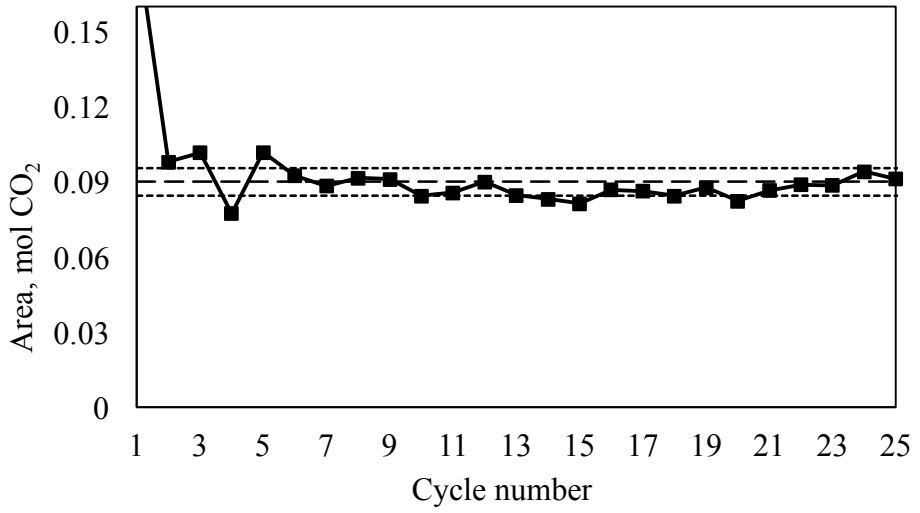

Figure 5.20 Total moles of carbon dioxide evolved per cycle for 25 cycles of SCF operation.

5.3.2 Cell, glucose and ethanol concentrations

The growth of the engineered yeast strain during SCF operation for each cycle for 23 cycles given by OD_{600} is presented in Figure 5.21. The optical density showed a stable, repeatable pattern after the first cycle. An average optical density value of 4.65 $\pm$ 0.13 at the end of the cycles and 2.46 $\pm$ 0.12 at the start of the cycles was obtained.

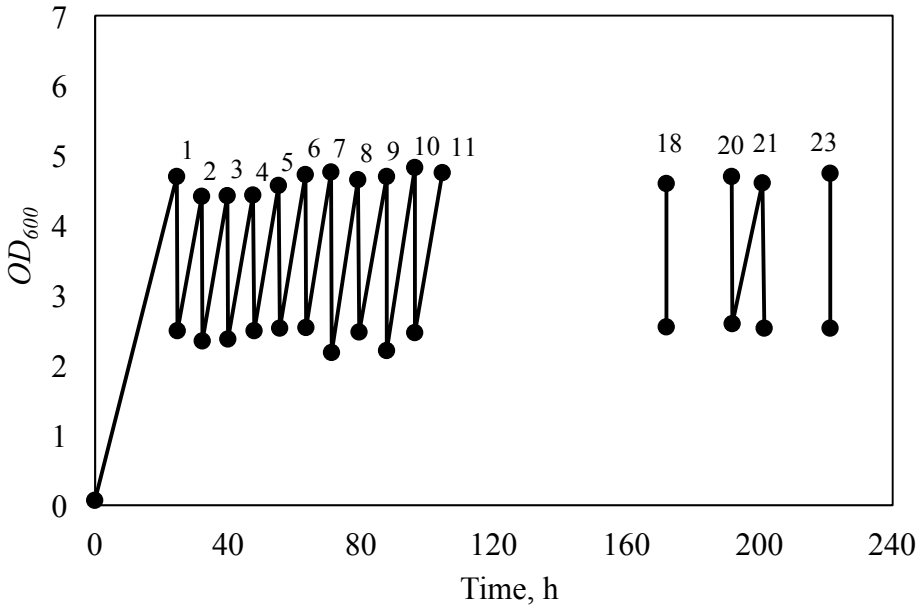

Figure 5.21 Optical density at the start and end of each cycle for 23 cycles of SCF operation. Cycle numbers are shown above the end-of-cycle data points.

The glucose concentration at the start and end of each cycle for 21 cycles during SCF operation of the engineered yeast strain is presented in Figure 5.22. At the beginning of the first cycle, the glucose concentration was 20 $g \cdot L^{-1}$. After the emptying/refilling step, where half the fermenter volume was harvested and 0.5 L of fresh medium was added, the glucose concentration was approximately half of that. The average glucose concentration at the beginning of each cycle after the first cycle was 9.28 $g \cdot L^{-1}$ $\pm$ 0.42. At the end of each cycle, no glucose was detected in the fermentation broth.

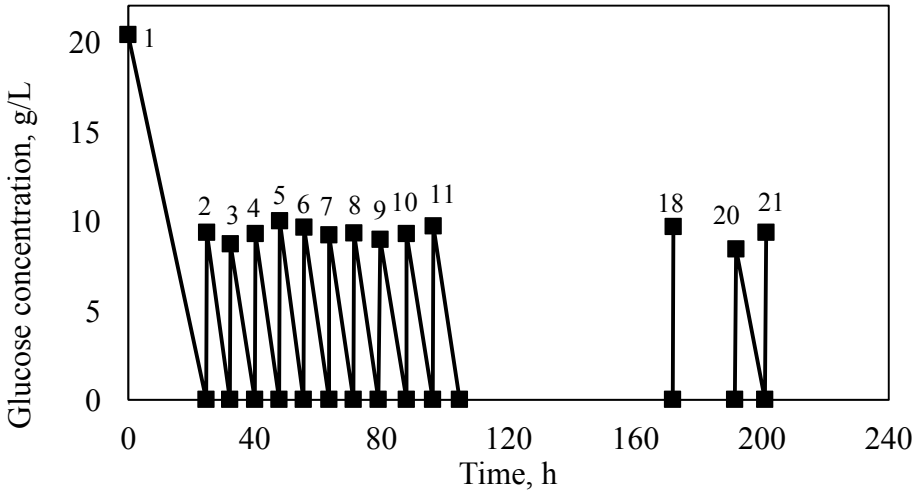

Figure 5.22 Glucose concentration at the start and end of each cycle for 21 cycles of SCF operation. Cycle numbers are shown above the start-of-cycle data points.

Similarly, the ethanol concentration at the start and end of each cycle for 21 cycles during SCF operation is shown in Figure 5.23. This figure illustrates a decreasing trend for the ethanol concentration at the end of each cycle as SCF operation propagated. At the end of the first cycle, the ethanol concentration achieved was 0.63 v/v%. At the end of cycle 21, the ethanol concentration reached a value of 0.47 v/v%. This is a 25% reduction in the observed ethanol concentration at the end of a cycle.

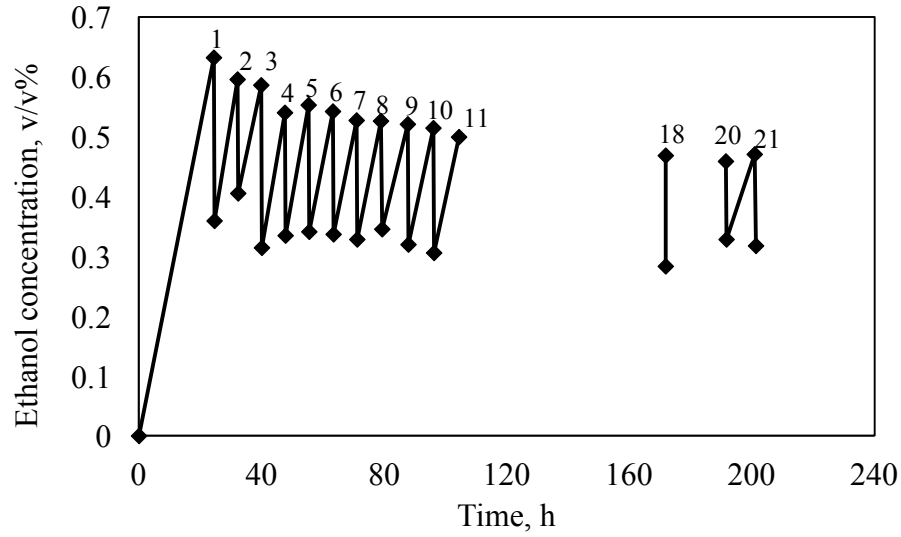

Figure 5.23 Ethanol concentration at the start and end of each cycle for 21 cycles of SCF operation. Cycle numbers are shown above the end-of-cycle data points.

5.3.3 Shikimic acid production: yield, selectivity, and specific productivity

The shikimic acid concentration at the start and end of each cycle for 23 cycles during SCF operation of the engineered strain is presented in Figure 5.24. This figure shows an increasing trend for the shikimic acid concentration from cycle to cycle. At the end of the first cycle, a shikimic acid concentration of approximately 0.11 $g \cdot L^{-1}$ was achieved, which is comparable to values obtained at the end of the exponential phase obtained in batch shake flask experiments and 1-L batch fermenters. At the end of cycle 23, the shikimic acid concentration reached 0.39 $g \cdot L^{-1}$. This is more than a three-fold increase in the observed shikimic acid concentration at the end of a cycle.

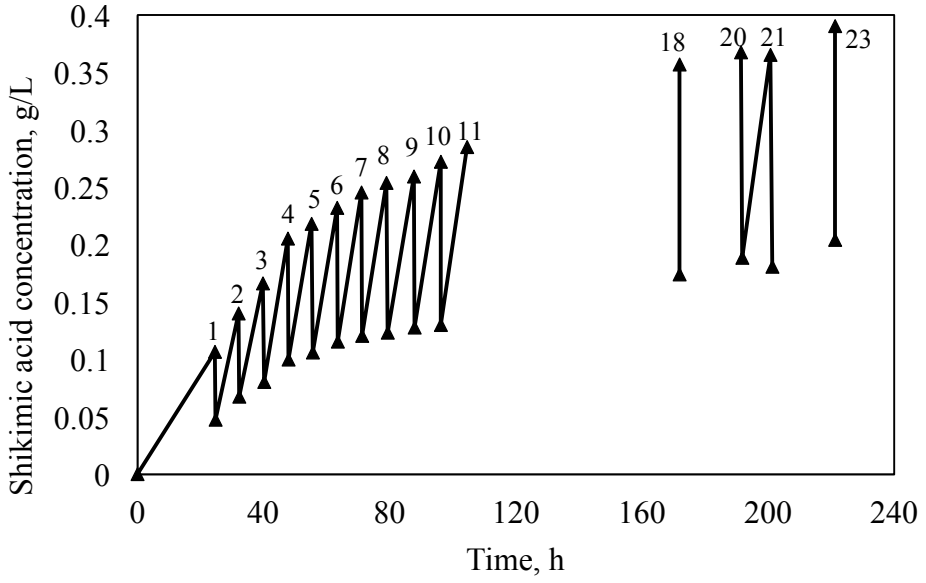

Figure 5.24 Shikimic acid concentration at the start and end of each cycle for 23 cycles of SCF operation. Cycle numbers are shown above the end-of-cycle data points.

Figure 5.25 illustrates the overall selectivity of shikimic acid over cell number and ethanol for 23 and 21 cycles, respectively. Similarly, Figure 5.26 presents the instantaneous selectivity over cell number and ethanol with respect to normalized time for cycle 11 and 21. The overall selectivity over cell number is given by the ratio of the produced shikimic acid in moles and number of cells produced in a cycle. Similarly, the overall selectivity over ethanol is given by the ratio of moles of produced shikimic acid over the moles of produced ethanol. The instantaneous selectivity over both cell number and ethanol are given as the ratio of the absolute value of rate of

formation of shikimic acid over the rate of formation of either cell concentration or ethanol within a cycle, accordingly. The time was normalized with respect to the period of the cycle. Figure 5.25 shows that as cycle number increased, the overall selectivity over both cell number and ethanol increased. Compared to the selectivity values obtained during a batch process (cycle 1), a three-fold and four-fold increase in the overall selectivity over cell number and ethanol, respectively, was achieved. Figure 5.26A shows that the selectivity over cell number is high early within the cycle for both cycles 11 and 21. However, larger selectivity values were obtained for cycle 21 at peak values. Figure 5.26B shows that the selectivity over ethanol peaks roughly mid-cycle for both cycles 11 and 21. Again, the selectivity values for cycle 21 was larger than in cycle 11 at peak values.

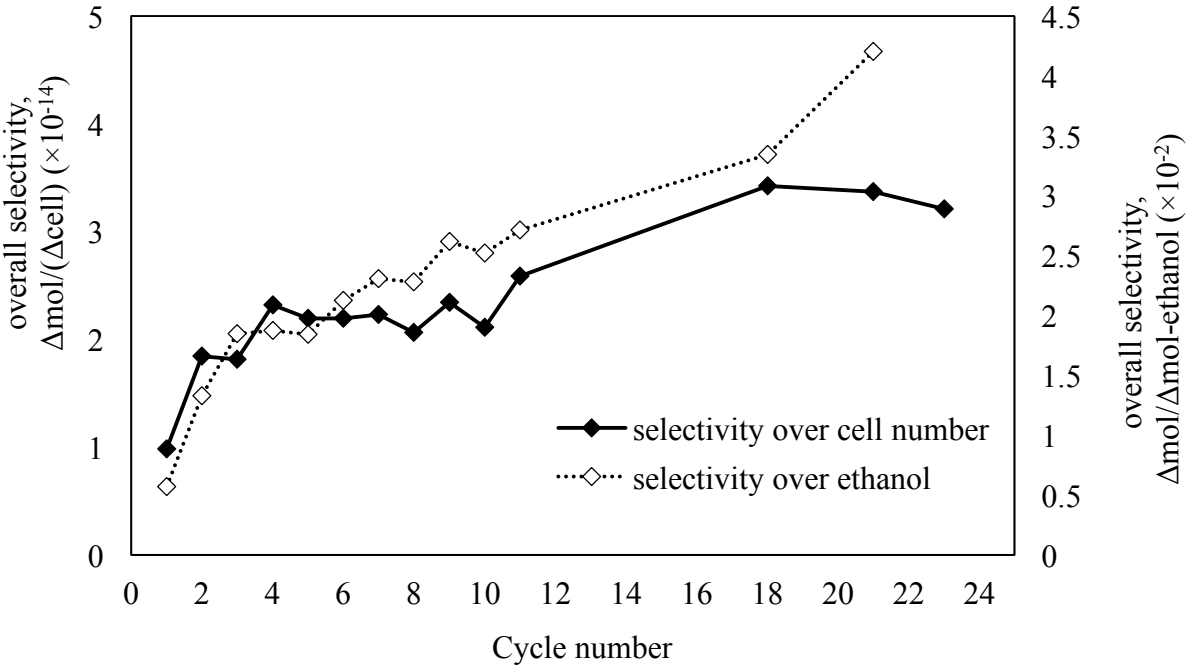

Figure 5.25 Overall selectivity of shikimic acid over cell number and ethanol for 23 and 21 cycles, respectively

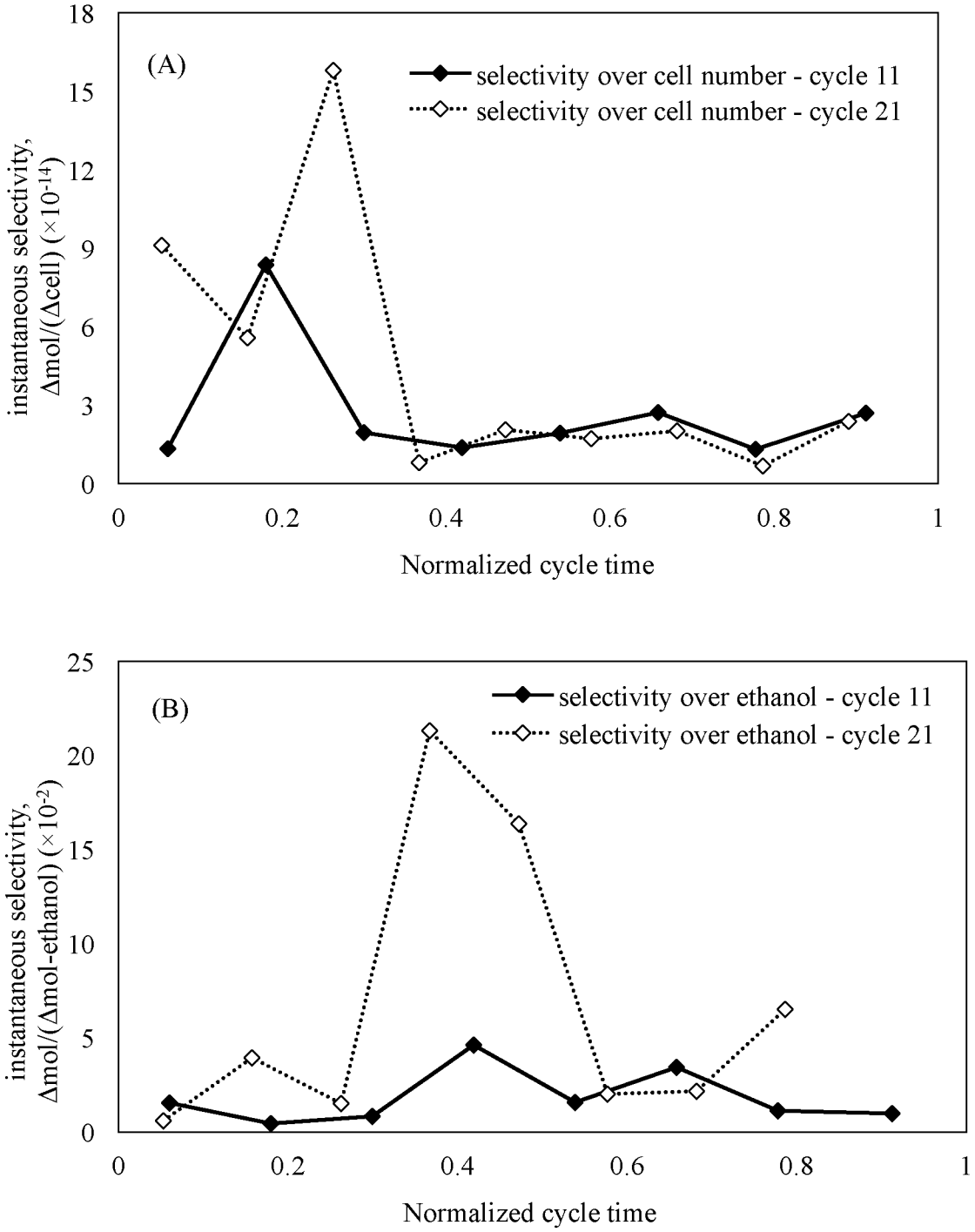

Figure 5.26 Instantaneous selectivity of shikimic acid over cell number (A) and ethanol (B) for cycle 11 and 21.

Figure 5.27 shows the yield of shikimic acid on glucose. This yield was calculated as either the ratio of moles of shikimic acid produced per mole of glucose consumed for each cycle or the

ratio of moles of shikimic acid produced per moles of carbon of glucose consumed. The figure illustrates an increasing trend in yield as cycle number increased. Between the first cycle and cycle 21, a four-fold increase in yield was observed. A two-fold increase was achieved when cycle 21 was compared to the yield of shikimic acid during batch growth on glucose (Figure 5.14).

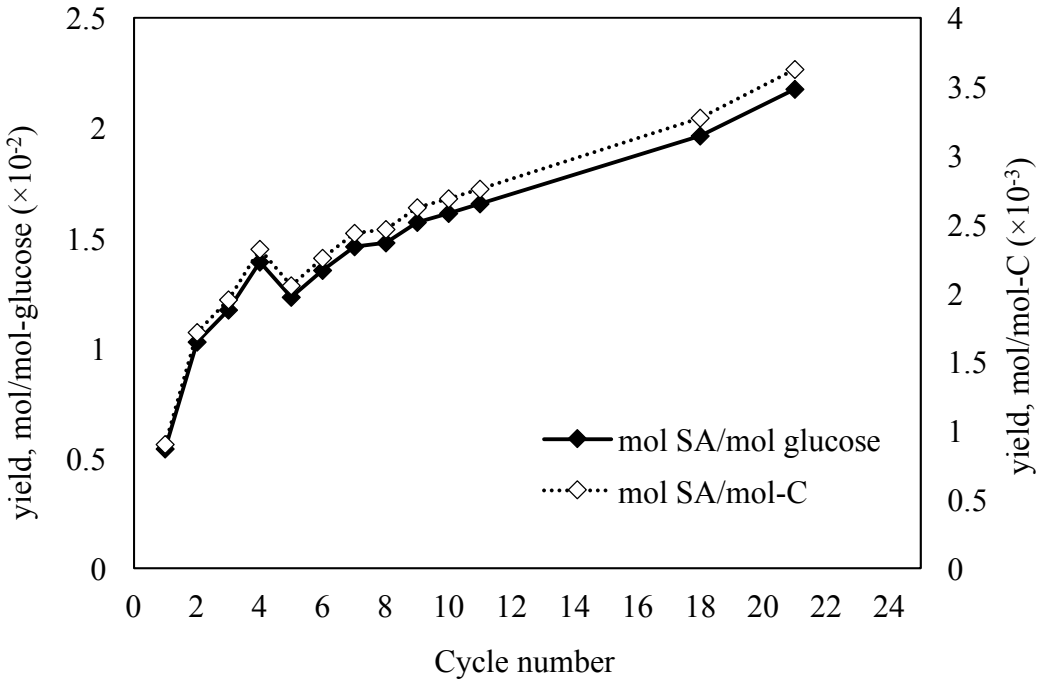

Figure 5.27 Molar yield of shikimic acid on either moles of glucose consumed or moles of carbon in glucose consumed for 21 cycles of SCF operation.

Figure 5.28 illustrates the productivity and integrated specific productivity of shikimic acid for each cycle. The productivity is given by the concentration of shikimic acid in mol·L^{-1} within a cycle per cycle time of the corresponding cycle. The integrated specific productivity was calculated as the concentration of shikimic divided by the integral of cell concentration for a given cycle. The cell concentration was obtained using the correlation curve given in Figure B6 of Appendix B. For cycle 11 and 21, the integral of actual intra-cycle cell counts were used. A sharp increase in productivity was observed between cycle 1 and 4, followed by a slow increase as cycle number increased. Between cycle 23 and cycle 1, an approximate four-fold and three-fold increase was achieved for productivity and specific productivity, respectively.

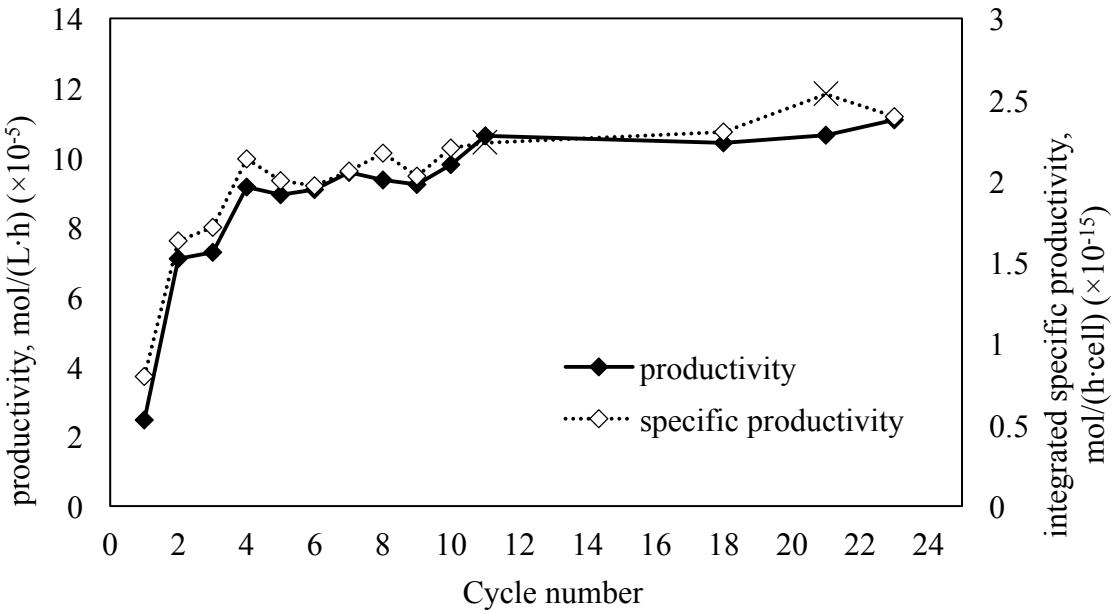

Figure 5.28 Productivity and integrated specific productivity of shikimic acid for 23 cycles of SCF operation. The integrated specific productivity for cycle 11 and 21 (×) were calculated using intra-cycle cell counts.

Figure 5.29 shows the intra-cycle productivity (A) and integrated specific productivity (B) against the normalized cycle time for cycles 11 and 21 of SCF operation. The normalized cycle time was determined by dividing the time point a sample is taken for analysis by the total cycle time. The productivity was calculated by dividing the moles of shikimic acid produced per time within the cycle. The integrated specific productivity was determined by dividing the cumulative $mol \cdot L^{-1}$ of shikimic acid produced by the integral of the cell number up to the corresponding time point. The cell number was counted for each time point. The correlation curve obtained for a batch process between optical density and cell number cannot be used within a cycle. This is because the optical density is not a true measure of cell number within a cycle during SCF operation. Figure 5.29A shows an increasing trend in productivity for both cycles 11 and 21 as time increased. Figure 5.29B shows a parabolic trend in integrated specific productivity for both cycles 11 and 21 as time increased. However, the parabola is skewed to the right for cycle 21 where the largest increase in specific productivity occurs near the beginning of the cycle.

A summary of the intra-cycle data for cycle 21 showing optical density, glucose consumption, shikimic acid production, CER and dCER is shown in Figure B12 in Appendix B.

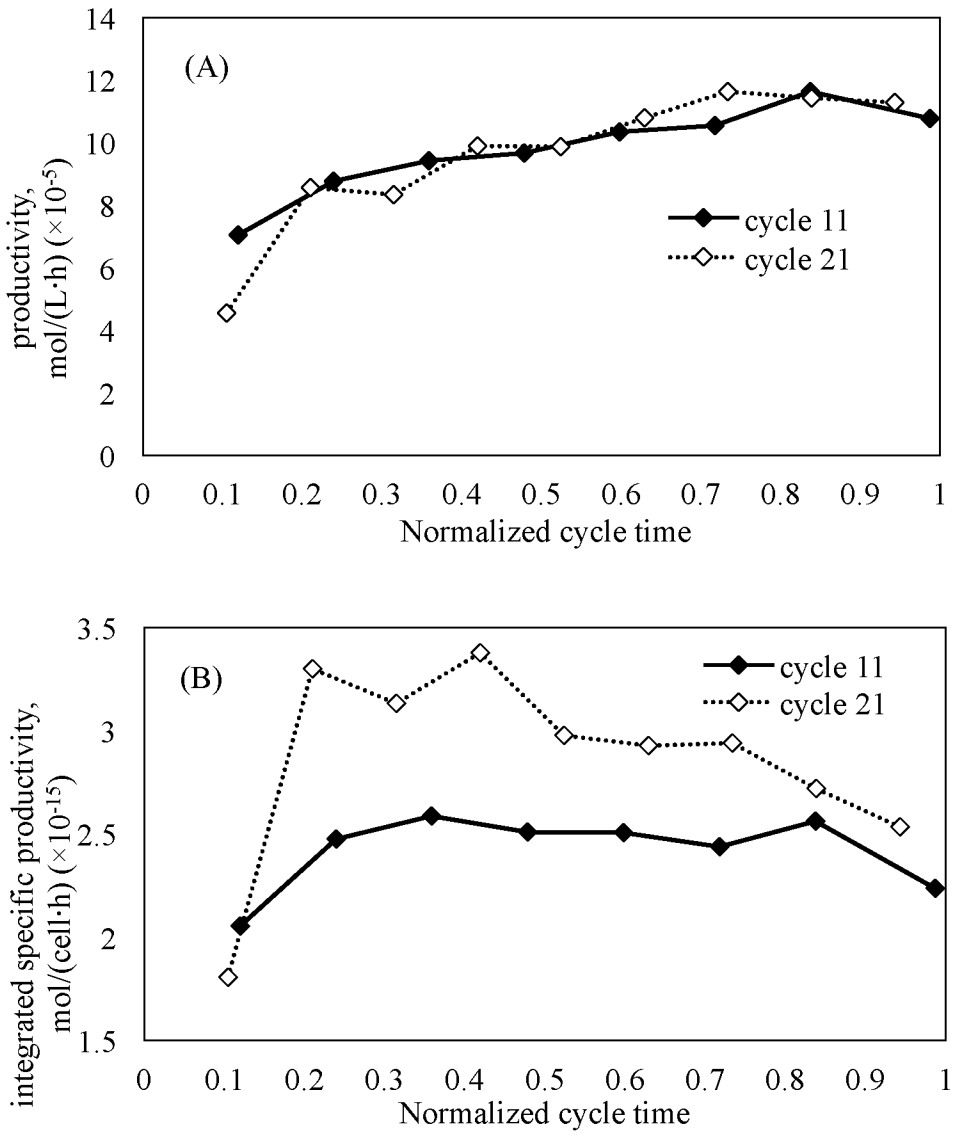

Figure 5.29 Intra-cycle productivity (A) and integrated specific productivity (B) of shikimic acid for cycle 11 and 21 of SCF operation.

5.3.4 Harvesting of cells at the end of a cycle

At the end of cycle 2 and cycle 20, the SCF fermenter was harvested to determine the shikimic acid production beyond the exponential phase, when shikimic acid is produced from ethanol. Figure 5.30 shows the shikimic acid concentration after an additional 60 h of culture in shake flasks after the end of the SCF cycle. The results are representation of the yield of shikimic acid on the produced ethanol from cycles 2 and 20, which is shown in Figure 5.31. For both cycles, an increase in shikimic acid concentration was observed. Despite the higher absolute concentration

obtained in cycle 20 at hour 72 (0.54 $g \cdot L^{-1}$ as compared to 0.32 $g \cdot L^{-1}$ for cycle 2), the slopes of both curves are equal, which implies that the amount of shikimic acid produced is relatively similar for both cycles after the growth phase. This is confirmed by Figure 5.31 where the yields of shikimic acid on ethanol for both cycles are the same.

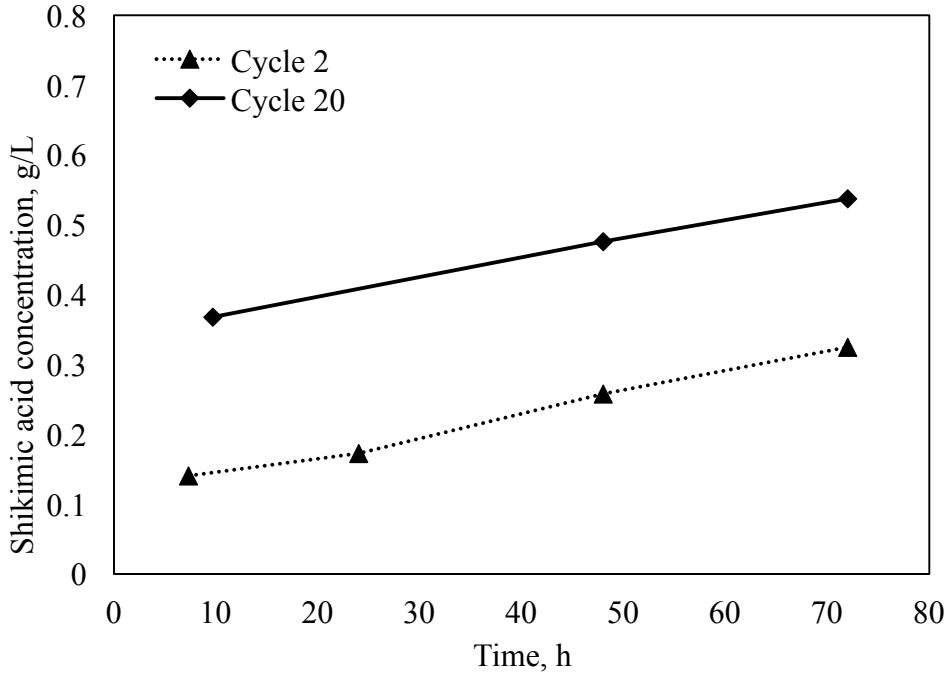

Figure 5.30 Shikimic acid concentration after an additional 60 h of growth in shake flasks for cells harvested at the end of cycle 2 and 20 of SCF operation.

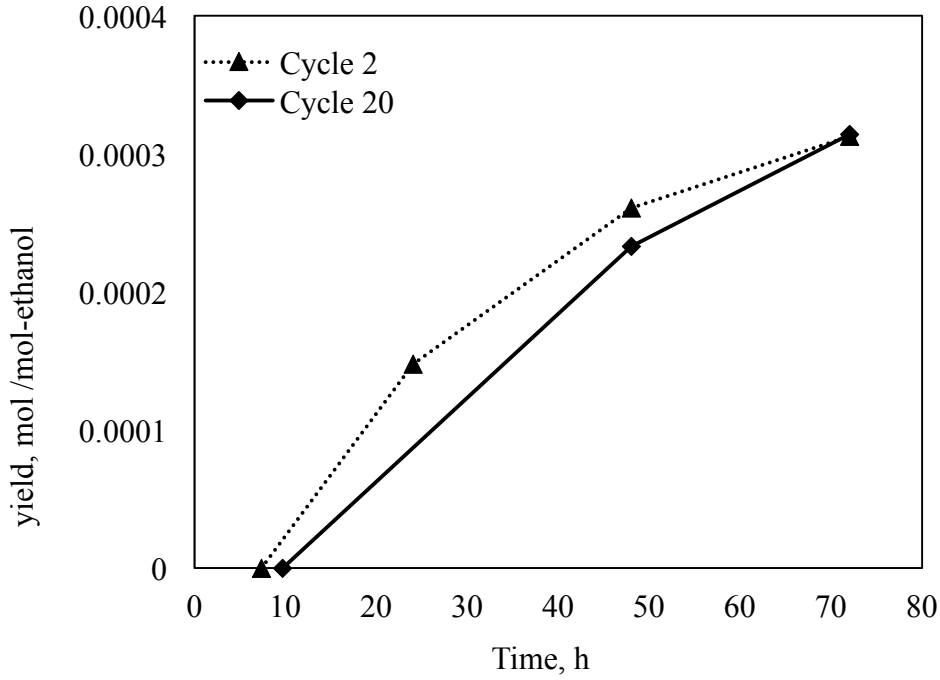

Figure 5.31 Yield of shikimic acid on produced ethanol for cycles 2 and 20 of SCF operation.

5.4 Cell synchrony

SCF operation induces synchrony in microbial populations (Sheppard and Cooper 1990; Brown and Cooper, 1992; McCaffrey and Cooper, 1995; Wentworth and Cooper, 1996; Sauvageau, et *al.,* 2010; Storms, e*t al.*, 2012). Thus, the degree of synchrony attained within the population of engineered yeast was assessed in order to determine if the increase in productivity of shikimic acid was linked to the synchronization of the yeast population. In addition, other possibilities for the increase in shikimic acid production were explored.

5.4.1 Shikimic acid positive feedback

The possible positive effect of the presence of shikimic acid on its own production by the engineered yeast strain was investigated. Figure 5.32 shows the shikimic acid concentration (A) and yield (B) for a growing culture of the engineered strain in fresh medium with varying starting concentrations of shikimic acid. Figure 5.32A shows that an increasing trend in concentration was observed for all four initial shikimic acid concentrations tested throughout the fermentation period. Despite the higher absolute concentration obtained in the experiment initiated with 0.90 $g \cdot L^{-1}$ of shikimic acid (1.2 $g \cdot L^{-1}$) as compared to that of the experiment initiated without shikimic acid

(0.34 $g \cdot L^{-1}$), the slope of all four curves imply that the amount of shikimic acid produced for all conditions are similar. Again, this is confirmed by Figure 5.32B, where the yields of shikimic acid on the total moles of carbon consumed are consistent for all four conditions tested.

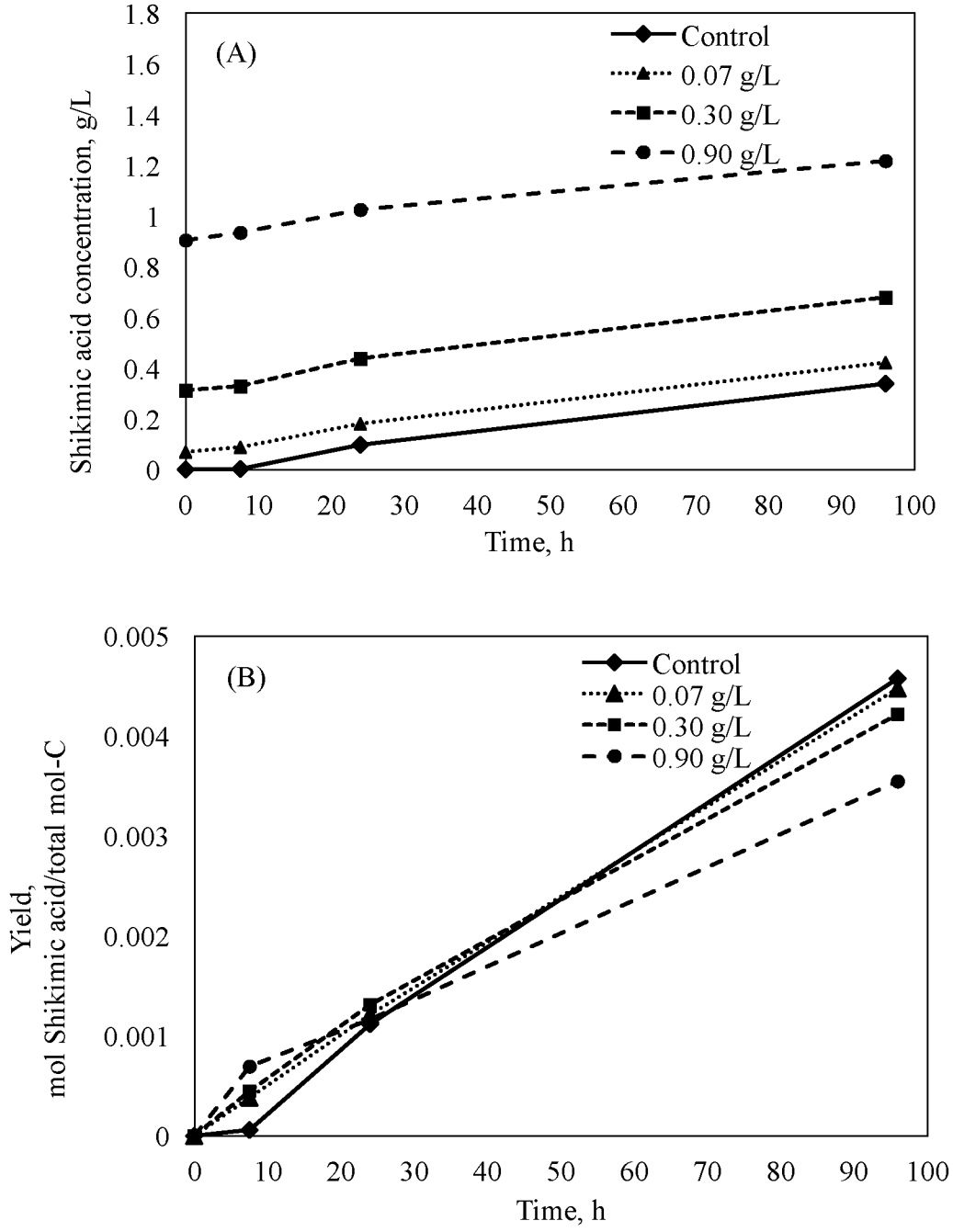

Figure 5.32 Shikimic acid concentration (A) and yield (B) for shake flask experiments initiated with 0 $g \cdot L^{-1}$ (♦), 0.07 $g \cdot L^{-1}$ (▲), 0.30 $g \cdot L^{-1}$ (■), and 0.90 $g \cdot L^{-1}$ (●) of shikimic acid.

5.4.2 Cell number and cell division

The change in cell concentration during the course of cycles 11, 16, 21, and 38 of SCF operation is shown in Figure 5.33. The measurements of cell concentration were normalized with respect to the initial cell concentration for each cycle. The time was normalized with respect to the length of the cycle. Figure 5.33 shows the progression in the cell density within cycles for 4 cycles. For cycle 38, the synchrony index (Equation 2.1) was 0.68 as compared to 0 for cycles 11 and 16. For cycle 21, the synchrony index was 1.01; this synchrony index was achieved because the ratio of cell concentration between the beginning and end of the cycle for cycle 21 was greater than 2 which implies that the population more than doubled within the cycle. This is most likely due to experimental error in cell counts.

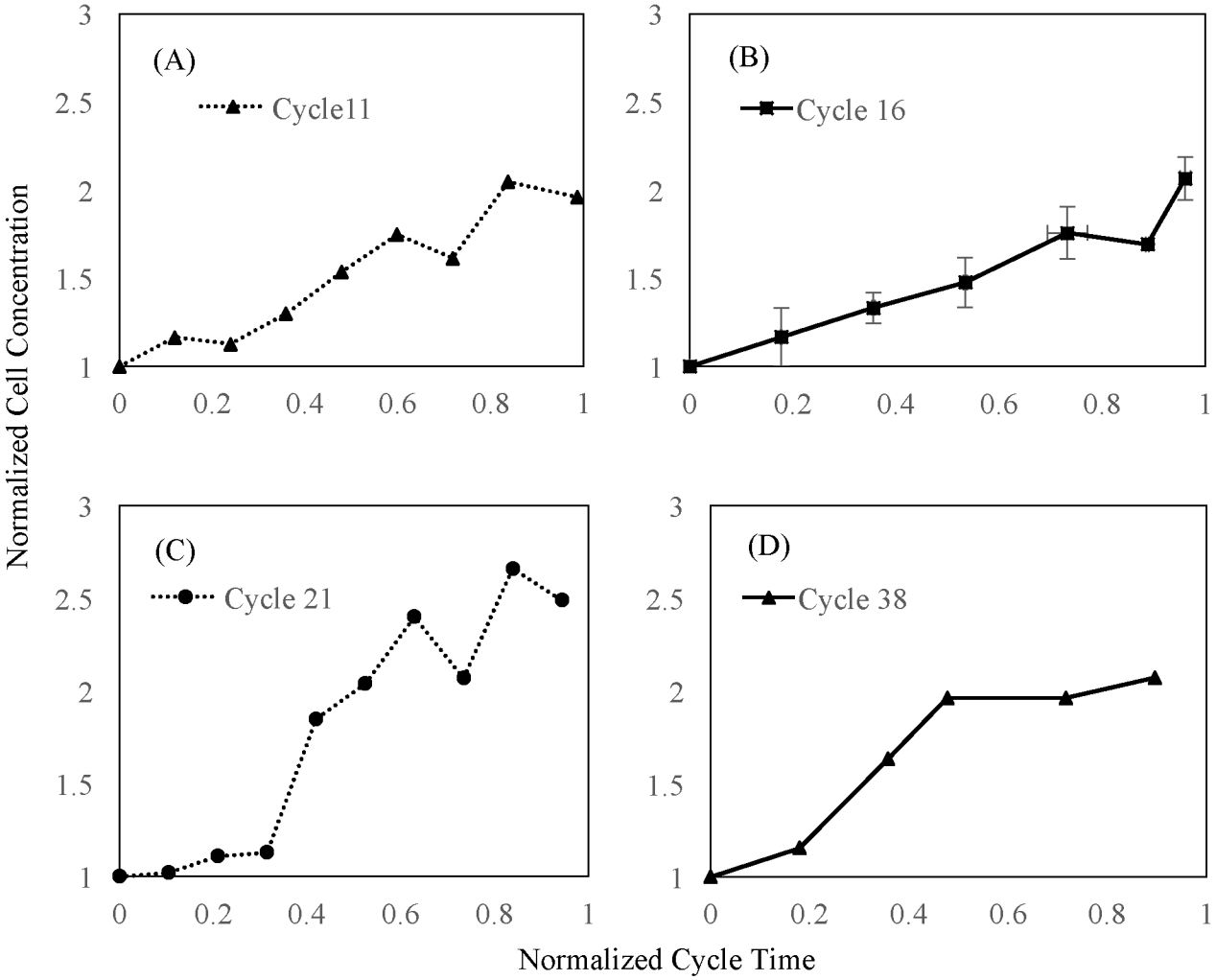

Figure 5.33 Cell density during SCF cycles for cycle 11 (A), 16 (B), 21 (C), and 38 (D).

5.4.3 Cell morphology

Figure 5.34A shows an example of a microscope image of the engineered yeast strain after 30 h of batch growth in a shake flask. The proportion of the yeast population with more than one bud was 23%. Figure 5.34B is a microscope image of the engineered yeast strain after 120 h of growth in a 1-L batch fermenter. The proportion of the cell population with more than one bud was 25%. Figure 5.34C portrays yeast cells after 8.5 h of growth in cycle 16 of SCF operation. It shows a yeast population with 35% of cells with more than one bud. This result is congruent with the idea that the cell population may have more than doubled within the cycle for cycle 21 during SCF operation; this also hints at a cell population under stress.

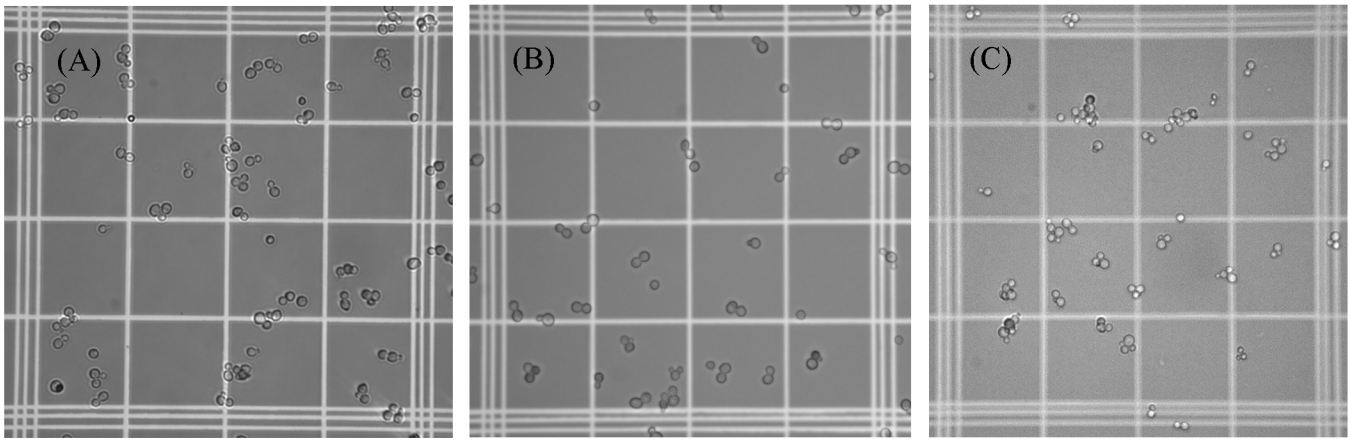

Figure 5.34 Microscopy images of the engineered *S. cerevisiae* after (A) 30 h of batch growth in a shake flask; (B) 120 h of growth in a 1-L batch fermenter; and (C) at the end of cycle 16 of SCF operation (cycle time of 8.5 h). The images were taken at 40X magnification using a hemocytometer.

5.4.4 pH measurement

The pH of the minimal YNB medium before inoculation was approximately 5.0. When the parent and engineered yeast strains were grown in shake flask cultures, the pH of the fermentation broth after 72 h of growth were approximately 3.0 for both strains. Under SCF operation of the parent strain, the pH of the fermentation broth after 6 cycles had dropped to 2.5. Similarly for the engineered strain, the pH of the fermentation broth at the beginning and end of cycle 10 was 2.6 and 2.4, respectively.

6. Discussion

The results obtained in this study demonstrated that the use of SCF increased the yield and specific productivity of shikimic acid in *Saccharomyces cerevisiae* engineered to accumulate shikimic acid. Moreover, it illustrated other conditions that improve the fermentation of yeast for the production of this compound.

6.1 Batch growth of yeast

The modified *Saccharomyces cerevisiae* was engineered to increase the production of the desired metabolite, shikimic acid. Though only 20% of the approximate 6200 predicted genes in yeast are essential (Tong, *et al.*, 2001), the engineered yeast strain was grown in minimal medium in batch cultures to confirm its viability after the performed deletions and plasmid insertion. The growth profile of the parent strain was used as a reference.

6.1.1 Measurement of plasmid retention

The pYES vector is the heterologous expression plasmid used in the engineered strain. It contains a 2μ origin for maintenance and replication at high copy numbers (approximately 10-40 copies per cell) in yeast (Invitrogen, 2009). It was necessary to verify that the inserted plasmid was maintained and replicated during growth to ensure that the plasmid encoding for improved shikimic acid production did not get lost over many rounds of replication (Mead, *et al.,* 1986; Karim, *et al.*, 2013). When the engineered strain was plated in non-selective and selective agar plates, the number of colony forming units were within error for both conditions (Figure 5.2). This suggests that the engineered strain was able to retain the plasmid, allowing the cells to proliferate in uracil-lacking medium. Ultimately, this experiment ensured that cell viability and metabolite production should not cease due to loss of plasmid.

6.1.2 Biomass growth

The biomass growth for both parent and engineered strain followed a similar profile (Figure 5.1). Both strains had a 6 h lag phase, which is a period characterized by the adaptation of inoculated cells to a new environment (Shuler and Kargi, 2002). This was followed by a rapid exponential phase until 15 h of fermentation. After 15 h of growth, both cell populations entered a decelerated growth phase where the cell population continued to increase but with a slowed growth

rate caused by the near depletion of the limiting nutrient (Shuler and Kargi, 2002); this occurred until approximately 24 h of fermentation where stationary phase began to take place. Afterwards, a continued increase in biomass was observed with an even slower growth rate. The continued slow growth was observed for both strains for 73 h (Figure 5.3). For the engineered strain, the slow growth ceased at approximately 100 h of fermentation (Figure 5.6).

The slow increase may be caused by cryptic growth. This is characterized by cellular growth on cells that have lysed at the onset of stationary phase (Shuler and Kargi, 2002). Upon inspection under the microscope however, no lysis products were observed and this hypothesis was discarded. A second possibility may be due to a bottleneck in the metabolic pathway of glucose, the primary carbon source. This hypothesis suggests that the kinetics of glucose catabolism is faster than that of a downstream metabolite. Thus, the downstream product of glucose would accumulate in the cell and subsequently would continue to feed the carbon needs for biomass growth (Dell and Frost, 1993). A metabolomics profile of the fermentation broth at specific time points could help elucidate the presence and concentration of various accumulating metabolites. A third possibility is related to the second; it involves the presence of a secondary carbon source caused by the respiratory bottleneck characteristic in many strains of yeast which result in diauxic growth (Käppeli, e*t al.*, 1986). Diauxic growth is caused by a shift in the metabolic functions of a cell population as it adapts from one carbon source to another after the primary carbon source has been depleted (De Deken, 1965; Shuler and Kargi, 2002).

In the fermentations tested, ethanol was observed in the medium (Figure 5.7). Its concentration peaked at roughly the same time as the occurrence of glucose depletion. After ethanol depletion, biomass growth stabilized. It is known that for some *S. cerevisiae* strains, ethanol, the primary product of anaerobic fermentation of yeast, is aerobically produced during glucose metabolism (Figure 5.7). This phenomenon is explained by the *Crabtree effect* (De Deken, 1965; Wills, 1990): a mixed respiro-fermentative metabolism in aerobic conditions at glucose concentrations higher than 0.08 mM (Otterstedt, e*t al.,* 2004). Aerobic fermentation has an energy yield of 2 ATP molecules per molecule of glucose which is derived solely from the glycolytic pathway (Shuler and Kargi, 2002; Russell, 2003). In comparison, the respiratory pathway has an energy yield of 36 molecules of ATP per glucose after the completion of glycolysis, the TCA cycle and oxidative phosphorylation (Shuler and Kargi, 2002; Russell, 2003). Despite the lower energy

yield of fermentation, it is the preferred metabolic state of many yeast strains due to its faster kinetics for glucose metabolism (van Urk, e*t al.*, 1989; van Dijken, e*t al.*, 1993). The kinetic preference towards fermentation is caused by fast glucose uptake into the cell and the limitations of the pyruvate dehydrogenase (PDH) complex in shuttling glycolytic products into the TCA cycle (Otterstedt, e*t al.,* 2004). Thus, the carbon flux shifts towards aerobic fermentation instead of respiration under high glucose concentration. As glucose levels drop, the yeast population switches to respiratory metabolism where pyruvate successfully enters the TCA cycle since the PDH complex is not overwhelmed with excess pyruvate. Consequently, the energy yield on glucose increases. Despite the higher energy yield however, the metabolic switch towards respiration leads to slower growth kinetics (Figure 5.7) which is characteristic of the second growth phase in diauxic growth (De Deken, 1965; Mohammed Al-mhanna, 2010). Ultimately, the produced ethanol during aerobic fermentation acts as the secondary carbon source for continued biomass growth.

The similarity in growth profile between the parent and engineered strain demonstrates that the genetic modifications performed on the engineered strain were not obviously detrimental to cell growth. The lower optical density measurements observed in Figure 5.1 and Figure 5.3 for the engineered yeast strain as compared to the parent strain denoted a decrease in cell density, as seen through microscope inspection (results not shown). It follows that though the genetic modifications did not significantly inhibit cell growth of the engineered strain, it did slightly lower its maximum growth rate. A study on the characterization of plasmid burden and copy number in yeast showed that the choice of auxotrophic markers, as is the case in the strain used in the present study, can decrease the growth rate of a plasmid-containing lab strain as compared to parent cells without plasmids (Karim, *et al.*, 2013). Thus, the decrease in growth rate and increase in doubling time in the engineered strain can most likely be attributed to the burden associated with the extra plasmid containing a *URA3* selection marker.

6.1.3 Shikimic acid production

The parent and engineered strains were grown in shake flask cultures for 73 h to quantify the growth, glucose consumption and shikimic acid production profiles. No shikimic acid was detected in the fermentation broth of the parent strain (Figure 5.4) even though it does contain a non-optimized shikimate pathway (Figure 2.3) (Braus, 1991). In comparison, the engineered strain accumulated shikimic acid for the entire duration of the 73-hour fermentation period. This shows

that the applied genetic modifications (Figure 4.1) successfully induced overproduction of shikimic acid in the engineered strain. Moreover, this shows that the accumulation of shikimic acid did not significantly inhibit its own continued production through negative feedback loops as was thought to occur since shikimic acid inhibits the activity of shikimic acid dehydrogenase (Dell and Frost, 1993). Furthermore, the production of ethanol due to the *Crabtree effect* affected shikimic acid synthesis. Shikimic acid, which is a growth-associated product (Bhangale, *et al.,* 2014; Kojima, *et al.,* 2015), continued to accumulate after the depletion of glucose, much like biomass (Figure 5.5, Figure 5.6, and Figure 5.7). Since ethanol induced a secondary growth phase, the continued production of shikimic acid on ethanol after glucose depletion was plausible. After ethanol depletion, shikimic acid concentration stabilized (Figure 5.7). Between the 96 and 120 hour time points however, a slight increase in shikimic acid concentration was observed despite the depletion of ethanol and glucose. This may be explained by the metabolism of other fermentation products such as acetic acid or the effect of a downstream glycolytic metabolite that had accumulated, or a combination of both.

Figure 5.8 shows that 1.8% of moles of carbon from glucose went to the production of shikimic acid as compared to 6.4% moles of carbon from ethanol having gone to shikimic acid. This is surprising because shikimic acid production enters the shikimate pathway by the condensation of phosphoenolpyruvate (PEP) from glycolysis with erythrose-4-phosphate (E4P) from the pentose phosphate pathway (Floss, e*t al.*, 1972). Both of these metabolites are readily produced through the glycolytic catabolism of glucose. On ethanol, a possible pathway for the production of shikimic acid is through gluconeogenesis (Figure 2.2) (Wills, 1990; Fraenkel, 2011). In this process, ethanol is converted to acetaldehyde and shuttled into the TCA cycle. Eventually, the carbon in ethanol is found in malate which is converted into oxaloacetate. Once in the cytoplasm, oxaloacetate is converted to PEP. The gluconeogenesis pathway then produces glucose-6-phosphate (G6P) which is the primary substrate for the pentose phosphate pathway (Figure B10) (Wills, 1990; Fraenkel, 2011). Though the pathway toward shikimic acid production from ethanol is more complex, the ATP yield during aerobic respiration on ethanol is higher than that of aerobic fermentation on glucose, as stated above. Therefore, the higher ATP yield may provide enough energy to drive the gluconeogenesis reaction forward, which resulted in increased concentrations of shikimic acid. Another possible reason for the higher apparent yield on ethanol may be caused by differences in biomass growth rates under glucose and ethanol metabolism. During aerobic

fermentation of glucose, the carbon flux is directed towards biomass formation (Figure 5.7). During ethanol metabolism, biomass growth was slower. Thus, more carbon from ethanol was available for shikimic acid production. Also, the greater cell concentration available during ethanol metabolism may positively influence shikimic acid production (i.e. greater "man power" available for product formation).

Since shikimic acid production during respiratory metabolism on ethanol seemed to give rise to higher product yield, ethanol as the primary carbon source for shikimic acid production and growth was investigated. Biomass growing solely on ethanol had a longer lag phase (not shown). This may be due to the production of internal components in the yeast cell necessary for survival in high concentrations of ethanol (Wills, 1990; Birch and Walker, 2000). In addition, the ethanol concentration decreased after 25 hours of growth before any shikimic acid production was observed (Figure 5.9B). This illustrates how the carbon in ethanol is not as readily available for metabolism as that in glucose (Figure 5.9A) since the uptake of ethanol does not immediately result in biomass growth and product formation. This may also suggest that the cellular machinery for ethanol metabolism was being synthesized which contributed to the longer lag phase (Wills, 1990; Shuler and Kargi, 2002). Figure 5.9 also shows that the shikimic acid concentration when ethanol was the primary carbon source was lower than when glucose was the primary substrate. The lower overall shikimic acid yield suggests that the carbon in ethanol was split between biomass and shikimic acid formation. In contrast, the carbon flux was directed towards biomass growth during aerobic fermentation on glucose (with appreciable amounts of shikimic acid still being produced). Once glucose was depleted, only a small proportion of the carbon in fermentation products were allocated to biomass growth and the rest could be shuttled towards product formation. Ultimately, it could be deduced that the full metabolism of glucose yields a higher production of shikimic acid compared to growing the engineered strain in ethanol as the primary carbon source.

6.2 Characterization of engineered yeast for SCF operation

As seen from the previous discussion, there are many conditions that affect the production of shikimic acid in engineered yeast such as the growth profile of the yeast population due to the available carbon source and the eventual conversion of an accumulating secondary substrate. The synchronization of the yeast population via SCF shows advantages that can utilize the above effects

and maximize product formation (Dawson, 1972). In order to assess the conditions required to operate under SCF, the engineered yeast was characterized in a 1-L batch fermenter for growth kinetics, substrate consumption, and product formation. This was done to select an appropriate control parameter for stable SCF operation while maximizing the productivity of shikimic acid (Sheppard and Cooper, 1990; McCaffrey and Cooper, 1995; Brown, 2001). More specifically, the SCF control scheme must be coupled with the natural metabolism of the yeast population such that the period of a cycle is related to the doubling time of the organism (Sauvageau, e*t al.*, 2010). This is important because if the cycle time is faster than the doubling rate, the culture would wash out (Sheppard and Cooper, 1990; Brown, 2001). Furthermore, the cycle time must at least coincide with the depletion of an essential nutrient, in this case the primary carbon source, to prevent substrate accumulation leading to unstable SCF operation (Brown, 2001). Finally, the control parameter signalling the initiation of the cycling sequence must be accurate, reliable, and easy to use for stable SCF operation (Sauvageau, e*t al.*, 2010).

6.2.1 Choosing the cycling initiation time point

The growth profile, carbon-source consumption, and shikimic acid formation of the engineered yeast strain during glucose metabolism was similar when grown in a 1-L batch fermenter (Figure 5.10) as in shake flask cultures (Figure 5.7). However during ethanol metabolism, significantly less shikimic acid was produced in the 1-L batch fermenter. The growth conditions between shake flask and 1-L batch fermenter differed in the volume of culture, the agitation rate, and the aeration rate. Of these, the aeration rate had the most significant effect in the system. In some fermentation scale-ups, the increase in liquid volume and agitation rate can negatively affect the productivity of a process. An increase in liquid volume of a culture may affect cell viability due to a reduced mixing quality creating substrate concentration gradients (Larsson, e*t al.,* 1996; Bylund, e*t al.,* 1998; Enfors, e*t al.,* 2001). An increase in agitation rate may cause a higher shear force exerted on the cells due to the rotation of the impeller which could eventually lead to lower cell density (Shuler and Kargi, 2002). However, these effects must be negligible in the current system since the biomass growth and shikimic acid production profile during glucose metabolism is similar in both shake flask and 1-L fermenter. In contrast, the increase in aeration rate led to the ethanol being stripped from the liquid fermentation broth and thus leaving the reactor in the outlet gas stream; this left less carbon available for growth and product formation after

glucose depletion (Taylor, 1995). In fact, the rate of ethanol loss in the 1-L fermenter was determined, through an abiotic experiment, to be approximately 6.4×10^{-3} mol-C·(L·h)$^{-1}$ (Figure B8 in Appendix B). This corresponds to a convective mass transfer coefficient (k_c) of 1.465 (m^2·h)$^{-1}$. A simplified mass balance comparing the yield of moles of carbon of shikimic acid on moles of carbon from ethanol in both conditions (with and without stripping) revealed that the rate at which ethanol was stripped in the fermenter was consistent with the lower product yield (see Appendix C for sample calculation). Thus in terms of maximum productivity in the self-cycling fermenter, the point at which the cycling process must occur during SCF operation should be at the point of glucose depletion, and no later.

Glucose is the primary substrate in the fermentation broth; it must be depleted before cycling occurs to ensure that it does not accumulate and cause unstable SCF operation (Sauvageau, e*t al.*, 2010). Based on the batch experiment, cycling should occur between 21 to 41 hours of growth (Figure 5.10). From shake flask cultures, glucose depletion occurred after 25 hours of growth. However the ethanol concentration was at its peak at this point. If cycling were initiated, the ethanol in the fermentation broth would be expected to accumulate. This can be problematic as increased levels of ethanol is toxic to cells (Birch and Walker, 2000; Galeote, e*t al.,* 2001). Therefore, an extended cycle time triggered at the depletion of ethanol could be beneficial for two reasons: it would avoid the potential cycle-to-cycle accumulation of ethanol in subsequent cycles and it could maximize the amount of shikimic acid produced in the fermenter. However, this would create cycles lasting up to 90 hours, caused by the slower kinetics of respiration during ethanol metabolism. This situation would lead to increases in shikimic acid yield (Figure 5.14) at the expense of shikimic acid productivity (Figure 5.15). Therefore, it was decided to initiate cycling shortly after the point of glucose depletion to minimize ethanol accumulation and avoid long cycle times.

Multiple approaches can be used to assess the optimal production of shikimic acid. Figures 5.12 and 5.13 only show three points for the selectivity over ethanol because ethanol started to get consumed at subsequent sample points, leading to negative selectivity values. Both figures illustrate that the overall and instantaneous selectivity over ethanol is at its peak at complete glucose depletion. Similarly, a local maximum is observed for the selectivity over cell number at this time point. However, the maximum overall and instantaneous selectivity over cell number

occurred later, around the time at which ethanol was depleted. A similar trend was observed for the yield of shikimic acid on the total moles of carbon consumed (Figure 5.14). This shows that shikimic acid, a primary metabolite, is maximally produced at the end of carbon-source metabolism (Shuler and Kargi, 2002). However, importantly, the maxima in productivity and specific productivity of shikimic acid both occurred at the end of glucose consumption. The subsequent decrease in productivity was due to the slower kinetics encountered during ethanol metabolism. Taking all these factors into account, the time at which glucose became depleted indicate the best point at which cycling should occur for optimal production of shikimic acid. Again, while this strategy does not yield the maximum shikimic acid concentration possible, it yields the highest productivity. Another advantage of tying the cycling to the glucose consumption is that it avoids the dependence on ethanol, which was shown to strip in the aerated fermenter (Figure 5.10).

6.2.4 Choosing the feedback control parameter

Glucose depletion marks the switch in metabolism from glucose to ethanol and a slower growth rate. Since glucose concentration is difficult to measure in real time during fermentation, previous studies have used the change in OD to signal glucose depletion (Rishpon, *et al.,* 1989; Hatch and Veilleux, 1995; Veloso, *et al.,* 2009). However, OD probes are expensive and susceptible to fouling during longer fermentation periods (van Walsum and Cooper, 1993; Sauvageau, e*t al.*, 2010). Furthermore, the *Crabtree effect* observed in the engineered yeast strain causes a continued slow increase in OD readings. For all these reasons, OD is not a good indicator of glucose depletion.

Previous studies on aerobic cultures have used the dissolved oxygen (DO) levels in the fermenter as the control parameter during SCF operation. In these cases, DO signalled substrate depletion and the onset of stationary phase (Brown and Cooper, 1991; van Walsum and Cooper, 1993; Zenaitis and Cooper, 1994; McCaffrey and Cooper, 1995; Wentworth and Cooper, 1996; Marchessault and Sheppard, 1997). Though this has worked well in the past, several issues can arise. To ensure that changes in DO are detected, microorganisms had to be grown under oxygen limitation. This was necessary so that when the actively growing culture depletes the limiting nutrient, the change in DO signal is large enough to be detected to initiate the cycling process. However, oxygen limitation inhibits maximal growth of cell culture and subsequently results in

sub-optimal product formation. In addition, a DO probe has many of the same limitations as an OD probe in terms of its tendency to foul after many cycles. This necessitates the removal and replacement of the probe which increases the risk of contamination during the fermentation process or the restarting of a new series of cycle periods (Sauvageau, e*t al.*, 2010).

More recently, the CER and dCER were used as monitoring parameter during SCF operation of *E.coli* (Sauvageau, e*t al.*, 2010; Storms, e*t al.*, 2012). In both studies, the CER was not used as the principal parameter because the maximum in CER did not coincide with the depletion of the limiting nutrient. However, the point at which the dCER curve crossed the x-axis for the second time clearly marked this time point. Thus, the dCER was used as the control parameter for SCF operation. Using dCER, it was not imperative to grow the cultures under oxygen limitation; nor was the use of a probe in direct contact with the medium necessary, avoiding risks of fouling or contamination. Furthermore, dCER as the control parameter led to cycle periods with less variability and cell synchrony was achieved at earlier cycles than in studies using DO.

The CER and dCER trends monitored during the batch growth of the engineered yeast strain (Figure 5.16 and 5.17) were similar to those observed for *E. coli* (Sauvageau et al. 2010). The maximum in CER coincided with the beginning of the deceleration of the growth on glucose but not the depletion of glucose. The rapid drop in CER observed at 22 h in Figure 5.17A signalled the end of the exponential phase of growth and glucose depletion. At this point, the dCER curve decreased significantly before rising towards the x-axis and stabilizing at approximately 25 hours of growth (Figure 5.17B). Unlike in the Sauvageau study, the point at which the dCER curve crosses the x-axic cannot be used as the control parameter for cycling since the dCER level is erratic around the axis when CER is at a maximum. Thus, a more robust control parameter for cycling which signals glucose depletion is a combination of both CER and dCER readings. As shown in Figure 5.17, the CER was below 3000 ppm and the dCER was zero at approximately 25 hours of growth which was the point at which glucose was fully consumed. Figure B7 in Appendix B shows a schematic of the control scheme for the chosen cycling condition.

6.3 Self-cycling fermentation operation

After choosing glucose depletion as the point at which cycling is initiated and the coupled readings of CER and dCER as the control parameter for the feedback control loop triggering cycling, the engineered strain was grown under SCF conditions.

6.3.1 Stability of operation

In literature, the use of the CER as the control parameter for the feedback control strategy during SCF operation provided stable cycles as measured by reproducible cycle lengths and CER pattern between cycles (Sauvageau, e*t al.*, 2010; Storms, e*t al.*, 2012). In the current study, the CER pattern and cycle period were not the only parameters used to infer stability; they were used to calculate the total carbon dioxide evolved per cycle.

In SCF operation, the first cycle is analogous to a batch process. In this study, the difference was that the first cycle ended when the cycling process was initiated due to glucose depletion whereas the batch process continued into ethanol catabolism. After five cycles, the CER data followed a relatively stable repeatable pattern (Figure 5.18), even if, in the case shown, cycles 14-22 had low maximum CER compared to preceding and subsequent cycles. These cycles also showed longer cycle times (Figure 5.19). Conversely, the cycles with high CER maxima tended to have shorter cycle times. Despite these small differences, the total moles of carbon dioxide evolved was shown to be reliably consistent beyond 5 cycles (Figure 5.20). This is an improvement from SCF studies using DO as the control parameter where a stable pattern was not observed before ten cycles (van Walsum and Cooper, 1993; Wentworth and Cooper, 1996).

Another measure of stability can be seen in the reproducibility of the OD pattern (Figure 5.21). The end of cycle OD became reproducible immediately after the first cycle. This implies that the cells were not accumulating from cycle to cycle or being washed out due to potential early cycling. The reproducibility of the end of cycle glucose and ethanol concentrations can also be used as evidence of the stability of operation. The starting glucose concentration was twice the concentration used for subsequent cycles (Figure 5.22). This procedure, as opposed to using the same glucose concentration for all cycles, leads to immediate repeatable cycling patterns (Storms, e*t al.*, 2012). Furthermore, the cycling process was initiated only when glucose was fully consumed; for all cycles, the end of the cycle coincided with a glucose concentration of zero. This was beneficial for stable SCF operation as it prevented substrate accumulation. On the other hand, despite previous concerns that ethanol accumulation may occur due to cycling conditions, the end of cycle ethanol concentration stayed low and even decreased over the period of operation (Figure 5.23). This decrease may be due to the continual stripping of ethanol caused by the aeration

in the fermenter and/or a decrease in ethanol production caused by different metabolic regimes under synchrony.

One surprising observation was that the average cycle time (8.87 h) after the first cycle was significantly longer than the doubling time observed in a batch culture for the engineered strain (2.06 h). In earlier studies of the SCF system, the period of nutrient dosing was shown to coincide with the natural doubling time of the cell (Sheppard and Cooper, 1990; Sheppard and Dawson, 1999). However, it has also been shown that stable SCF operation can be achieved with the doubling of cells occurring in the middle of the cycle when a delay was imposed on the normal cycling process to extend the cycle period (McCaffrey and Cooper, 1995). Even more recent studies have shown that the doubling of cells of *E. coli* may naturally occur in the middle of cycles during stable SCF operation (Sauvageau, e*t al.*, 2010; Storms, e*t al.*, 2012). These studies are most consistent with the results from the present study. The delay between the doubling of cells and the end of a cycle may be attributed to the presence of a short lag phase immediately after cycling, or a metabolic process associated with the synchronization of the cell population (Sheppard and Dawson, 1999; Sauvageau, e*t al.*, 2010). Based on the intra-cycle OD data for cycle 11 and 21 (Figure B9 in Appendix B), no lag phase was observed. Thus, the extended cycle time was likely caused by the process of synchronization in the engineered yeast strain. It was proposed, in a different study, that synchronization in yeast cells may lead to metabolic oscillations longer than the doubling times caused by the presence of ethanol in the medium; ethanol decreases the critical cell size for bud initiation (Porro, e*t al.,* 1988).

6.3.2 Shikimic acid production: yield, selectivity, and productivity

Previous SCF experiments have been conducted where the cycling process was extended past the point of depletion of the limiting nutrient to improve the production of a secondary metabolite (McCaffrey and Cooper, 1995). In another SCF experiment for the production of non-growth associated products, biomass production was uncoupled from product formation where secondary vessels were used for the production stage (van Walsum and Cooper, 1993). In the current study, the yeast population was kept in exponential phase for many generations to maximize the production of shikimic acid, a primary metabolite. Moreover, biomass production and product formation was done in the same vessel. With this set-up, an increasing trend in the yield, selectivity, and productivity of shikimic acid was observed as cycle number increased

(Figures 5.24-5.28). Compared to the selectivity, yield, and productivity obtained during batch growth of the engineered strain (Figures 5.12-5.15), the values obtained during SCF operation were consistently higher. Specifically, an almost five-fold increase was observed when comparing the maximum productivity of the engineered strain after 20 hours of batch growth in a 1-L fermenter (Figure 5.15) to the productivity obtained after 23 cycles in the SCF (Figure 5.28). This increase in productivity may be due to a positive feedback loop caused by the presence of shikimic acid-related products in the medium, which would maintain a high intracellular level of shikimic acid. Alternatively, the increase may be due to the effects of synchronization during SCF operation (McCaffrey and Cooper, 1995; Wentworth and Cooper, 1996; van Walsum and Cooper, 1993; Zenaitis and Cooper, 1994, Storms, e*t al.*, 2012).

Interestingly, the intra-cycle instantaneous selectivity over cell number (Figure 5.26A) for both cycles 11 and 21 had maximum values early in the cycle. This is in contrast to the results obtained in the 1-L batch fermenter (Figure 5.13) where the maximum values of instantaneous selectivity over cell number occurred at the end of carbon-source consumption (i.e. a local maximum at glucose depletion and an absolute maximum at ethanol depletion). The maximum selectivity value obtained for cycle 21 corresponds to time points before cell division within the cycle (Figure 5.33C). Thus, Figure 5.26A suggests that shikimic acid may be continually produced within the cycle while the cell number increase happens at a narrow time frame, suggesting a synchronized cell division. Similarly, the intra-cycle instantaneous selectivity over ethanol (Figure 5.26B) for cycle 21 reaches a peak value mid-cycle as opposed to the end of glucose consumption (Figure 5.13). This maximum corresponds to time points during cell division within the cycle (Figure 5.33C). This suggests that shikimic acid may be produced preferentially over ethanol during cell division. For both selectivity over cell number and ethanol, the trends observed are more pronounced in cycle 21 as compared to cycle 11, suggesting synchronization may have an effect on specific shikimic acid production. However, the same deductions done on cycle 21 cannot be made for cycle 11, since the cell number steadily increased within the cycle and the time frame for cell division cannot be determined easily (Figure 5.33A).

While the productivity increased for the whole duration of a cycle (Figure 5.29A), the integrated specific productivity showed a parabolic profile (Figure 5.29B). In cycle 21, the parabolic curve is more pronounced and skews to the right with two maxima in productivity

occurring at normalized times of 0.21 and 0.42, which should correspond to the onset and end of cell division within the cycle (Figure 5.33C). A previous study on the production of a recombinant protein by a lysogenized *E. coli* undergoing SCF operation showed the presence of two distinct maxima in productivity at the onset and end of cell division in synchronized cultures (Storms, e*t al.*, 2012). Unlike that study however, the local minimum between the two maxima coincided with the onset of cell replication (Figure 5.33C). As with selectivity, the high productivity before cell division in cycle 21 may imply that shikimic acid production was faster before cell division was initiated. The maximum after cell replication may imply that the new cells impact the shikimic acid production. Thus, the local minimum found between these maxima would result from the production of shikimic acid slowing down as cells divide. It should be noted that this trend was not observed for cycle 11 (Figure 5.29B), which also did not exhibit cell synchrony (Figure 5.33A).

6.3.3 Shikimic acid production beyond glucose consumption

Two-stage SCF systems can be used to decouple the growth/synchronizing phase from the production phase (van Walsum and Cooper, 1993; Sauvageau and Cooper, 2010). Depending on the requirements of the process of interest, different approaches can be taken with the second vessel. For example, McCaffrey and Cooper (1994) proposed to add a secondary carbon source to increase the yield of secondary metabolites. Sauvageau and Cooper (2010) and Storms *et al.* (2012) demonstrated that this approach could be used to trigger production in inducible systems.

In the present study, during exponential growth on glucose in the later cycles of SCF operation, cells produced more shikimic acid (Figure 5.24). To investigate whether cells from later cycles would produce more shikimic acid from the ethanol they had produced, cells were harvested from cycles 2 and 20 and cultured for an additional 60 h to allow for the complete conversion of ethanol. In these cases, the final shikimic acid concentration for cycle 20 was higher than that of cycle 2 (Figure 5.30). First, this confirms that using a secondary vessel to allow for longer periods of production could lead to increased shikimic acid titers. However, as was seen from batch fermentations, this increase in titer would come at the expense of productivity, which had a tendency to decrease during the consumption of ethanol (Figure 5.15). Another interesting observation comes from Figures 5.30 and 5.31, which show that the yields on ethanol for cells in cycle 2 and 20 were actually comparable. This implies that the mechanism of ethanol metabolism was the same for cells harvested from early and late cycles.

6.4 Cell synchrony

Implementing SCF for the engineered yeast strain was shown to increase dramatically the specific productivity and yield of a primary metabolite. Possible explanations for these increases rely on a potential product positive feedback and on the impact of synchronizing cells on metabolic activity.

6.4.1 Shikimic acid positive feedback

The case for the potential positive feedback is based on the fact that each cycle starts with some shikimic acid (and other cellular products) remaining from the previous cycle. The presence of these molecules could stimulate further production of shikimic acid. Figures 5.32 illustrate that the rate and yield of shikimic acid production was similar, regardless of the starting shikimic acid concentration in the medium. From these results, it is highly unlikely that shikimic acid would be the cause of the increase product formation in the later cycles of SCF operation. Also, though shikimic acid did not stimulate further production of itself, both figures show that it does not significantly inhibit product formation either. This is important since the synthesis of certain enzymes in the shikimic acid pathway are subject to regulation by the presence of aromatic acids and their related precursors (Teshiba, e*t al.,* 1986; Braus, 1991).

6.4.2 Cell number and cell division

The increase in shikimic acid production may be caused by the synchronizing effects of the self-cycling fermenter. Synchronized cultures occur when the majority of cells in a population are in the same phase of development (Dawson, 1972). The synchronization of cells has many advantages. Primarily, the metabolism of a synchronized cell population represents that of a single cell (Dawson, 1972). Thus, the metabolism of a single cell can be studied from synchronized cells instead of the average cell population. By doing so, parameters and environmental conditions that directly affect the growth of a cell and its capabilities to form products can be more readily investigated. Furthermore, the synchronization of cells mitigate the effects of product inhibition in negative feedback loops. In biological processes, the formation of products is often regulated by feedback loops to ensure that metabolites are formed only in proportion to the needs of the cells and to avoid toxicity. Thus, a downstream product may deregulate an upstream enzyme. This effect is amplified in asynchronous cultures where the formation of product from one cell inhibits nearby

cells from synthesizing the same metabolite (Madigan, *et al.,* 2009). If the cell population is synchronized, cells manufacture products within roughly the same time frame. Thus, maximum productivity can be achieved. This is beneficial in the current system since the presence of shikimic acid negatively inhibits the activity of shikimic acid dehydrogenase, the enzyme that converts DHS to shikimic acid (Dell and Frost, 1993).

The synchrony index was developed as a measure of synchrony (Blumenthal and Zahler, 1962). Values above 0.6 indicate that the population has a significant degree of synchrony. The cell concentration at the beginning and the end of a cycle are used to calculate the synchrony index. However, it is important to note that the determination of cell concentration cannot be done via OD. This is because OD measures the scattering and absorption of light of a cell population. This measure correlates with the number of cells present in a sample of a randomly distributed population; but in synchronized cultures, all cells grow and divide in a narrow time period, which means that OD increases with increases in cell volumes even if the number of cells has not changed. A more suitable measure of cell number for synchrony is the actual cell count. In asynchronous cultures, the cell number pattern increases steadily (Sauvageau, et *al.,* 2010) while in synchronized cultures, the cell number doubles in a narrow time frame within a cycle. In the SCF, synchrony is usually thought to occur when a stable pattern is achieved in the monitored parameters (Brown and Cooper, 1992; McCaffrey and Cooper, 1995; Wentworth and Cooper, 1996; Sauvageau, et *al.,* 2010; Storms, e*t al.*, 2012). Based on the previous discussion, synchrony of the engineered yeast strain was expected to be achieved after five cycles. However, intra-cycle cell counts for cycle 11 and 16 revealed that the cultures were still not synchronized, with synchrony indexes of zero (Figure 5.33A, 5.33B). This is surprising since yeast cells subjected to SCF operation have been shown to achieve synchrony after 10 to 11 cycles (Wentworth and Cooper, 1996). By cycle 38, the synchrony index was 0.68 which indicates synchrony in the cell population (Figure 5.33D). Cycle 21 gave a synchrony index of 1.01 (Figure 5.33C); this value was achieved because the ratio of cell concentration at the beginning and end of the cycle was greater than two, likely due to measurement errors.

While obtaining intra-cycle cell counts, it was possible to observe a high degree of cells with multiple buds (Figure 5.34C). This may partially explain the synchrony index obtained in cycle 21 and the low synchrony values obtained in previous cycles. In previous studies of

synchronized yeast cells, the morphology observed was that of asymmetric cell division where the mother cell is larger than the budding daughter cell despite equal partitioning of genetic content (Dawson, 1972; Thomas, *et al.,* 1980). Thus, the occurrence of multiple buds during the replication of the engineered yeast strain in SCF indicates a population under stress where the checks within the replication cycle have been overridden (Madigan, *et al.,* 2009). Stress during microbial growth is caused by a deviation from optimal conditions. These include environmental factors such as temperature, pH, osmolarity, dissolved oxygen concentration, nutrient supply, and ethanol concentration (Gibson, *et al.,* 2007; Madigan, *et al.,* 2009). Of these, the most plausible cause for stress in the SCF system was the pH.

The optimal pH for yeast growth is between pH 4 and 5; although yeast are capable of good growth in pH ranges from pH 3.5 to 6 (Russell, 2003). The pH of the liquid medium before inoculum was approximately pH 5. After the growth of both parent and engineered yeast strain in the liquid medium in shake flask cultures, the pH dropped to pH 3. During SCF operation of the parent and engineered yeast strain, the pH at the end of the cycle dropped to approximately pH 2.4 (it was approximately pH 2.6 at the beginning of the cycle). The decrease in pH mostly results from the production of carbonic acid from carbon dioxide, the secretion of organic acids, and the consumption of ammonium sulfate, the nitrogen source used in this study (Shuler and Kargi, 2002). Of these, the consumption of ammonia from ammonium sulfate, which stimulates the secretion of hydrogen protons, is the greatest contributor to the decrease in pH. The lower pH observed during SCF compared to batch operation was a result of the use of medium from the previous cycle. Since only half of the reactor was harvested, fresh medium at pH 5 was mixed with pH-reduced medium from the previous cycle.

Upon inspection for the number of buds, the cells grown in batch cultures (Figure 5.34A, 5.34B) showed a lower degree of multiple buds as compared to the cells grown under SCF operation (Figure 5.34C). This implies that the cells in the SCF system were under more stress than cells grown in batch cultures, despite the drop in pH in both conditions. The difference lies in the way the cells were cultured. During batch operation, the pH during exponential growth on glucose remained relatively close to optimum since fresh medium is used before inoculation. Thus, cells can divide in favourable conditions. Once the limiting nutrient was depleted and appreciable amounts of the nitrogen source had been consumed, which lowered the pH, the cells entered

aerobic respiratory metabolism on ethanol. Under aerobic respiration, the ATP yield is high. Therefore, cells were able to use the extra ATP molecules to actively pump dissociated hydrogen molecules out of the cell which allow them to continue to grow normally despite a decrease in pH (Ingledew, 2009). Finally, it was shown that haploid strains of *Saccharomyces cerevisiae* increase the expression of cell wall-related genes in minimal medium where the pH has been reduced from pH 5 to 3.5 (Kapteyn*, et al.,* 2001). As the cells enter stationary phase, the increased expression of cell-wall related genes protect the cell from the acidic environmental conditions. Ultimately, yeast cells in batch cultures can grow relatively normally and remain viable as the pH decreases.

In the SCF system however, the pH during exponential growth of glucose decreased for subsequent cycles due to the half of the reactor volume which remains between each cycle. Since no other pH adjustments were performed, the cells were growing in sub-optimal pH conditions. Moreover, the metabolism on glucose undergoes aerobic fermentation. Though kinetically faster than aerobic respiration, the ATP yield is low. Thus, the cells may not have enough energy to successfully pump the accumulating hydrogen ions out of the cytoplasm leading to abnormal budding patterns. These conditions are then exacerbated as the cycle number increases and hydrogen ions accumulate in the fermentation broth. In terms of the measurement of synchrony, the cell number then is not indicative of the degree of synchrony in the system. This is because the synchrony attained by the yeast cells as the cycle number increases may be masked by the formation of multiple buds. Therefore, a next step would be to incorporate pH control in the SCF system to maintain optimal pH for all cycles. An alternative to this would be to investigate the use of a different nitrogen source, such as urea, that would not result in the dissociation of hydrogen ions in the fermentation broth. The latter may be more practical for scale-up purposes as it bypasses added costs related to the addition of a base for pH control, and the separation of conjugate salts in the broth due to neutralizing reactions.

Despite the stress placed on the cells and the resulting slower growth kinetics, it is interesting and important to note that the yield, productivity, and specific productivity were all greatly improved under SCF operation.

7. Conclusion

The present work demonstrated that the coupled strategy of metabolically engineering *Saccharomyces cerevisiae* to overproduce shikimic acid and the implementation of the SCF process increased the yield, productivity, and specific productivity of this compound. More specifically, the following conclusions can be made from the obtained results:

The genetic modifications performed on the CEN.PK 113-13D strain of *S. cerevisiae* increased the production of shikimic acid as compared to a parent strain that contains a non-optimized shikimic acid pathway. Moreover, the inserted plasmid was retained after many rounds of replication which ensures cell viability and continued metabolite overproduction. Despite the decrease in growth kinetics and increase in doubling time caused by the burden associated with the presence of the inserted plasmid, these genetic modifications were not obviously detrimental to cell growth. Furthermore, the overproduction of shikimic acid did not inhibit its own continued production through negative feedback loops. Finally, the production of shikimic acid, a primary metabolite, is tied to the growth of the yeast population as shown by the continued production of this compound on both glucose, ethanol, and possibly other fermentation products produced during aerobic fermentation.

The implementation of the SCF process for the growth of engineered *S. cerevisiae* showed that the selection of a proper feedback control parameter facilitated stable SCF operation. More specifically, the point at which a cycle should be initiated was shortly after the depletion of glucose, the primary carbon source. As well, the coupled readings of the CER and dCER proved to be an appropriate feedback control parameter to trigger cycling.

The use of SCF improved the yield, productivity, and specific productivity of shikimic acid as compared to batch fermentation. In addition, intra-cycle studies illustrated that the maximum specific productivity and instantaneous selectivity was achieved before cell division, which suggests the mechanism of growth-associated product formation in yeast during SCF operation is favoured at this point in the growth cycle. As well, the results obtained from shikimic acid production beyond glucose consumption showed that the use of a two-stage SCF system for the production of shikimic acid would not be beneficial for high productivity, despite the achievement of increased shikimic acid titers.

The improved results obtained through SCF operation was not due to a hypothesized positive feedback effect of shikimic acid. Also, though synchrony has been reported in previous studies for different microbial populations subjected to SCF, it is not clear if the increased productivity of shikimic acid can be attributed directly to the synchronizing effects of the SCF system. This is because the method through which synchrony is affirmed was masked by a high degree of multiple bud formation observed during cell division during SCF operation. This indicates a yeast population under stress most likely due to the lack of pH control in the system. Moreover, the cycling sequence of the SCF system can exacerbate the effect pH has on the growing culture. Despite the stress experienced by the yeast population, it is important to keep in mind that the implementation of the SCF system greatly improved the yield and specific productivity of shikimic acid.

8. Future Work and Recommendations

Although the present work revealed several aspects of the SCF system on the production of shikimic acid in engineered strains of *S. cerevisiae*, further areas of exploration could be pursued.

First of all, the implementation of pH control on the SCF system is an area that can mitigate the stress placed on the yeast population. This could minimize the formation of multiple buds during cell division and subsequently highlight the true onset of synchrony during SCF operation. Moreover, this could improve metabolite productivity.

Secondly, different areas of optimization can be explored for the production of shikimic acid in engineered yeast. Some examples include determining an optimal carbon source and concentration, the use of inhibitors such as glyphosate which has been shown to improve shikimic acid titers in other fermentative systems, or the type of nitrogen source. A surface response analysis could be applied on the system to determine the optimal growth and production conditions.

Thirdly, the use of the SCF system affected the metabolic rates of the yeast population. Thus, the SCF can be used a means to obtain synchronized cultures for physiological studies. Namely, the changes in intracellular mechanism of the yeast population at the molecular level could be explored and elucidated by a metabolomics study.

Finally, this present study is a proof of concept for the production of metabolites through the coupled strategy of using a synthetic biology yeast platform and the SCF system. Therefore, it would be interesting to apply these same principles to other metabolites of interest in different engineered microbe platforms. Moreover, the introduction of heterologous biosynthetic pathways into yeast hosts for the production of high-value plant-specific metabolites for specialty chemical ingredient production, in conjunction with the increased productivity obtained during SCF operation, could be an area of further study.

References

Ahn J.O., Lee H.W., Saha R., Park M.S., Jung J.K., Lee D.Y. (2008). *Exploring the effects of carbon sources on the metabolic capacity of shikimic acid production in Escherichia coli using in silico metabolic predictions.* J Microbio Biotechnol, 18, 1773-1784.

Amrhein N., Johanning J., Schab J.J., Schulz A. (1983). *Biochemical basis for glyphosate tolerance in a bacterium and plant tissue culture.* FEBS Lett., 157, 191-195.

Anderson K.A., Cobb W.T., Loper B.R. (2001). *Analytical method for determination of shikimic acid: Shikimic acid proportional to glyphosate application rates.* Commun Soil Sci Plant Anal, 32, 2831-2840.

Arndt K., Fink G.R. (1986). *GCN4 protein. A positive transcription factor in yeast, binds general control promoters at all 5'-TGACTC-3' sequences.* Proc. Antl. Acad. Sci. Biochem., 83, 8516-8520.

Ball S.G., Wickner R.B., Cottarel G., Schaus M., Tirtiaux C. (1986). *Molecular cloning and characterization of ARO7-OSM2, a single yeast gene necessary for chorismate mutase activity and growth in hypertonic medium.* Mol Gen Genet., 205(2), 326-330.

Bender S.L., Widlanski T., Knowles J.R. (1998). *Dehydroquinate synthase: the use of substrate analogues to prove the early steps of catalyzed reaction.* Biochemistry, 28, 7560-7572.

Bhangale R.P., Makandar A.Y., Kininge P.T. (2014). *Optimization of Fermentative Production of Shikimic Acid by Pseudomonas putida*. IJBR, 5(3), 524-532.

Birch, R.M. and Walker, G.M. (2000) *Influence of magnesium ions on heat shock and ethanol stress responses of Saccharomyces cerevisiae*. Enzyme Microb Technol 26, 678–687.

Birch A.J., Kelly L.F., Weerasuria D.V. (1988). *Facile synthesis of* (+)- *and* (–)-*shikimic acid with asymmetric deuterium labelling, using tricarbonyliron as a lateral control group.* J Org Chem, 53, 278-281.

Blumenthal K., Zahler S. (1962). *Index for measurement of synchronization of cell populations.* Science, 135, 724.

Bode R., Melo C., Birnbaum D. (1984). *Mode of action of glyphosate in Candida maltosa*. FEMS Microbiol. Lett., 140, 83-85.

Bode R., Schauer F., Birnbaum D. (1986). *Comparative studies on the enzymological basis for growth inhibition by glyphosate in some yeast species.* Biochem. Physiol. Pflanzen., 181, 39-46.

Braus G.H. (1991). *Aromatic Amino Acid Biosynthesis in the Yeast Saccharomyces cerevisiae: a Model System for the Regulation of a Eukaryotic Biosynthetic Pathway.* Microbiological Reviews. 55(3), 349-370.

Brown W.A., Cooper D.G. (1991). S*elf-cycling fermentation applied to Acinetobacter calcoaceticus RAG-1.* Applied Environmental Microbiology. 57, 2901-2906.

Brown W.A., Cooper D.G. (1992). *Hydrocarbon degradation by Acinetobacter calcoaceticus RAG-1 using the self-cycling fermentation technique.* Biotechnology and Bioengineering, 40, 797-805.

Brown W.A., Cooper D.G., Liss S.N. (1999). *Adapting the self-cycling fermentor to anoxic conditions.* Environ. Sci. Technol., 33(9), 1458-1463.

Brown W.A., Cooper D.G., Liss S.N. (2000). *Toluene removal in an automated cyclical bioreactor.* Biotechnol Prog., 16(3), 378-384.

Brown W.A. (2001). *The self-cycling fermentor – development, applications, and future opportunities.* Recent es. Devel. Biotech. & Bioeng., 4, 61-90.

Bohm B.A. (1965). *Shikimic acid (3,4,5-trihydroxy-1-cyclohexene-1-carboyxlic acid).* Chem Rev, 65, 435-466.

Burns V.W. (1964). *Synchronizatin of division in bacteria by nutritional changes.* In Zeuthen (ed.), Synchrony in cell division and growth. Interscience Publishers, NY, 433.

Bylund F., Collet E., Enfors E.O., Larsson G. (1998). *Substrate gradient formation in the large scale lowers cell yield and increases by-product formation.* Bioprocess Eng, 18, 171-180.

Chandran S.S., Yi J., Draths K.M., von Daeniken R., Weber W., Frost J.W. (2003). *Phosphenolpyruvate availability and the biosynthesis of shikimic acid.* Biotechnol Prog. 19, 804-808.

Crumplen R., DAmore T., Panchal C.J., Stewart C.G. (1989). *Industrial uses of yeast: present and future.* Yeast, 5, 3-9.

Curran K.A., Leavitt J.M., Karim A.S., Alper H.S. (2013). *Metabolic engineering of muconic acid production in Saccharomyces cerevisiae.* Metabolic Engineering, 15, 55-66.

Dangschat G., Fischer H.O.L. (1950) *Configurational relationships between naturally occurring cyclic plant acids and glucose transformation of quinic acid into shikimic acid.* Biocem Biophys Acta, 4, 199-204.

Dawson P.S.S., Anderson M., York A.E. (1971). *The cyclone column culture vessel for batch and continuous, synchronous or asynchronous, culture of microorganisms.* Biotechnology and Bioengineering, 13, 865-876.

Dawson P.S.S. (1972). *Continuously Syncrhonised Growth.* J. appl. Chem. Biotechnol. 22, 79-103.

De Deken R.H. (1966). *The Crabtree Effect: A Regulatory System in Yeast*. J. gen. Microbiol. 44, 149-156.

Dell A.K., Frost J.W. (1993). *Identification and Removal of Impediments to Biocatalytic Synthesis of Aromatics from D-Glucose: Rate-Limiting Enzymes in the Common Pathway of Aromatic Amino Acid Biosynthesis*. J. AM. Chem. Soc., 115, 11581-11589

Draths K.M., Knop D.R., Frost J.W. (1999). *Shikimic acid and quinic acid: replacing isolation from plant sources with recombinant microbial biocatalysis.* Am Chem Soc, 121, 1603-1604.

Duncan K., Edwards R.M., Coggins J.R. (1988). *The Saccharomyces cerevisiae ARO1 gene. An example of the co-ordinate regulation of five enzymes on a single biosynthetic pathway.* FEBS Lett., 241, 83-88.

Enfors S.O., Jahic M., Rozkov A., Xu B., Hecker M., Jurgen B., Kruger B., Schweder T., Hamer G., O'Bierne D., Noisommit-Rizzi N., Reuss M., Boone L., Hewitt C., McFarlane C., Nienow A., Kovacs T., Tragardh C., Fuchs L., Revstedet J., Frieber P.C., Hjertager B., Blomsten G., Skogman H., Hjort S., Hoeks F., Lin H.J., Neubauer P., van der Lans R., Luyben K., Vrabel P., Manelius A. (2001). *Physiological responses to mixing in large scale bioreactors.* J Biotechnol 85:175-185.

Enrich L.B., Scheuermann M.L., Mohadjer A., Matthias K.R., Eller C.F., Newman M.S. (2008). *Liquidambar styraciflua:* a renewable source of shikimic acid. Tetrahedron Lett, 49, 2503-2505.

Escalante A., Calderon R., Valdivia A., de Anda R., Hernandez G., Ramirez O.T., Gosset G., Bolivar F. (2010). *Metabolic engineering for the production of shikimic acid in an evolved Escherichia coli strain lacking the phosphoenolpyruvate: carbohydrate phosphotransferase system.* Microbial Cell Factories. 9:21.

Fleet G.W.J., Shing T.K.M., Warr S.M. (1984). *Enantiospecific synthesis of shikimic acid from D-mannose; formation of a chiral cyclohexene by intramolecular olefination of a carbohydrate-derived intermediate.* J Chem Soc Perkin Trans 1, 905-908.

Floss H.G., Onderka D.K., Carroll M. (1972). *Stereocheistry of the 3-deoxy-D-arabino-heptulosonate 7-phosphate synthetase reaction and the chorismate synthase reaction.* J. Biol. Chem. 247, 736-744.

Fossati E., Ekins A., Narcross L., Zhu Y., Falgueyret J.P., Beaudoin G.A. (2014). *Reconstitution of a 10-gene pathway for synthesis of the plant alkaloid dihydrosanguinarine in Saccharomyces cerevisiae.* Nat Commun, 4(5), 3283.

Fraenkel D.G. (2011). *Yeast Intermediary Metabolism.* Cold Spring Harbor Laboratory Press Cold Spring Harbor, NY.

Galeote, V.A., Blondin, B., Dequin, S. and Sablayrolles, J.M. (2001) *Stress effects of ethanol on fermentation kinetics by stationary-phase cells of Saccharomyces cerevisiae*. Biotechnol Lett 23, 677–681.

Ganem B. (1978) *Shikimate-derived metabolites. From glucose to aromatics – recent developments in natural-products of shikimic acid pathway.* Tetrahedron, 34, 3353-3383.

Ghosh S., Chisti Y., Banerjee U.C. (2012). *Production of shikimic acid.* Biotechnology Advances, 30(6), 1425-1431.

Gibson B.R., Lawrence S.J., Leclaire J.P.R., Powell C.D., Smart K.A. (2007). *Yeast responses to stresses associated with industrial brewery handling.* FEMS Microbiol Rev., 31, 535-569.

Gientka I., Duszkiewicz-Reinhard W. (2009). *Shikimate pathway in yeast cells: enzymes, functioning, regulation – a review.* Pol. J. Food. Nutr. Sci., 59(2), 113-118.

Gold N.D., Gowen C.M., Lussier F.X., Cautha S.C., Mahadevan R., Martin V.J.J. (2015). *Metabolic engineering of a tyrosine-overproducing yeast platform using targeted metabolomics.* Microbial Cell Factories, 14:73.

Graham L.D., Gillies F.M., Coggins J.R. (1993). *Over-experssion of the yeast multifunctional arom protein.* Biochem. Biophys. Acta, 1216, 417-424.

Hansen E.H., Moller B.L., Kock G.R., Buenner C.M., Kristensen C., Jensen O.R., Okkels F.T., Olsen C.E., Motawia M.S. Hansen J. (2009). *De novo biosynthesis of vanillin in fission yeast (Schizosaccharomyces pombe) and baker's yeast (Saccharomyces cerevisiae).* Appl. Environ. Microbiol., 75, 2765-2774.

Hatch R.T., Veilleux B.G. (1995). *Monitoring of Saccharomyces cerevisiae in commercial bakers' yeast fermentation.* Biotechnology and Bioengineering, 46, 371-374.

Harring T., Streibig J.C., Husted S. (1998). *Accumulation of shikimic acid: a technique for screening glyphosate efficacy.* J. Agric Food Chem, 46, 4406-4412.

Hartmann M., Schneider T.R., Pfeil A., Heinrich G., Lipscomb W.N., Braus G.H. (2003). *Evolution of feedback-inhibited beta/alpha barrel isoenzymes by gene duplication and a single mutation.* Proc. Natl. Acad. Sci. USA, 100, 862-867.

Herrmann K.M., Weaver L.M. (1999). *The shikimate pathway.* Annu Rev Plant Physiol Mol Biol., 50, 473-503.

Hinnebusch A.G. (1988). *Mechanism of gene regulation in the general control of amino acid biosynthesis in Saccharomyces cerevisiae.* Microb. Rev., 52, 248-273.

Hughes S.M., Cooper D.G. (1996). *Biodegradation of phenol using the self-cycling fermentation (SCF) process.* Biotechnology and Bioengineering, 51(1), 112-119.

Ingledew W.M. (2009) *Yeast stress in fermentation process. In: The alcohol textbook – a reference for the beverage, fuel, and industrial alcohol industries, 5th Ed.* W.M. Ingledew, D.R. Kelsall, G.D. Austin and C. Kluhspies (eds.), Nottingham University Press, Nottingham, UK, 115-126.

Invitrogen™. (2009). *pYES2/CT, pYES3CT, and PYC2/CT: Yeast expression vectors with c-terminal tags and auxotrophic markers*. User Manual.

Iomantas Y., Abalakina E.G., Polanuer B., Yampolskaya T.A., Bachina T.A., Kozlov J.I. (2002). *Method for producing shikimic acid.* US Patent 6436664.

Jiang H., Wood K.V., Morgan J.A. (2005). *Metabolic engineering of the phenylpropanoid pathway in Saccharomyces cerevisiae.* Appl. Environ. Microbiol., 71, 2962-2969.

Jiang S., McCullough K.J., Mekki B., Singh G., Wightman R.H. (1997). *Enantionspecific synthesis of* (-)-*5-epi-shikimic acid and* (-)-*shikimic acid.* Journal of the Chemical Society, Perkin Transactions 1, 12(12), 1805-1814.

Johansson L., Lindskog A., Silfversparre G., Cimander C., Nielsen K.F., Liden G. (2005) *Shikimic acid production by a modified strain of E. coli (W3110.shik1) under phosphate-limited and carbon-limited conditions.* Biotechnology and Bioengineering, 92, 541-552.

Käppeli O., Sonnleitner B., Blanch H.W. (1986). *Regulation of Sugar Metabolism in Saccharomyces-Type Yeast: Experimental and Conceptual Considerations.* Critical Reviews in Biotechnology. 4(3), 299-325.

Kapteyn J.C., ter Riet B., Vink E., Blad S., De Nobel H., van Den Ende H., Klis F.M. (2001). *Low external pH induces HOG-1 dependent changes in the organization of the Saccharomyces cerevisiae cell wall.* Mol Microbiol., 39(2), 469-479.

Karim A.S., Curran K.A., Alper H.S. (2013). *Characterization of plasmid burden and copy number in Saccharomyces cerevisiae for optimization of metabolic engineering applications.* FEMS Yeast Res., 13(1), 1-18.

Kim C.U., Lew W., Williams M.A., Zhang L., Liu H., Swaminathan S., Bischofberger N., Chen M.S., Tai C.Y., Mendel D.B., Laver W.G., Stevens R.C. (1997). *Influenza neuraminidase inhibitors possessing a novel hydrophobic interaction in the enzyme active site: Design, synthesis, and structural analysis of carbocyclic sialic acid analogs with potent anti-influenza activity.* J Am Chem Soc, 119(4), 681-690.

Knop D.R., Draths K.M., Chandran S.S., Barker J.L., von Daeniken R., Weber W., Frost J.W. (2001) *Hydroaromatic equilibration during biosynthesis of shikimic acid.* J Am Chem Soc, 123, 10173-10182.

Kojima M., Kimuar N., Miura R. (2015). *Regulation of Primary Metabolic Pathways in Oyster Mushroom Mycelia Induced by Blue Light Stimulation: Accumulation of Shikimic Acid.* Scientific Reports, 5: 8630 DOI: 10.1038/srep08630

Koreeda M., Ciufolini M.A. (1982). *Natural product synthesis via allylsilanes 1. Synthesis and reactions of (1E, 3E)-4-acetoxy-1-(trimethylsilyl)1,3-butadiene and its use in the total synthesis of* (±)-*shikimic acid.* J Am Chem Soc, 104, 2308-2310.

Krämer M., Bongaerts J., Bovenberg R., Kremer S., Müller U., Orf S., Wubbolts M., Raeven L. (2003). *Metabolic engineering for microbial production of shikimic acid.* Metabolic Engineering 5 (4), 277-283.

Kranich R., Busemann A.S., Bock D., Schroeter-Maas S., Beyer D., Heinemann B., Meyer M., Schierhorn K., Zahlten R., Wolff G, Aydt E.M. (2007). *Rational Design of Novel, Potent Small Molecule Pan-selectin Antagonists.* J. Med. Chem., 50, 1101-1115.

Krömer J.O., Nunez-Bernal D., Averesch N.J.H., Hampe J., Varela J., Varela C. (2012). *Production of aromatics in Saccharomyces cerevisiae – a feasibility study.* J. Biotechnol. http://dx.doi.org/10.1016/j/jbiotec.2012.04.014.

Künzler MG., Paravicini G., Egli Ch.M., Irniger S., Braus G.H. (1992). *Cloning, primary structure and regulation of the ARO4 gene, encoding the tyrosine-inhibited 3-deoxy-D-arabinoheptulosonate-7phophate synthase from Saccharomyces cerevisiae.* Gene, 113, 67-74.

Larsson G., Tomkvist M., Wernersson E.S., Tragard C., Noorman H., Enfors S.O. (1996). *Substrate gradients in bioreactors: origin and consequences.* Bioprocess Eng 14, 281-289.

Lederer I., Schulzki G., Gross J., Steffen J.P. (2006). *Combination of TLC and HPLC-MS/MS methods. Approach to a rational quality control of Chinese star anise.* J Agric Food Chem, 54, 1970-1974.

Liu L., Redden H., Alper H.S. (2013). *Frontiers of yeast metabolic engineering: diversifying beyond ethanol and Saccharomyces.* Current Opinion in Biotechnology, 24, 1023-1030.

Lloyd D., Poole R.K., Edwards S.W. (1982). *The cell division cycle: temporal organization and control of cellular growth and reproduction.* Academic Press Publication, NY.

Luttik M.A.H., Vuralhan Z., Suir E., Braus G.H., Pronk J.T., Daran J.M. (2008). *Alleviation of feedback inhibition in Saccharomyces cerevisiae aromatic amino acid biosynthesis: quantification of metabolic impact.* Metab. Eng., 10, 141-153.

Madigan M.T., Martinko J.M., Dunlap P.V., Clark D.P. (2009). *Brock Biology of Microorganisms 12th Ed.* Pearson Education Inc., CA.

Marchessault, P., Sheppard, J.D., 1997. *Application of self-cycling fermentation technique to the production of poly-hydroxybutyrate*. Biotechnol. Bioeng. 55, 815–820.

Martin E., Duke J., Pelkki M., Clausen E.C., Carrier D.J. (2010). Sweetgum (*Liquidambar styraciflua L): extraction of shikimic acid coupled to dilute acid pretreatment.* Appl Biochem Biotechnol, 162, 1660-1668.

McCaffrey W.C., Cooper D.G. (1995). *Sophorolipids Production by Candida bombicola using self-cycling fermentation.* Journal of fermentation and bioengineering, 79(2), 146-151.

McCrindle R., Overton K.H., Raphael R.A. (1960). *A stereospecific total synthesis of D*-(–)-*shikimic acid*. J Am Chem Soc, 1560-1566.

Mead D.J., Gardner D.C., Oliver S.G. (1986). *The yeast 2 micron plasmid: strategies for the survival of a selfish DNA.* Mol Gen Genet, 205(3), 417-21.

Mohammed Al-mhanna N.M. (2010). *Observation of Crabtree effect and diauxic behaviour of yeast by using absorption.* Chemical Engineering Transactions, 21, 1465-1470.

Mousdale D.M., Coggins J.R. (1985). *High-performance liquid chromatography of shikimate pathway intermediates.* Journal of chromatography, 329, 268-272.

Moxley J.F., Jewett M.C., Antoniewicz M.R., Villas-Boas S.G., Alper H., Wheeler R.T., Tong L., Hinnebusch A.G., Ideker T., Nielsen J., Stephanopoulos G. (2009). *Linking high-resolution*

metabolic flux phenotypes and transcriptional regulation in yeast modulated by the global regulator Gcn4p. Proc. Nat. Acad. Sci. USA, 106, 6477-6482.

Mueller T.C. (2003). *Shikimate accumulates in both glyphosate-sensitive and glyphosate-resistant horseweed (Conyza Canadensis L. Cronq.).* J Agric Food Chem, 51, 680-684.

Müller J., Dawson P.S.S. (1968). *The oxygen uptake of phased yeast cultures growing at different doubling times on nitrogen- and energy-limited media.* Canadian Journal of Microbiology, 14, 1127.

Naesby M., Nielsen S.V.S., Nielsen C.A.F., Green T., Tange T.O., Simon E., Kneschtle P., Hansson A., Schwab M.S., Titiz O., Folly C., Archilia R.E., Maver M., Fiet S.V.S., Boussemghoune T., Janes M., Kumar A.S.S., Sonikar S.P., Mitra P.P., Benjamin V.A.K., Korrapati N., SUman I., Hansen E.H., Thybo T., Goldsmith N., Sorensen A.S. (2009). *Yeast artificial chromosomes employed for random assembly of biosynthetic pathways and production of diverse compounds in Saccharomyces cerevisiae.* Microbial Cell Factories, 8, 45.

Neelakantam V.N., Power R. (2005). *Relationship between pH and medium dissolved solids in terms of growth and metabolism of Lactobacilli and Saccharomyces cerevisiae during ethanol production.* Appl. Environ. Microbiol., 71(5), 2239-2243.

Nevoigt E. (2008). *Progress in metabolic engineering of Saccharomyces cerevisiae.* Microbiol Mol Biol Rev., 72(3), 379-412.

Nielsen J., Jewett M.C. (2008). *Impact of systems biology on metabolic engineering of Saccharomyces cerevisiae.* FEMS Yeast Research, 8(1), 122-131.

Nielsen J. (2013). *Production of biopharmaceutical proteins by yeast. Advances through metabolic engineering.* Bioengineered, 4(4), 207-211.

Oda Y., Ouchi K. (2000). *Sacharomyces. In: Encylopedia of food microbiology.* R.K. Robinson (editor-in-chief), Academic Press, San Diego, CA, 1907-1912.

Ohira H., Torii N., Aida T.M., Watanabe M., Smith Jr R.L. (2009). *Rapid separation of shikimic acid from Chinese star anise (Illicium verum Hook. F.) with hot water extraction.* Sep Purif Technol, 69, 102-108.

Ostergaard S., Olsson L., Nielsen J. (2000). *Metabolic engineering of Saccharomyces cerevisiae.* Microbiol. Mol. Biol. Rev., 64(1), 34-50.

Otterstedet K., Larson C., Bill R.M., Stahlberg A., Boles E., Hohmann S., Gustafsson L. (2004). *Switching the mode of metabolism in the yeast Saccharomyces cerevisiae*. EMBO, 5(5), 532-537.

Payne R., Edmonds M. (2005). *Isolation of shikimic acid from star anise seeds.* J Chem Educ, 82, 599-600.

Porro D., Martegani E., Ranzi B.M., Alberghina L. (1988). *Oscillations in continuous cultures of budding yeast: a segregated parameter analysis.* Biotechnology and Bioengineering, 32(4), 411-417.

Prather K.L.J., Martin C.H. (2008). *De novo biosynthetic pathways: rational design of microbial chemical factories.* Current Opinion in Biotechnology, 19(5), 468-474.

Pravicini G., Mösch H.U., Schmidheini T., Braus G. (1989). *The general control activator protein GCN4 is essential for basal level of ARO3 gene expression in Saccharomyces cerevisiae.* Mol. Cell Biol., 9, 144-151.

Raghavendra T.R., Vaidyanathan P., Swathi H.K., Ramesha B.T., Rabikanth G., Ganeshaiah K.N. (2009). *Prospecting for alternate sources of shikimic acid, a precursor of Tamilflu, a bird-flu drug.* Curr Sci, 96(6), 771-772.

Rishpon J., Shabtai Y., Rosen I., Zibenherg Y., Tor R., Freeman A. (1990). *In Situ Glucose Monitoring in Fermentation Broth by "Sanwiched" Glucose-Oxidase Electrode (SGE).* Biotechnology and Bioengineering, 35, 103-107.

Rohloff J.C., Kenneth M.K., Postich M.J., Becker M.W., Chapman H.H., Kelly D.E. (1998). *Practical total synthesis of anti-influenza drug GS-4104.* J Org Chem, 63, 4545-4550.

Russell I. (2003). *Understanding yeast fundamentals. In: The alcohol textbook – A reference for the beverage, fuel, and industrial alcohol industries,* 4th Ed. KA Jacques, TP Lyons, DR Kelsall (eds.), Nottingham University Press, Nottingham, UK, 86-119.

Sadaka M., Garcia A. (1999). *Extraction of shikimic and quinic acids.* Chem Eng Commun. 173, 91-102.

Salvado Z., Arroyo-Lopez F.N., Guillamon J.M., Salazar G., Querol A., Barrio E. (2011). *Temperature adaptation markedly determines evolution within the genus Saccharomyces.* Appl Environ Microbiol. 77(7), 2292-2302.

Sarkis B.E., Cooper D.G. (1994). *Biodegradation of aromatic compounds in a self-cycling fermenter (SCF).* The Canadian Journal of Chemical Engineering, 72(5) 874-880.

Sauvageau D., Cooper D.G. (2010). *Two-stage, self-cycling process for the production of bacteriophages.* Microbial Cell Factories, 9:81.

Sauvageau D., Storms Z., Cooper D.G. (2010). *Synchronized populations of Escherichia coli using simplified self-cycling fermentation.* Journal of Biotechnology, 149, 67-73.

Sheppard J.D., Cooper D.G. (1990). *Development of computerized feedback control for the continuous phasing of Bacillus subtilis.* Biotechnology and Bioengineering, 36, 539-545.

Sheppard J.D., Cooper D.G. (1991). *The response of Bacillus-subtilis ATCC-21332 to manganese during continuous-phased growth.* Applied Microbiology and Biotechnology, 35, 72-76.

Sheppard J.D., Dawson P.S.S. (1999). *Cell Synchrony and Periodic Behaviour in Yeast Populations.* The Canadian Journal of Chemical Engineering, 77, 893-902.

Shnappauf G., Harmann M., Künzler M.G., Braus G.H. (1998). *The two 3-deoxy-D-arabinoheptulosonate-7-phosphate synthase isoenymes from Saccharomyces cerevisiae show different kinetic models of inhibition.* Arch. Microbiol., 169, 517-524.

Shuler M.L., Kargi F. (2002). *Bioprocess Engineering: Basic Concepts.* 2nd Ed. Upper Saddle River, NJ: Pearson Education Inc.

Snyder C.D., Rapoport H. (1973). *Stereochemistry of quinate-shikimate conversions. Synthesis of* (-)-4-*epi-shikimic acid.* J. Am. Chem. Soc., 95(23), 7821-7828.

Stansfield I., Stark M.J.R. (2007). *Yeast Gene Analysis 2nd Ed.* Academic Press, NY.

Storms Z.J., Brown T., Sauvageau D., Cooper D.G. (2012). *Self-cycling operation increases productivity recombinant protein in Escherichia coli.* Biotechnology and Bioengineering, 109(9), 2262-2270.

Sui R.H. (2008). *Separation of shikimic acid from Pine needles.* Chem Eng Technol, 31, 469-473.

Taylor F., Kurantz M.J., Goldberg N., Craig Jr., J.C. (1995). *Continuous Fermentation and Stripping of Ethanol.* Biotechnol Prog. 11, 693-698.

Teshiba S., Furter R., Niederberger P., Braus G., Paravicini G., Hutter R. (1986). *Cloning of ARO2 gene of Saccharomyces cerevisiae and its regulation.* Mol. Gen. Genet., 205, 353-357.

Thomas K.C., Dawson P.S.S., Gamborg B.L. (1980). *Differential growth rates of Candida utilis mother and daughter cells under phased cultivation.* Journal of Bacteriology, 141(1), 1-9.

Tong A.H.Y., Evangelista M., Parsons A.B., Xu H., Bader G.D., Page N., Robinson M., Raghibizadeh S., Hogue C.W.V., Bussey H., Andrews B., Tyers M., Boone C. (2001). *Systematic Genetic Analysis with Ordered Arrays of Yeast Deletion Mutants.* Science, 294, 2364-2367.

van Dijken J.P., Weusthuis R.A., Pronk J.T. (1993). *Kinetics of growth and sugar consumption in yeasts.* Antonie van Leeuwenhoek, 63, 343-352.

van Dijken J.P., Bauer J., Brambilla L., Duboc P., Francois J.M., Gancedo C., Giuseppin M.L.F., Jeignen J.J., Hoare M., Lange H.C., Madden E.A., Niederberger P., Nielsen J., Parrou J.L., Petit T., Porro D., Reuss M., van Riel N., Rizzi M., Steensma H.Y., Verrips C.T., Vindelov J., Pronk J.T. (2000). *An interlaboratory comparison of physiological and genetic properties of four Saccharomyces cerevisiae strains.* Enzyme and Microbial Technology, 26, 706-714.

Vannelli T., Wei Q., Sweigard J., Gatenby A.A., Sariaslani F.S. (2007). *Production of p-hydroxycinnamic acid from glucose in Saccharomyces cerevisiae and Escherichia coli by expression of heterologous genes from plants and fungi.* Metabolic Engineering, 9, 142-151.

van Urk H., Postma E., Scheffers W.A., van Dijken J.P. (1989). *Glucose transport in Crabtree-positive and Crabtree-negative yeasts.* Journal of general microbiology, 135, 2399-2406.

van Walsum G.P., Cooper D.G. (1993). *Self-cycling Fermentation in a Stirred Tank Reactor.* Biotechnology and Bioengineering, 42(10), 1175-1180.

Van Zandycke S. (2009). *Yeast biology, monitoring and identification. In: The alcohol textbook – a reference for the beverage, fuel and industrial alcohol industries, 5th edition.* V.M. Ingledew, D.R. Kelsall, G.D. Austin, C. Klushpies (eds.), Nottingham University Press, Nottingham, UK, 95-100.

Veloso A.C.A., Rocha I., Ferreira E.C. (2009). *Monitoring of fed-batch E.coli fermentations with software sensors.* Bioprocess Biosyst Eng, 32, 381-388.

Verduyn C., Zomerdijk T.P.L., van Dijken J.P., Scheffers W.A. (1984). *Continuous measurement of ethanol production by aerobic yeast suspension with an enzyme electrode.* Appl. Microbiol Biotechnol., 19, 181-185.

Walker G.M. (2009). *Yeasts. In: Encyclopedia of Microbiology, 3rd ed.* M. Schaechter (editor-in-chief), Oxford: Academic Press, Ipswich, MA, 478-491.

Wang Y., Yu O. (2012). *Synthetic scaffolds increased resveratrol biosynthesis in engineered yeast cells.* J. Biotechnol., 157, 258-260.

Wang G.W., Hu W.T., Huang B.K., Qin L.P. (2011). *Illicium verum: a review on its botany, traditional use, chemistry and pharmacology.* J Ethnopharmacol, 136, 10-20.

Wentworth, S.D., Cooper, D.G., 1996. *Self-cycling fermentation of a citric acid producing strain of Candida lipolytica*. J. Ferment. Bioeng. 81, 400–405.

Wills, C. (1990). *Regulation of sugar and ethanol metabolism in Saccharomyces cerevisiae.* Crit Rev Biochem Mol Biol., 25(4), 245-80.

Wilson D.J., Patton S., Florova G., Hale V., Reynolds K.A. (1998). *The shikimic acid pathway and polyketide biosynthesis.* J Ind Microbiol Biotechnol, 20, 299-303.

Yeast metabolome database, (2015). *Shikimic acid.* http://www.ymdb.ca/compounds/YMDB00216.

Yi J., Draths K.M., Li K., Frost J.W. (2003). *Altered glucose transport and shikimate pathway product yields in E. coli.* Biotechnol Prog. 19, 1450-1459.

Yoshida N., Ogasawara K. (2000). *An enantioconvergent route to* (–)-*shikimic acid via a palladium-mediated elimination reaction. Org Lett, 2, 1461-1463.*

Zenaitis M.G., Cooper D.G. (1994). *Antibiotic production by Streptomyces aureofaciens using self-cycling fermentation.* Biotechnology and Bioengineering, 44, 1331-1336.

Zeuthen E. (1964). *Synchrony in cell division and growth*. John Wiley & Sons Inc., NY.

Appendix A: Supplementary Tables

Table A1 Components of yeast nitrogen base (YNB) medium without amino acids.

Component	Concentration (Amount/Liter)
Nitrogen Source	
Ammonium sulfate	5.0 g
Salts	
Potassium phosphate monobasic	1.0 g
Magnesium sulfate	0.5 g
Sodium chloride	0.1 g
Calcium chloride	0.1 g
Vitamins	
Biotin	2.0 µg
Calcium pantothenate	400.0 µg
Folic acid	2.0 µg
Inositol	2,000.0 µg
Nicotinic acid	400.0 µg
p-Aminobenzoic acid	200.0 µg
Pyridoxine HCl	400.0 µg
Riboflavin	200.0 µg
Thiamine HCl	400.0 µg
Citric acid	0.1 g
Trace Elements	
Boric acid	500.0 µg
Copper sulfate	40.0 µg
Potassium iodide	100.0 µg
Ferric chloride	200.0 µg
Manganese sulfate	400.0 µg
Sodium molybdate	200.0 µg
Zinc sulfate	400.0 µg

Table A2 Amino acid component of yeast synthetic drop-out media supplement.

Component	Concentration (mg/L)
Adenine	18
p-Aminobenzoic acid	8
Leucine	380
Alanine	76
Arginine	76
Asparagine	76
Aspartic acid	76
Cysteine	76
Glutamic acid	76
Glutamine	76
Glycine	76
Histidine	76
myo-Inositol	76
Isoleucine	76
Lysine	76
Methionine	76
Phenylalanine	76
Proline	76
Serine	76
Threonine	76
Tryptophan	76
Tyrosine	76
Valine	76

Appendix B: Supplementary Figures

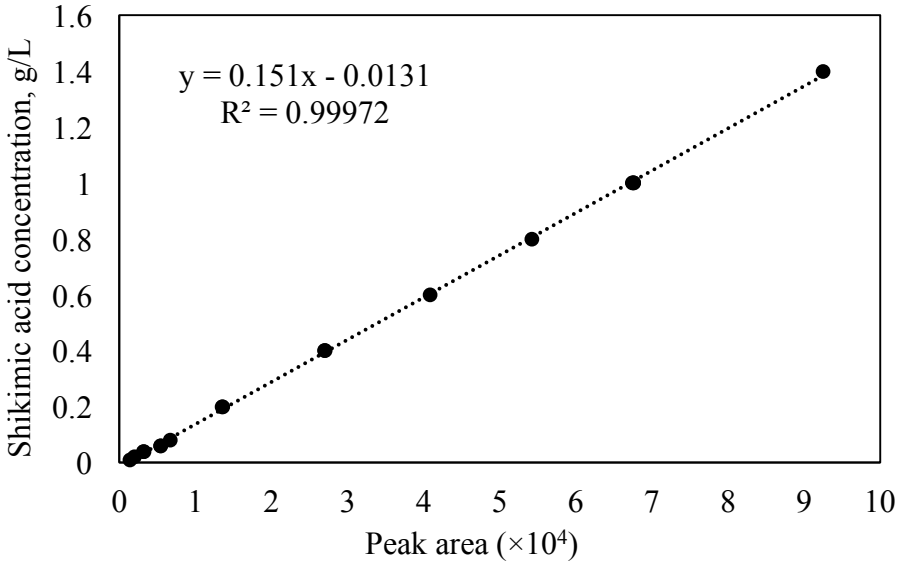

Figure B1 Calibration curve for shikimic acid concentration measured using HPLC.

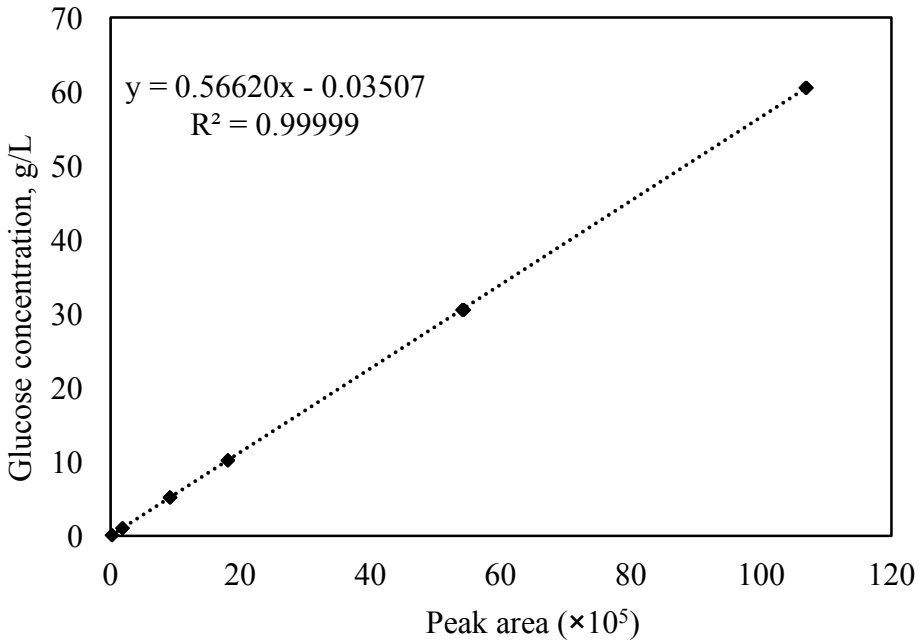

Figure B2 Calibration curve for glucose concentration measured using HPLC.

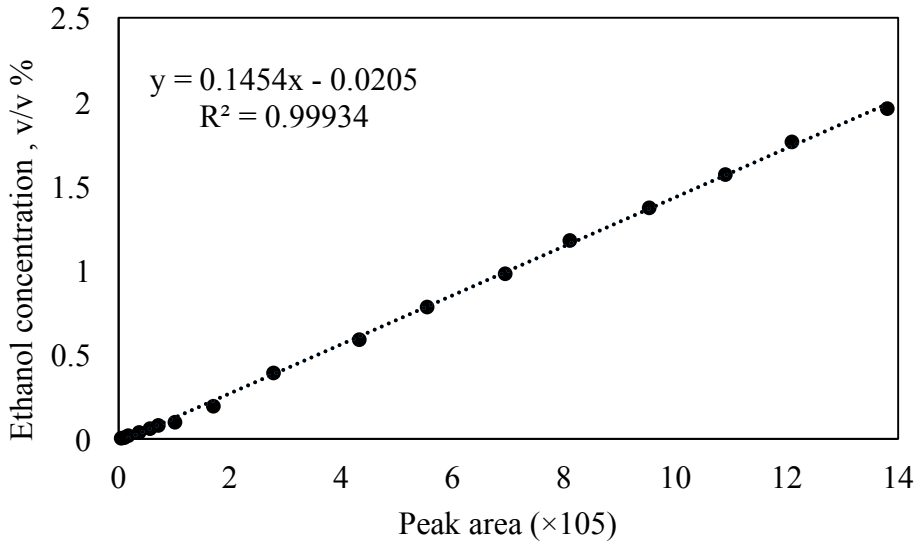

Figure B3 Calibration curve for ethanol concentration measured using HPLC.

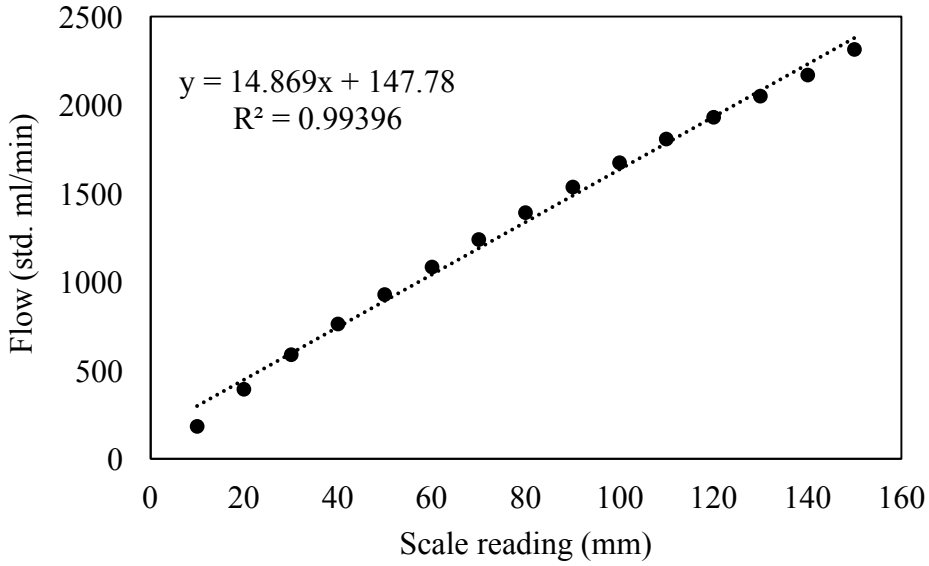

Figure B4 Cole Parmer flowmeter calibration data for aeration rate control.

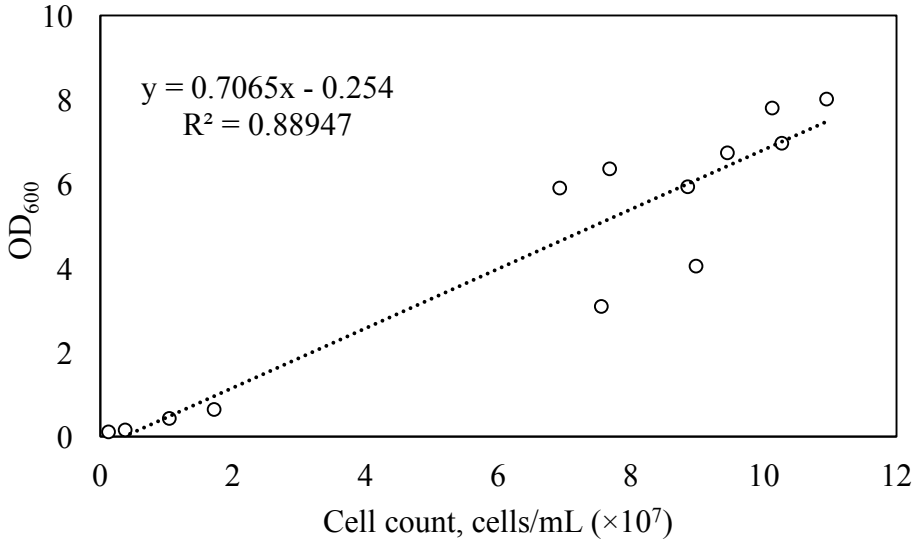

Figure B5 Correlation curve between cell count and OD_{600} for the parent strain.

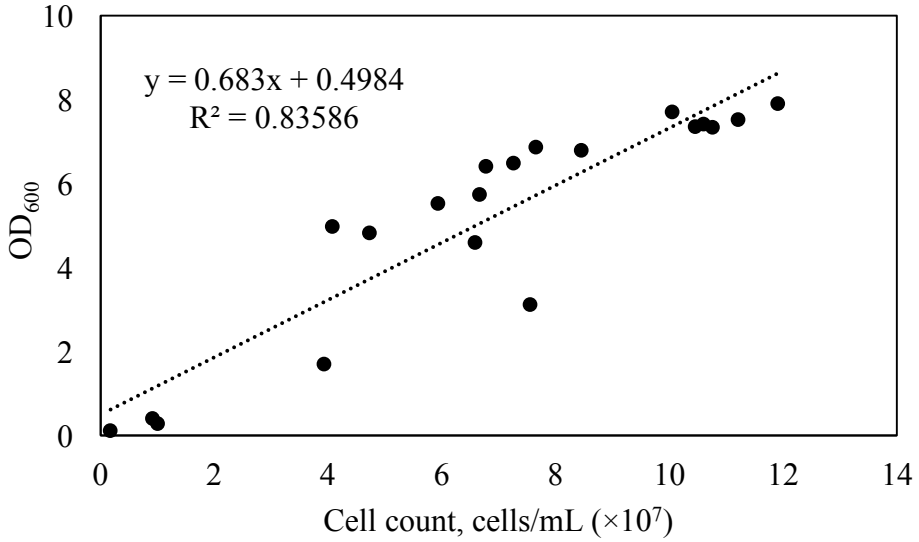

Figure B6 Correlation curve between cell count and OD_{600} for the engineered type strain.

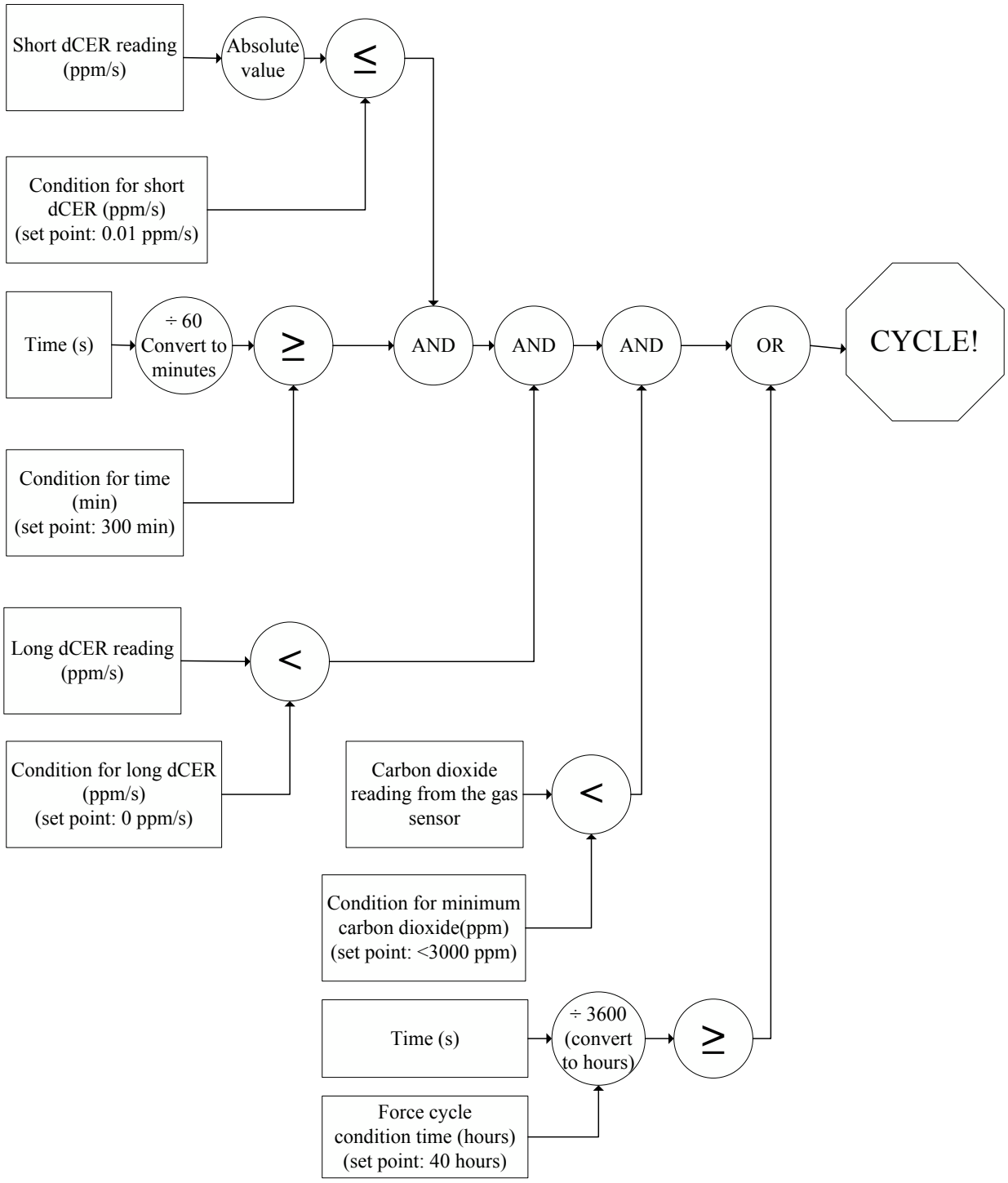

Figure B7 Schematic of the control scheme for the cycling condition. The short and long dCER were calculated with CER data collected in the previous 7 and 15 minutes, respectively. The time condition (in minutes) ensured that cycling did not occur during lag phase of growth. The condition for minimum carbon dioxide controlled the occurrence of cycling at a specific time frame. The timed force cycle condition (in hours) was placed to enable cycling when other parameters were not met.

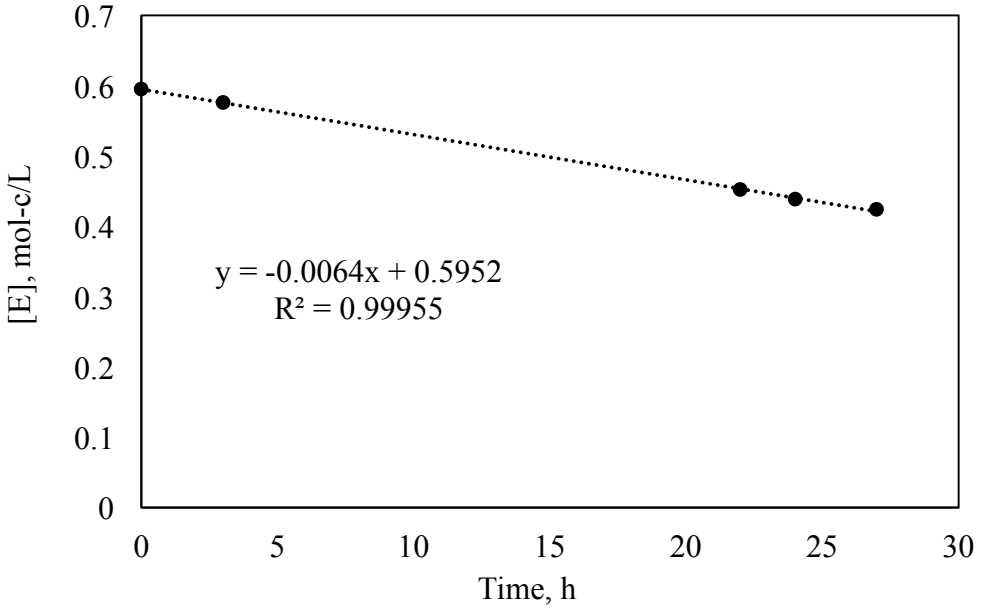

Figure B8 Rate of ethanol loss in a 1-L fermenter due to aeration.

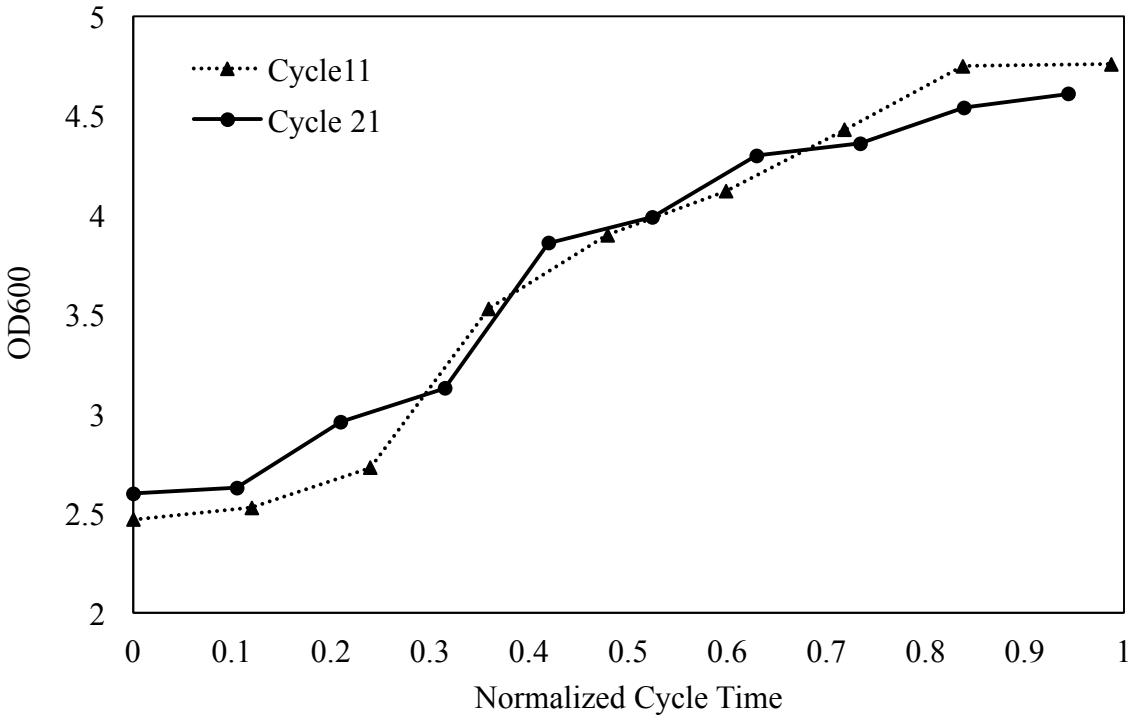

Figure B9 Intra-cycle OD_{600} for cycle 11 and 21 during SCF operation.

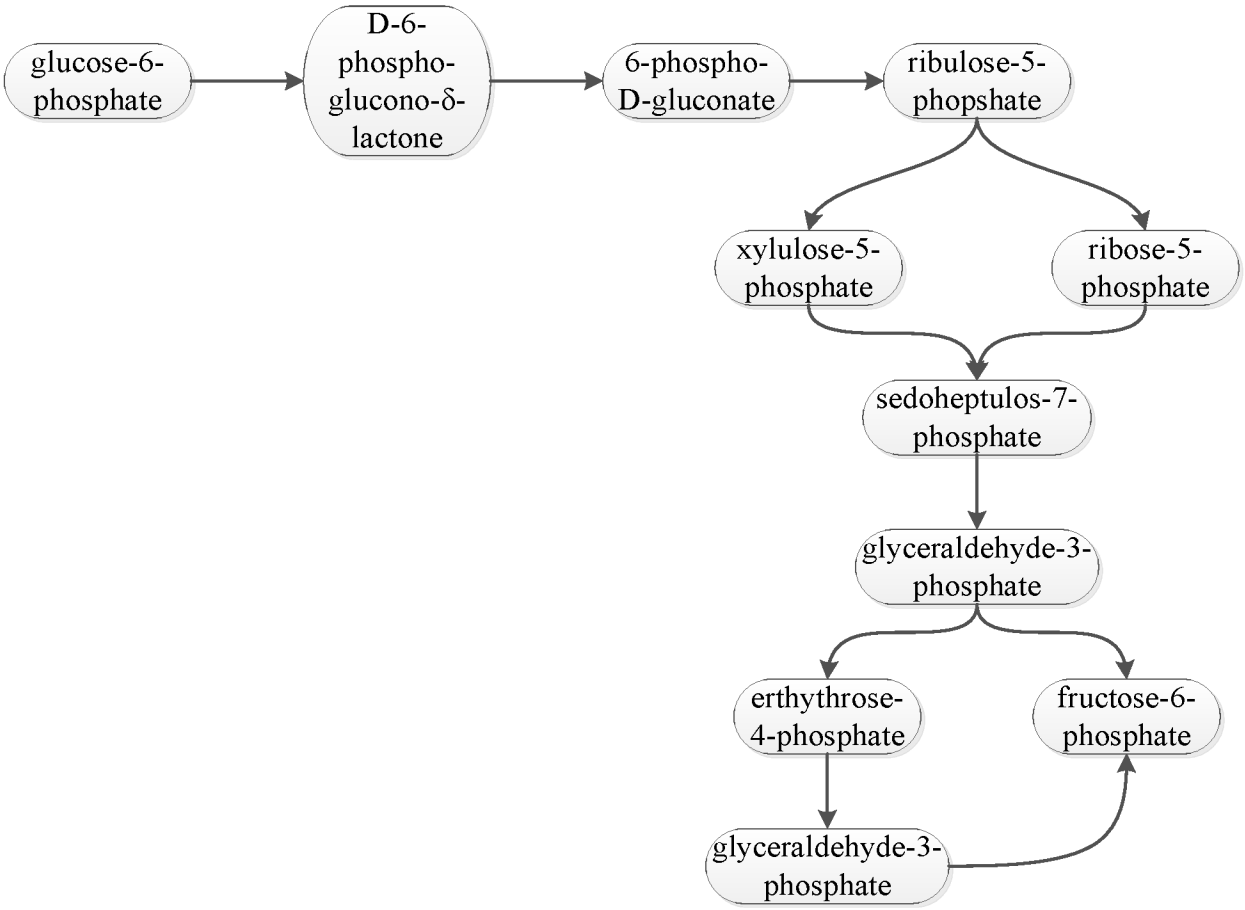

Figure B10 Pentose-phosphate pathway in *Saccharomyces cerevisiae*.

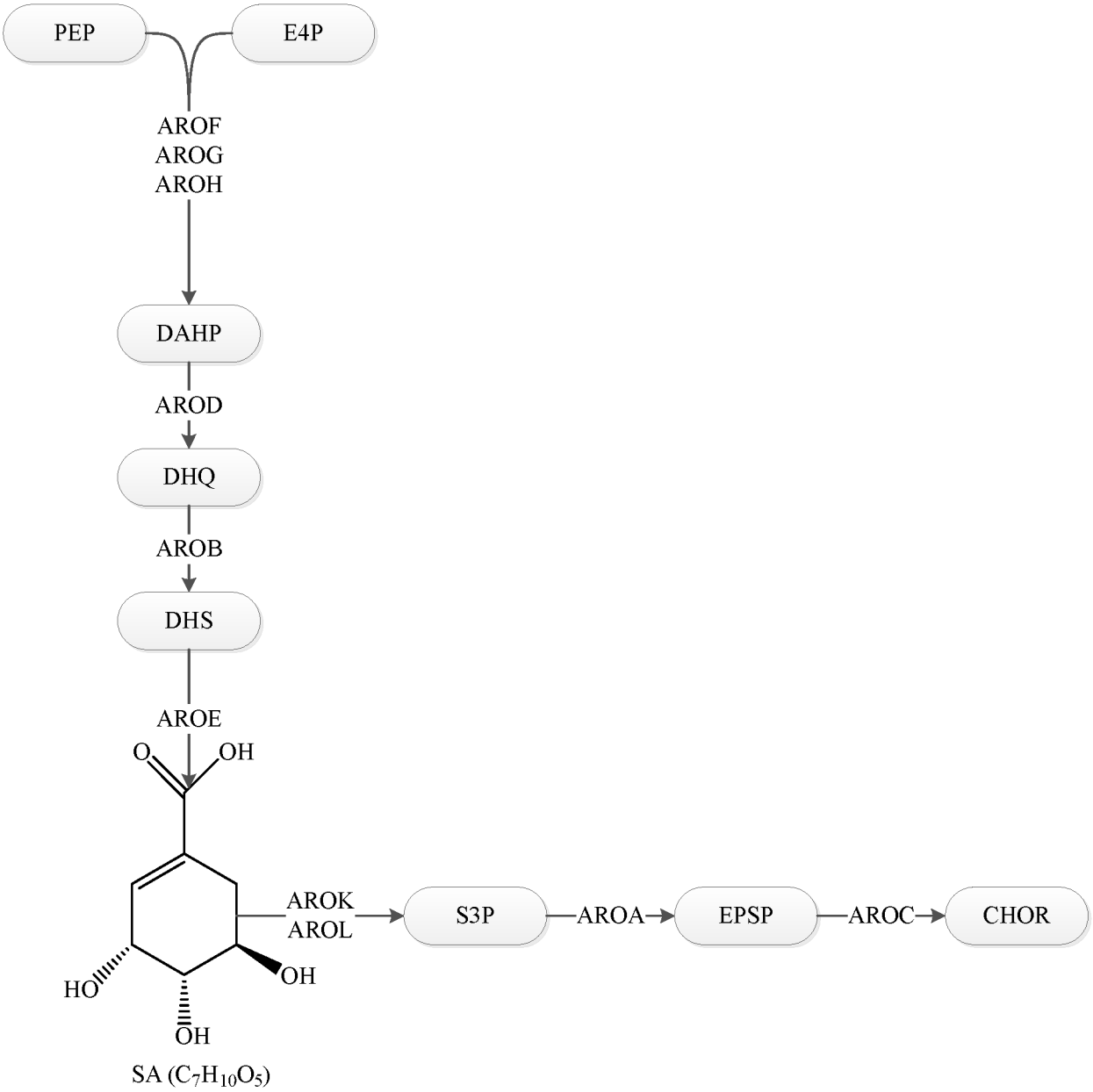

Figure B11 Shikimic acid pathway in *E. coli*.

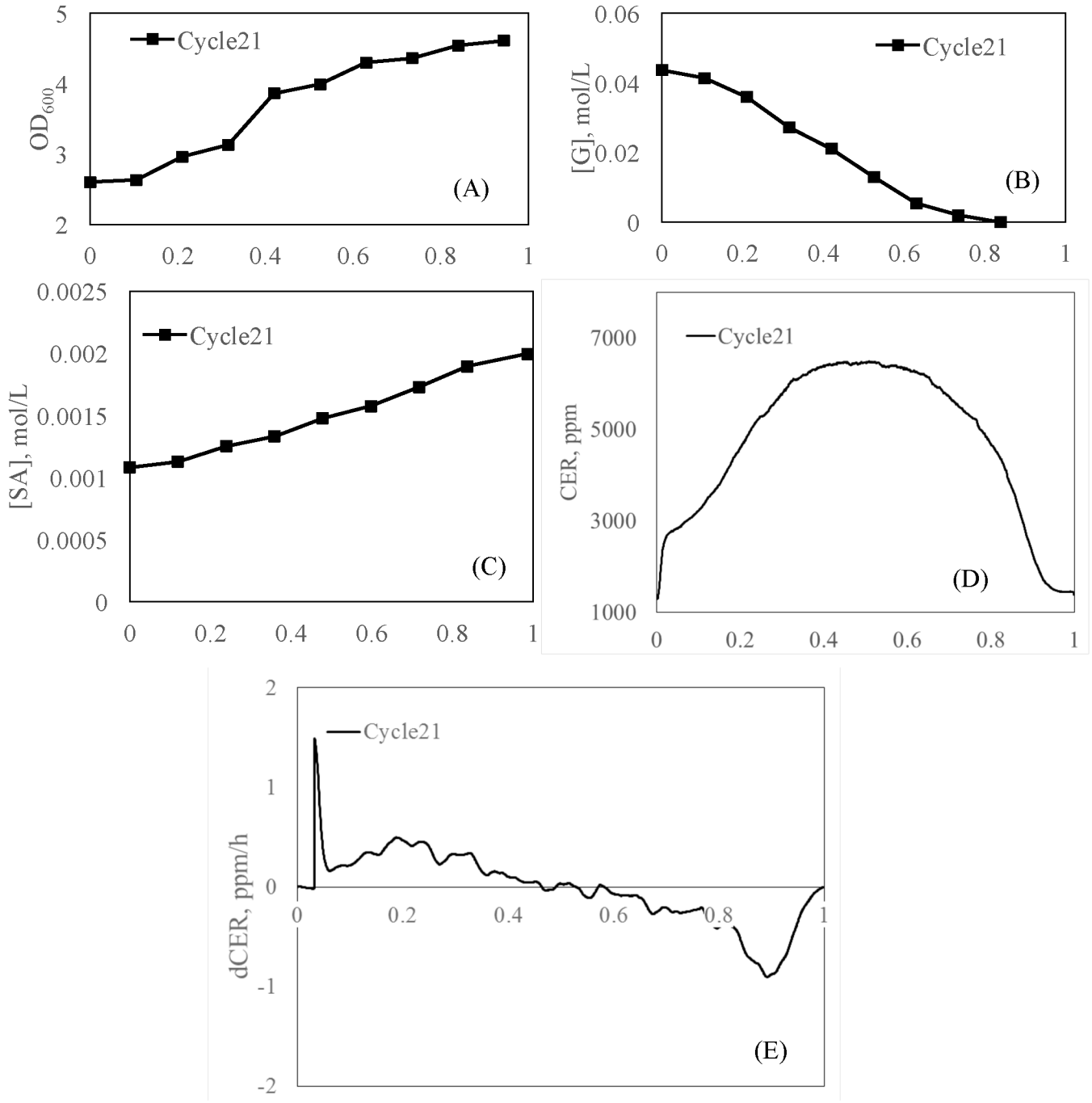

Figure B12 Intra-cycle data for cycle 21. The optical density (A), glucose concentration (B), shikimic acid concentration (C), CER (D), and dCER (E) are shown. The x-axis for all graphs is in terms of the normalized cycle time.

Appendix C: Sample Calculations

A. Theoretical maximum yield of shikimic acid on glucose

Assuming that all the carbon in glucose is used for product formation, the theoretical chemical balance is then given as:

$$C_6H_{12}O_6 + \alpha O_2 \rightarrow \beta C_7H_{10}O_5 + \gamma CO_2 + \delta H_2O$$

Taking a 1-mole basis on glucose, an elemental balance gives three equations:

C-balance: $6 = 7\beta + \gamma$

H-balance: $12 = 10\beta + 2\delta$

O-balance: $6 + 2\alpha = 5\beta + 2\gamma + \delta$

The final equation is given by the respiratory quotient (RQ). The respiratory quotient is defined as the amount of carbon dioxide produced (moles) per mole of oxygen consumed. It has been found that the respiratory quotient for glucose-metabolizing yeast is RQ = 3.88 ≈ 4. Thus, $4 = \gamma/\alpha$. After solving the system of equations, the values obtained were $\alpha = 0$, $\beta = 0.8571$, $\gamma = 0$, $\delta = 1.7143$. This shows that all carbon in glucose ends up in shikimic acid where 0.8571 moles of shikimic acid is maximally produced per mole of glucose. This value is an unattainable ceiling since in reality, the metabolized glucose is used to produce biomass, carbon dioxide, and other carbon-containing products.

B. Comparison between shikimic acid yield on ethanol between shake flask and 1-L fermenter batch cultures.

1. Shake flask batch experiment

In Figure 5.8, 0.67 mol-C of glucose produced 0.25 mol-C of ethanol and 0.0057 mol-C of shikimic acid. Then, 0.016 mol-C of shikimic acid is produced from the ethanol. This gives a 6.4% yield on ethanol.

$$yield\ on\ ethanol = \frac{0.016\ mol - C\ SA}{0.25\ mol - C\ E} = 0.064\ \frac{mol - C\ SA}{mol - C\ E}$$

2. 1-L Fermenter batch experiment

In Figure 5.11, 0.54 mol-C of glucose produced 0.23 mol-C of ethanol and 0.0031 mol-C of shikimic acid. Then, 0.0076 mol-C of shikimic acid is produced from the ethanol. This gives a 3.3% yield on ethanol.

$$yield\ on\ ethanol = \frac{0.0076\ mol - C\ SA}{0.23\ mol - C\ E} = 0.033\ \frac{mol - C\ SA}{mol - C\ E}$$

Figure B8 in Appendix B shows the rate at which ethanol was being stripped (6.4×10^{-3} mol-C·(L·h)$^{-1}$) during an abiotic experiment due to aeration in the 1-L fermenter. From this, the convective mass transfer coefficient (k_c) can be determined from the following equation:

$$N_A = k_c(C_i^* - C_L^*) \qquad \text{Equation C1}$$

where N_A is the mass transfer rate of ethanol in mol-C·(L·h)$^{-1}$, k_c has units of (m^2·h)$^{-1}$, C_L^* is the average bulk concentration of ethanol in the liquid phase in mol-C·Area·(L)$^{-1}$ and C_i^* is the average concentration of ethanol on the interface (which is assumed to be equivalent to the bulk concentration in the gas phase) with the same units. C_i^* is assumed to be zero since the bulk concentration of ethanol in the gas phase is negligible.

Therefore, Equation C1 can be reduced to

$$N_A = -k_c(C_L A) \qquad \text{Equation C2}$$

where A is the gas-liquid interface area in m^2 (8.66×10^{-3} m^2). Using a first order linear model to fit the data from the abiotic experiment, the value of k_c can be determined.

$$\frac{dC_L}{dt} = N_A = -k_c(C_L A) \qquad \text{Equation C3}$$

$$\int \frac{dC_L}{dt} = \int -k_c(C_L A) \qquad \text{Equation C4}$$

$$\int \frac{dC_L}{C_L} = -k_c A \int dt \qquad \text{Equation C5}$$

$$\ln C_L = -k_c A t \qquad \text{Equation C6}$$

Using the least squared approach, the value of k_c was estimated at 1.465 (m^2·h)$^{-1}$.

To determine the amount of ethanol stripped when the engineered yeast strain was cultured in a 1-L fermenter, k_c is used to find N_A in the system where 0.23 mol-C of ethanol was produced.

$$N_A = -k_c C_L A = \left(1.465\ \frac{1}{m^2 h}\right) \times \left(0.23\ \frac{mol-C}{L} \times (8.66 \times 10^{-3} m^2)\right) = -2.92 \times 10^{-3}\ \frac{mol-c}{L \cdot h}$$

In that system (Figure 5.11), it took 51 h to deplete ethanol (i.e. ethanol production peaked at 45h and was completely depleted by 96h of fermentation). Therefore, the amount of ethanol stripped during this time is given as:

$$Ethanol_{stripped} = \left(-2.92 \times 10^{-3}\ \frac{mol-c}{L \cdot h}\right) \times 51h = -0.149\ \frac{mol-c}{L}$$

Therefore, the true yield on ethanol in a 1-L fermenter is 9.5%

$$yield\ on\ ethanol = \frac{0.0076\ mol-C\ SA}{0.081\ mol-C\ E} = 0.094\ \frac{mol-C\ SA}{mol-C\ E}$$

This value is an overestimation due to the assumptions made in the calculations. The rate at which ethanol is lost into the gas phase as determined through the abiotic experiment is most likely higher than the true ethanol stripping rate in biotic experiments. This is because the fermentation broth contains cells, different substrates, and other products which can interfere with the diffusion of ethanol through the bulk phase into the gas-liquid interface. Moreover, the starting ethanol concentration in the abiotic experiment is 2% v/v (~0.6 mol-C of ethanol) whereas the maximum ethanol concentration produced by the cell population was 0.7% (~0.23 mol-C ethanol). A more diluted ethanol solution may show a decreased mass transfer rate. It is important to note however that despite these discrepancies, the aeration in the fermenter does play a role in the stripping of ethanol in the medium which, in turn, affect the biomass growth and shikimic acid production of the engineered yeast population on the produced ethanol.